



HAL
open science

Evaluating hydrological changes in semi-arid West Africa : Detection of past trends in extremes and framework for modeling the future

Catherine Wilcox

► **To cite this version:**

Catherine Wilcox. Evaluating hydrological changes in semi-arid West Africa : Detection of past trends in extremes and framework for modeling the future. Climatology. Université Grenoble Alpes, 2019. English. NNT : 2019GREAU016 . tel-02307847

HAL Id: tel-02307847

<https://theses.hal.science/tel-02307847v1>

Submitted on 8 Oct 2019

HAL is a multi-disciplinary open access archive for the deposit and dissemination of scientific research documents, whether they are published or not. The documents may come from teaching and research institutions in France or abroad, or from public or private research centers.

L'archive ouverte pluridisciplinaire **HAL**, est destinée au dépôt et à la diffusion de documents scientifiques de niveau recherche, publiés ou non, émanant des établissements d'enseignement et de recherche français ou étrangers, des laboratoires publics ou privés.

THÈSE

Pour obtenir le grade de

**DOCTEUR de la Communauté UNIVERSITÉ
GRENOBLE ALPES**

Spécialité : **Océan, Atmosphère, Hydrologie (CEOAH)**

Arrêté ministériel : 25 mai 2016

Présentée par

Catherine Wilcox

Thèse dirigée par **Théo Vischel**
et co-encadrée par **Gérémy Panthou**

préparée au sein **Institut des Géosciences de l'Environnement (IGE)**
dans l'école doctorale **Terre Univers Environnement**

**Evaluating hydrological changes in semi-
arid West Africa:**

**Detection of past trends in extremes and
framework for modeling the future**

Thèse soutenue publiquement le **1 juillet 2019**,
devant le jury composé de :

Sandrine Anquetin

DR CNRS, IGE, Présidente

Florence Habets

Directrice de Recherche CNRS, laboratoire de Géologie de l'ENS , Rapporteuse

Michel Lang

Ingénieur de Recherche, IRSTEA Lyon, Rapporteur

András Bárdossy

Prof. Dr. rer.nat. Dr.-Ing. Institute for Modelling Hydraulic and Environmental
Systems, Dept. of Hydrology and Geohydrology , Examineur

Théo Vischel

Maitre de conférences, Université Grenoble Alpes, Directeur de thèse



Acknowledgements

As most of those I would like to thank are French speakers, most of the following will be in French.

Comme la plupart de mes remerciements sont destinés à des personnes francophones, la partie suivante sera majoritairement rédigée en français.

À tous ceux qui m'ont accueillie lorsque je suis arrivée, un peu perdue, à l'IGE. Notamment, à mes excellents co-bureaux : François qui m'a fait un superbe accueil au labo - je ne le remercierais jamais assez. Avec lui et Carlos j'ai osé rire pour de vrai. Merci beaucoup pour tous ce temps partagé ensemble. Merci aussi à Tania, Louise, Philippe, Basile, ainsi que tous les Phyreviens. Je remercie Galateia et Luciano avec qui j'ai passé de bon moments dans la suite de ma thèse. Je n'oublie pas non plus tous les autres doctorants, stagiaires, post-docs, et chercheurs avec qui j'ai eu le plaisir d'échanger au cours de ces années, notamment Morgane et Léa à la fin de la thèse.

Une mention spéciale aux services administratifs et informatiques : à Carméline qui a tellement lutté pour nous les doctorants dans nos démarches, et aussi à Odette, Valérie, et Wajdi pour votre soutien sans faille. Vous êtes géniaux, l'IGE fonctionne largement grâce à vous.

À Christine et Florence dans l'école doctorale, toujours en soutien.

À Magda, Pati, Gabriela, Claudio, et Mabe, pour les pauses déjeuners/goûters/sportives, les rires et échanges et moments précieux partagés tout au long de ma thèse. Je suis ravie d'avoir trouvé un tel groupe d'amis !

À Jean, qui m'a soutenu avec bien plus qu'un "Coup de Pouce" ! Ton accompagnement était toujours avec l'équilibre parfait entre écoute, encouragement, et rappels à l'ordre (le travail ne sera pas fait si je ne le fais pas). J'ai beaucoup apprécié ces moments avec toi.

Aux membres de mon comité de thèse, mon jury, et mes coauteurs, qui

ont enrichi ce travail de thèse avec leurs commentaires et discussions.

À mes camarades scouts - Manu, Pô, Jû, Anouk, Gab, Annette, Cédric, et tous les Éclaireurs de la Nature avec qui j'ai eu le plaisir de vivre plein de choses. Vous m'avez accompagnée au long de mon voyage scout qui était très souvent en parallèle du voyage de ma thèse. Être cheftaine scout m'a aidée à retrouver la confiance que j'avais au fond de moi-même et à retrouver le moi-même qui était déjà là. À mes enfants scouts, les Voyageuses et Voyageurs de Grenoble, qui m'inspirent et me poussent à m'améliorer en continu et à explorer la magie du monde qui m'entoure.

À mes amis musiciens et danseurs - Yves, Catherine, José Luis, Daniel, Xavier, Elliott, et tous les Bayardiens du mardi soir. Un mot en plus à Catherine qui a souvent écouté mes soucis de thèse ; à Yves pour les conversations et le partage de son amour de la danse ; et à Daniel pour son encouragement avec les uilleann pipes - et jeux de mots aussi!

To my Complice friends, who, though far, perhaps followed my PhD more closely than anyone. Thank you for always encouraging me to "work well" and keep my head on straight. Thanks as well to the creators of all the wonderful "productivity hacks" that kept me going in the right direction, in particular Complice and writtenkitten.

À Théo et Gérémy, qui j'ai eu beaucoup de chance et de plaisir d'avoir comme encadrants. J'ai toujours apprécié votre bonne humeur, positivité, et vos encouragements. Un progrès professionnel ainsi que personnel énorme a été rendu possible grâce à votre soutien et investissement. Vous continuez à m'inspirer comme des modèles à suivre pour la suite. Merci d'avoir cru en moi.

For my family that I love so much and that was often in my thoughts during my PhD.

Et finalement, à Abdul, meilleur de mon monde. Le voyage de la thèse se termine ici, mais il nous reste plein de voyages pour la vie à venir !

Summaries

Abstract

The semi-arid regions of West Africa are known for their dry conditions which have predominated since the 1970s. In recent years, however, West Africa has witnessed a series of severe flooding events which caused widespread fatalities and socioeconomic damages. The emergence of this new problem demonstrates the sensitivity of the region to changes in the hydroclimatic system and calls for an improved characterization of flood hazard and the mechanisms that generate it. It also signals the need to develop projections for how flood hazard may evolve in the future in order to inform appropriate adaptation measures.

In this context, the following PhD thesis seeks to answer three main questions:

1. Is there a significant trend in extreme streamflow in West Africa, or are the documented flooding events isolated incidences?
2. How can one model mesoscale convective systems, the primary driver of runoff in the region, in order to explore the properties of precipitation that drive streamflow?
3. Based on potential climate change in the region, what trends might be observed in streamflow in the future?

First, changes in extreme hydrological events West Africa over the past 60 years are evaluated by applying non-stationary methods based on extreme value theory. Results show a strong increasing trend in extreme hydrological events since the 1970s in the Sahelian Niger River basin and since the 1980s in the Sudano-Guinean catchments in the Senegal River basin. Return levels

calculated from non-stationary models are determined to exceed those calculated from a stationary model with over 95% certainty for shorter return periods (<10 years).

Next, recent developments are presented for a stochastic precipitation simulator (Stochastorm) designed for modeling mesoscale convective storms, the main rainfall source in the Sahel. Developments include a model for storm occurrence, the explicit representation of extreme rainfall values, and an improvement in the modeling of sub-event intensities. Using high-resolution data from the AMMA-CATCH observatory, simulation outputs were confirmed to realistically represent key characteristics of MCSs, showing the simulator's potential for use in impact studies.

Finally, a modeling chain for producing future hydrological projections is developed and implemented in a Sahelian river basin (Dargol, 7000km²). The chain is original as it is the first attempt in West Africa to encompass the continuum of scales from global climate to convective storms, whose properties have major impacts on hydrological response and as a result local flood risk. The modeling chain components include the convection-permitting regional climate model (RCM) CP4-Africa, the only RCM (to date) explicitly resolving convection and providing long-term simulations in Africa; a bias correction approach; the stochastic precipitation generator Stochastorm; and a rainfall-runoff model specifically developed for Sahelian hydrological processes. The modeling chain is evaluated for a control period (1997-2006) then for future projections (ten years at the end of the 21st century). Hydrological projections show that peak annual flow may become 1.5-2 times greater and streamflow volumes may double or triple on average near the end of the 21st century compared to 1997-2006 in response to projected changes in precipitation.

The results raise critical issues notably for hydrological engineering. Current methods used to evaluate flood risk in the region do not take non-stationarity into account, leading to a major risk of underestimating potential floods and undersizing the hydraulic infrastructure designed for protecting against them. It is also suggested to not only consider rainfall changes but also societal and environmental changes, interactions, and feedbacks in order to better attribute past hydrological hazards and their future trajectories to related causes.

Résumé

Malgré des conditions sèches qui prédominent depuis les années 1970, l'Afrique de l'Ouest a subi au cours des deux dernières décennies des épisodes d'inondations sévères qui ont provoqué de nombreux décès et dommages socio-économiques. L'émergence de ce nouveau problème montre une nouvelle facette de la sensibilité de cette région aux changements hydro-climatiques, appelant à une meilleure caractérisation de l'aléa inondation, des processus qui le génèrent, ainsi que la mise en place de méthodes permettant de projeter les évolutions futures de cet aléa pour mieux s'en prémunir.

Dans ce contexte, la thèse cherche à répondre à trois questions principales :

1. L'augmentation des dommages liés aux inondations s'est-elle accompagnée d'une intensification des crues extrêmes en Afrique de l'Ouest?
2. Comment modéliser les orages de mousson, premier facteur de génération du ruissellement, afin d'explorer l'impact de leurs caractéristiques sur les crues?
3. Compte tenu des changements climatiques à l'œuvre dans la région, à quelles tendances hydro-climatiques peut-on s'attendre dans le futur ?

Dans un premier temps, on évalue l'évolution des crues en Afrique de l'Ouest au cours des soixante dernières années en utilisant de méthodes basées sur la théorie de valeurs extrêmes. Les résultats montrent une augmentation forte des événements hydrologiques extrêmes depuis les années 1970s dans les sous-bassins Sahéliens du fleuve Niger et depuis les années 1980s dans les sous-bassins soudano-guinéens du fleuve Sénégal. Les niveaux de retour calculés à partir des modèles non-stationnaires dépassent ceux qui ont été calculés avec un modèle stationnaire avec plus de 95% de certitude pour les périodes de retour les plus courtes (<10 ans).

On présente ensuite des développements récents apportés à un simulateur stochastique d'orages de mousson à meso-échelle (StochaStorm). Ils incluent: une modélisation de l'occurrence de ces orages, la représentation explicite des valeurs de pluie extrêmes et une amélioration du schéma temporel d'intensité infra-événementielle. Implémenté et évalué à partir des données haute-résolution de l'observatoire AMMA-CATCH, le générateur montre de très bonnes capacités à reproduire les propriétés des orages, confirmant son potentiel pour des études d'impact hydrologique.

Enfin, une chaîne de modélisation est élaborée afin de proposer des projections hydrologiques pour le futur sur un bassin sahélien de meso-échelle (Dargol, 7000 km²). L'originalité de cette chaîne provient de la prise en compte du continuum d'échelles entre climat global et impact local à travers la représentation du régime des pluies à l'échelle des orages de mousson, dont les propriétés d'occurrence et d'intensité ont des impacts majeurs sur la réponse hydrologique. La chaîne de modélisation inclut le modèle climatique CP4-Africa, unique modèle à convection explicite fournissant des simulations de long terme en Afrique ; une méthode de débiaisage statistique; le simulateur Stochastorm ; et un modèle pluie-débit spécifiquement adapté aux processus hydrologiques sahéliens. La chaîne est évaluée sur une période de contrôle 1997-2006 puis utilisée pour des projections futures montrant une hausse par un facteur 1,5-2 des débits maximum annuels et un doublement (voire triplement) des volumes moyens annuels à l'horizon 2100.

Les résultats ont des implications majeures notamment pour l'ingénierie hydrologique. Les méthodes actuellement utilisées pour appréhender les risques hydrologiques dans la région ne prennent pas en compte la non-stationnarité hydro-climatique risquant de sous-évaluer l'aléa hydrologique et sous-dimensionner les ouvrages hydrauliques utilisés pour s'en protéger. La thèse suggère aussi quelques pistes afin mieux définir les trajectoires hydrologiques passées et futures en incluant, au-delà des précipitations, les changements sociétaux et environnementaux, leurs interactions et rétroactions dans les approches de modélisation.

Contents

1	Introduction	13
1.1	Rivers in a changing world	13
1.1.1	Changes in the global water cycle	13
1.1.2	Changes due to local societies	14
1.1.3	Floods of the present and future	14
1.2	Changing hydrology in West Africa	15
1.2.1	Climatological context	15
1.2.2	Hydrological context	17
1.2.3	Climate evolution	17
1.2.4	Observed changes in West African hydrology	19
1.2.5	Potential causes of recent hydrological changes in the Sahel	19
1.2.6	Changing societal context	20
1.3	Increased extreme streamflow in West Africa: critical questions	20
1.4	Methodological framework	23
1.4.1	Methodology for hydrological extremes trend detection: Extreme Value Theory in a nonstationary context	23
1.4.2	Methodology for flood drivers modeling: Precipitation as a main driver of Sahelian hydrological extremes . . .	24
1.4.3	Methodology for hydrological projection: Modeling chain from global climate model to river basin outlet .	26
1.5	Study areas	28
1.5.1	Study area for trends in extreme streamflow in West Africa	28
1.5.2	Study area for high-resolution precipitation modeling .	29
1.5.3	Study area for modeling chain for hydrological projections	29

1.6	Summary of thesis objectives	29
1.7	Thesis outline	30
2	Trend detection of hydrological extremes in West Africa	31
2.1	Introduction to article 1	31
2.1.1	Personal contributions	32
2.2	Article: Trends in hydrological extremes in the Senegal and Niger Rivers	34
2.3	Introduction	34
2.4	Region of study and data	39
2.4.1	West African hydro-climatic features	39
2.4.2	Study catchments and datasets	40
2.5	Theoretical framework and methodology	44
2.5.1	Selection of extreme discharge values	45
2.5.2	Formulation of statistical models	46
2.5.3	Model fitting	50
2.5.4	Selection of the best GEV model	50
2.5.5	Return level evaluation	51
2.5.6	Uncertainty assessment	52
2.6	Results	53
2.6.1	Selected GEV model	53
2.6.2	Extreme discharge tails behavior	55
2.6.3	Return level estimates of selected models	56
2.6.4	Scale effects of drainage area	60
2.7	Discussion	61
2.7.1	Comparison of results with literature	61
2.7.2	Evaluation of the parameter ξ	62
2.7.3	Sensitivity analyses: robustness of the results	63
2.8	Conclusions and implications	65
3	Precipitation modeling and scenario generation	70
3.1	Introduction to article 2	70
3.1.1	Personal contributions	71
3.2	Stochastorm: A stochastic rainfall simulator for the intertropical zone	73
3.3	Introduction	74
3.4	Stochastorm presentation	77

3.4.1	Description of the previous version of the stochastic rainfall model	77
3.5	New developments and technical definitions	79
3.5.1	Season limits and intra-seasonal variability of parameters	79
3.5.2	Event occurrence	80
3.5.3	Marginal distribution of cumulative event rainfall . . .	81
3.5.4	Spatial dependency: Gaussian fields with censored likelihood	82
3.5.5	Temporal disaggregation	84
3.5.6	Overview of calibration	85
3.5.7	Simulation procedure	85
3.6	Application to Sahelian storms	86
3.6.1	Sahelian hydroclimatology	86
3.6.2	Model implementation	88
3.7	Evaluation of the model using AMMA-CATCH data (Sahel) .	95
3.7.1	Event occurrence	95
3.7.2	Event-based rain fields	97
3.7.3	Temporal disaggregation	101
3.8	Conclusion	103
4	Modeling chain for using a convection-permitting regional climate model to drive hydrological projections	108
4.1	Introduction to article 3	108
4.1.1	Personal contributions	109
4.2	Article: An original statistico-dynamical modeling chain for hydrological projections under future changes in convective rainfall	110
4.3	Introduction	111
4.4	Region and data	115
4.4.1	Study site: AMMA-CATCH network	115
4.4.2	Convection-permitting regional climate model: CP4-Africa	117
4.4.3	Hydrological study site and data	118
4.5	CP4 rainfall: preliminary evaluation	118
4.5.1	CP4 versus AMMA-CATCH	119
4.5.2	CP4 present versus CP4 future projections	121
4.6	Methodology	122
4.6.1	Bias correction methods	122

4.6.2	Stochastic precipitation model	124
4.6.3	Hydrological model description: Phorm	125
4.7	Results and discussion	126
4.7.1	Bias correction results	126
4.7.2	Hydrological modeling results	130
4.8	Conclusions and perspectives	134
4.8.1	Methodological advances	134
4.8.2	Limitations and future work	134
5	Conclusions and future research directions	136
5.1	Summary and implications of thesis work	136
5.2	Future research directions	143
5.2.1	NSGEV models for trends in hydrological extremes	143
5.2.2	Stochastic precipitation generator	144
5.2.3	Limits of applicability of bias-corrected CP4	146
5.3	Attribution of trends in hydrological extremes	146
5.3.1	Background for attribution in climatology	147
5.3.2	Methods for attribution	148
5.3.3	Attribution of changes in hydrological extremes	150
5.3.4	Precipitation or land cover? Natural or human-induced?	151
5.3.5	Land use scenarios	154
5.3.6	Flood risk and societal dynamics	155
5.3.7	Practical next steps for attribution framework	155
	Appendices	157
A	Supplementary information for article 1	158
A.1	Available data	158
A.2	Hydrological data evaluation, selection and cleaning	160
A.3	Hydroclimatological data sensitivity testing	162
A.3.1	Testing GEV parameters	165
A.3.2	The case of the Koriziena station	166
A.4	Specific discharge evolution	167
B	Supplementary information for article 2	170
B.1	Exploratory precipitation analysis	170
B.2	Seasonal cycle	171
B.2.1	Fitting a distribution to IET	173

B.3	Interannual non-stationarity	180
B.4	Conclusions	187

Chapter 1

Introduction

1.1 Rivers in a changing world

The amount of water flowing on the surface of the earth is an issue of concern for multiple reasons. The right amount sustains human life. Too little limits the capacity of agricultural production and drinking water. At other times, an excess of water produces floods that endanger human life and infrastructure.

The quantity and distribution of water in rivers is constantly evolving. It is changed by influences ranging from large-scale global planetary change to small-scale local changes.

1.1.1 Changes in the global water cycle

The water flowing in rivers or otherwise on the surface of the earth is just a small component of the interconnected water cycle. Precipitation is the primary generator of surface runoff. The processes of infiltration, evapotranspiration, and subsurface flow also determine the amount of water that flows on the surface and in rivers. On a larger scale, flood-generating processes are linked to global components of the water cycle such as atmospheric moisture and climate dynamics. The status of the water within this cycle is not static, but constantly transforming from one component of the cycle to another. The components of the water cycle are linked to each other, and when one is modified, others are modified too.

The processes governing the interconnected global water system are susceptible to change as well. One of the driving forces that can modify the water

cycle is global temperature. Natural and anthropic factors have had documented influence on global planetary temperatures, leading to an increase of approximately 1°C since the beginning of the industrial period (Intergovernmental Panel on Climate Change, 2018; Millar et al., 2017). This in turn modifies atmospheric water content and evapotranspiration, and changes the dynamics of the climate and the resulting precipitation. The result is a modification of the quantity in space and time of water distributed via surface hydrological processes (Hirabayashi et al., 2013; Trenberth, 1999). Global temperature increase and the resulting climatic non-stationarity are projected to continue over the course of the 21st century (Millar et al., 2017; Rogelj et al., 2016; Steffen et al., 2018). However, the amplitude of the increase and its impacts on eco-hydrological systems are uncertain, as well as the reversibility of the impacts (Steffen et al., 2018; Blöschl and Montanari, 2010).

1.1.2 Changes due to local societies

Anthropogenic climate change is not the only process that can alter surface hydrology. Human activities also have an impact at a more local scale. Land use changes, notably urbanization and agricultural expansion, change the surface cover by altering the presence of vegetation and the infiltration capacity of the soil. These modifications change the resulting amount and flow rate of water over the surface after a precipitation event.

Human societies also build infrastructures such as dams which alter river flow, whether for water storage for supply and demand management, irrigation, flood risk reduction, or hydroelectricity. Population is projected to continue to increase¹, which could mean increased development and increased modifications to surface hydrology. Increases in population lead to not only increased modifications to land surfaces, but also may lead to increased flood damage risk. The more people living in a flood zone, the more people at risk of being harmed.

1.1.3 Floods of the present and future

Floods are one of the most damaging natural disasters on the planet. They lead to large losses in life, as well as economic losses and material damage

¹<https://population.un.org/wpp/Graphs/Probabilistic/POP/TOT/>

(Miao, 2018). Approximately 6.8 million flood-related fatalities occurred during the 20th century, with over 500,000 between 1980-2009 (Doocy et al., 2013). Floods also cause billions of US dollars in economic and material losses annually worldwide (Hallegatte et al., 2013). These figures show the need for preventative measures in order to minimize flood-related damages.

Floods are generated by a variety of factors depending on local conditions. Changes in those factors could either increase or decrease river discharge (Arnell and Gosling, 2016). The resulting combined influence of these factors is little understood and little quantified, especially at smaller local scales. Understanding the mechanisms driving floods and having hydrological projections of how they might change improves the ability to adopt appropriate adaptation measures.

The focus of this work is on understanding past and future evolution of hydrological processes within West African, with a focus on the Sahelian region. West Africa is chosen as it features a nexus of strong climate signals, an increase in recent flood damages, and a rapidly changing societal context. All of these changes occur in a sensitive environment that reacts quickly to change, both environmental and socio-economical. The following sections present the hydroclimatic context of the PhD work (Section 1.2), followed by the key questions identified (Section 1.3), the methodology used to answer these questions (Section 1.4) and the specific study region used (Section 1.5).

1.2 Changing hydrology in West Africa

1.2.1 Climatological context

West Africa has two primary seasons per year: the wet season (Boreal summer) and the dry season (Boreal winter). These seasons are driven by the dynamics of the West African monsoon and the annual movements of the intertropical convergence zone (ITCZ) (Nicholson, 2013a), an area at latitudes near the equator where trade winds coming from the northeast and southeast converge. The ITCZ moves northward or southward seasonally, influencing regional climate. West African climate is also linked to large-scale climate oscillations (such as ENSO) and sea surface temperatures (SST) (Giannini et al., 2013; Sheen et al., 2017; Camberlin et al., 2001; Janicot et al., 2001), although the relationship is complex and appears to vary over time.

During the early months of the rainy season, moisture from the Atlantic

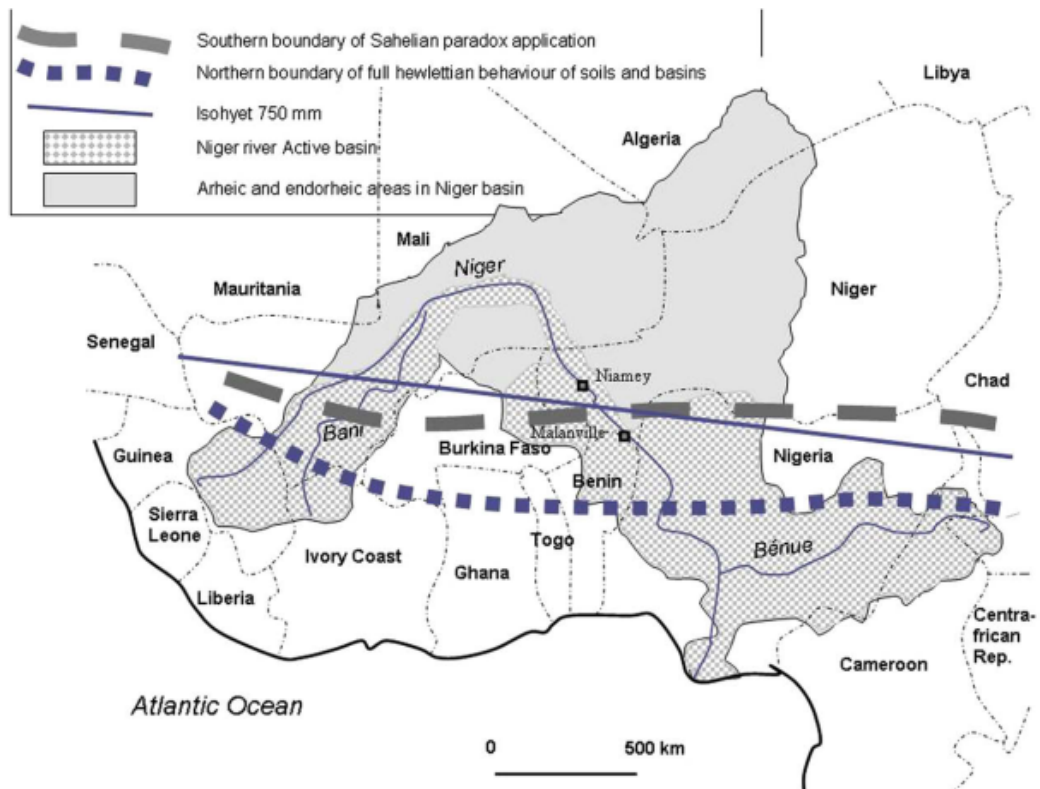


Figure 1.1: Hydrological and climatological boundaries between Sahelian and Sudano-Guinean phenomena. From Descroix et al. (2009).

Ocean/Gulf of Guinea is brought increasingly inland over the continent. The moisture meets with the heat of the continent, where convection occurs. The combination of heat and moisture leads to the formation of large storm complexes known as mesoscale convective systems (MCSs). The winds from the African Easterly Jet push the MCSs in a general westward direction after their formation. The magnitude and frequency of MCSs are greatest during the core of the rainy season in July through September. MCSs are the primary source of precipitation in the region (Mathon et al., 2002).

Subsaharan West Africa can be divided into two subregions that feature different hydroclimatic processes: the Sahelian zone and the Sudano-Guinean zone (Figure 1.1). The Sahel is located just south of the Sahara desert. It is often defined as being between the isohyetal lines of 250mm and 750mm of

precipitation per year, with a north-south precipitation gradient decreasing in higher latitudes (Descroix et al., 2009). It is considered to be a semiarid region as the potential evaporation due to high temperatures exceeds the quantity of annual precipitation. Precipitation increases further south into the Sudano-Guinean zone.

1.2.2 Hydrological context

The two subregions of West Africa have differing land surface properties that govern what happens to the precipitation once it hits the ground. The Sahel features sparse vegetation and crusted soils. Hydrological processes in the Sahel are characterized by Hortonian runoff, in which water infiltrates until the infiltration capacity is reached (Horton, 1933). The remainder of the precipitation runs off the land surface (Peugeot et al., 1997, 2003). Subsurface flow plays a minor or non-existent role in river discharge generation. Due to the characteristics of runoff generation in the Sahel, the factors of infiltration rate and precipitation intensity play a particularly large role in influencing runoff and river discharge.

In the Sudano-Guinean zone, however, there is more vegetation, notably with a relative abundance of trees and dense forests. Subsurface flow plays a dominant role in generating and sustaining river discharge.

West African hydrology also has marked seasonality, driven by the seasonal patterns of precipitation. Smaller river basins feature a high level of intermittency, and become dry for much of the year due to the long dry season. Large river basins are sustained year-round by the variety of hydrological processes found within their contributing watersheds; for example, the Niger River receives both direct and rapid inputs from runoff in the Sahelian zone during the rainy season, and delayed inputs from its sources in the Fouta Djallon ("water tower of Africa") area which receives 1000-1500mm of precipitation annually (Panthou et al., 2018). It also is fed by delayed underground flow from the wetter Guinean zone.

1.2.3 Climate evolution

West Africa has exhibited one of the most marked climate signals in recorded memory (Figure 1.2). The 1950s and 1960s witnessed annual precipitation levels that exceeded the documented norms. This trend was not to last: the wetter period was followed by an exceptionally severe and lasting drought

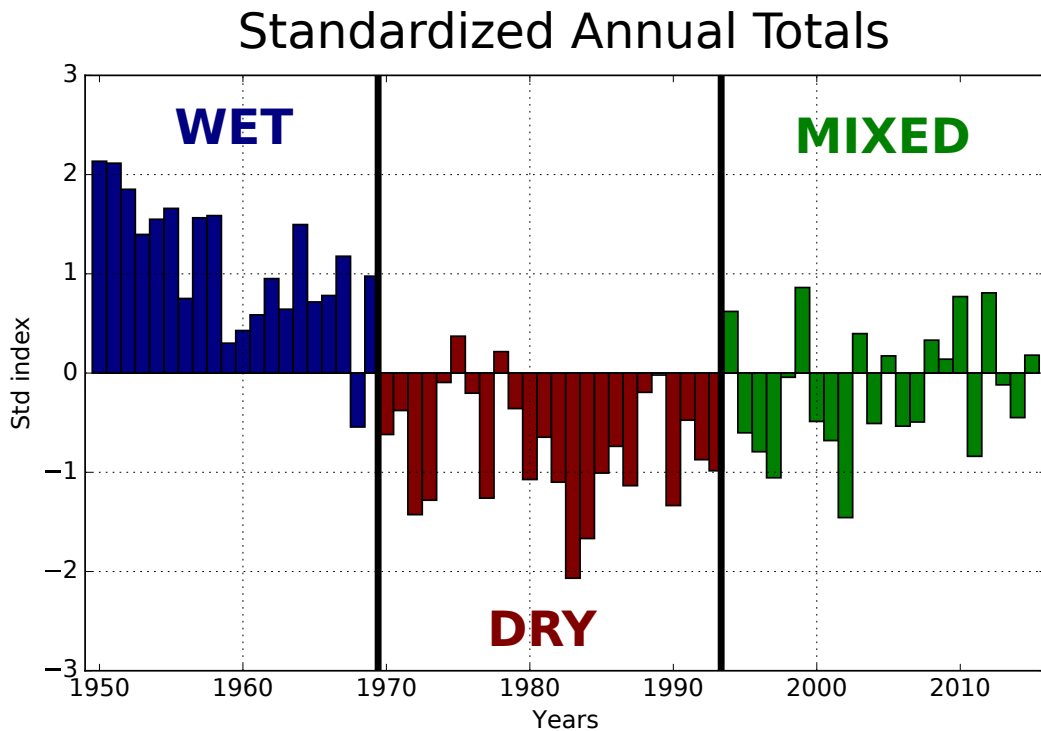


Figure 1.2: Standardized annual precipitation index calculated from 71 stations in the Sahel during the period 1950-2015. Updated from Panthou et al. (2018).

during the 1970s and 1980s that led to extensive fatalities and population displacements (Lamb, 1983; Le Barbé and Lebel, 1997; Nicholson, 2000; Camberlin et al., 2002; Le Barbé et al., 2002; L'Hote et al., 2002; Dai et al., 2004; Panthou et al., 2014; Bodian et al., 2011, 2016b).

In recent years, the signal has become more mixed. On average, the cumulative annual precipitation is greater than during the severe drought period, but still less than pre-drought levels (Lebel and Ali, 2009; Mahé and Paturel, 2009; Panthou et al., 2014; Tarhule et al., 2015; Diop et al., 2017). Notably, the contribution of extreme rainfall to annual totals is increasing (Panthou et al., 2014; Taylor et al., 2017). There is also evidence of persisting drought conditions (L'Hote et al., 2002; Ozer et al., 2009). Panthou et al. (2018) found that during the last three decades, there were not more rainfall events than during the great drought. However, the rainfall events were more intense when they occurred. This led Panthou et al. (2018) to define the last three decades as a period of hydroclimatic intensification as defined by Giorgi

et al. (2011), Trenberth et al. (2003), and Trenberth (2011).

1.2.4 Observed changes in West African hydrology

West African rivers have shown drastically different phases over the past century, linked to the decadal variability of rainfall regimes. However, the hydrological regime evolution differs within subregions of West Africa because of contrasts in hydrological processes and their relative sensitivity to rainfall variabilities.

In the decades prior to the 1970s, discharge levels in West African rivers were high. Droughts of the 1970s and 1980s featured decreased river levels throughout West Africa, but, paradoxically, an increase in some Sahelian rivers. Many studies have attributed the increase in streamflow to the crusting of soils at the surface and reduction in vegetation in response to the drought (Albergel, 1987; Descroix et al., 2009; Aich et al., 2015; Cassé et al., 2016; Gal et al., 2017; Boulain et al., 2009). This decreased infiltration capacity and increased the amount of runoff, in spite of the overall reduction in precipitation.

Over the past few decades, peak streamflow volumes appears to have increased. For instance, the Niger River has witnessed the new phenomenon of extremely large annual flood peaks. Although cumulative annual streamflow has not exceeded levels recorded during the 1950s and 1960s, the region has been struck by floods of unprecedented magnitude and frequency (Tarhule, 2005; Tschakert et al., 2010; Samimi et al., 2012; Sighomnou et al., 2013). Several flooding events have been particularly devastating, notably those of 2007, 2009, 2012, and 2013.

1.2.5 Potential causes of recent hydrological changes in the Sahel

As hydrology in the Sahel is highly sensitive to precipitation characteristics, the recent evolution of streamflow in the Sahel could be explained by changes in locally-generated precipitation. Notably, extreme rainfall events have increased in recent years, as have their overall contribution to annual cumulative precipitation (Panthou et al., 2014, 2018). Some recent studies have concluded that hydrological changes largely follow recent changes in precipitation (Cassé et al., 2016).

Changes in local climate are, however, not the only factor. Studies on Sahelian hydrology during the drought period have already shown the potential impact of changes in land surface properties, whether induced by local human impacts or by climate change itself (e.g. reduction in vegetation due to reduction in precipitation) (Seguis et al., 2004; Li et al., 2007; Leblanc et al., 2008; Gal et al., 2017).

1.2.6 Changing societal context

The aforementioned floods are occurring in a rapidly changing socioeconomic context. West Africa is currently undergoing rapid demographic change and development. Population is increasing by 3% per year (global average is 1.2%); by 2025, half of the projected population is expected to live in cities (UNEP, 2011). With greater population and demographic pressure comes greater risk of flood damages (Di Baldassarre et al., 2010). The recent events have already led to an increase in documented flood-related fatalities in West Africa, as shown in Figure 1.3.

Pertinent human-induced factors that may increase flood hazard include increased urbanization with proximity to flood dangers (Barrios et al., 2006), agricultural expansion and intensification, changing cultural land use practices, and vegetation depletion from migrating herds. Determining the causes of the floods would allow for the development of improved flood management and prevention strategies.

1.3 Increased extreme streamflow in West Africa: critical questions

The above context leaves us with numerous scientific questions. Although there is evidence of more floods recently in West Africa, there is little literature that specifically analyses changes in hydrological extremes in the region. The processes driving these extreme events have also not been extensively evaluated in the context of the water cycle in West Africa. It is even more uncertain how flood drivers and (as a result) hydrological extremes may continue to evolve in the future.

The issue of hydrological extremes is particularly important for the Sahel and similarly arid lands because water resources are sufficiently sparse that

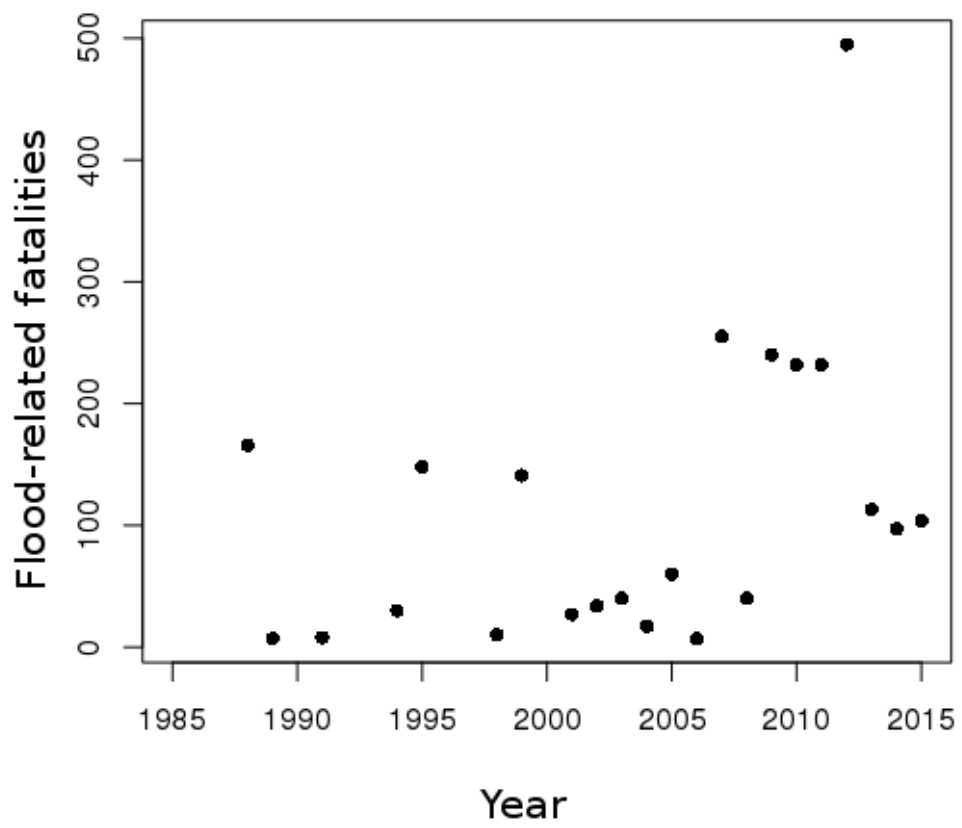


Figure 1.3: Flood-related fatalities in West Africa (Guha-Sapir et al., 2016).

changes in their frequency or distribution has higher importance. There is little long-term water storage in the region, and much local agriculture depends directly on local precipitation. With rapid development and changing demographics, the risk of damages from both floods and drought is increasing. Of particular note is the sharp increase in documented flood fatalities in West Africa (Figure 1.3).

The recent flooding events, coupled with a socioeconomic context that necessitates an understanding of the events, lead us to the following key questions that form the basis of this thesis:

Q1: Is there a significant trend in extreme streamflow in West Africa, or are the documented flooding events isolated incidences?

Q2: How can one model mesoscale convective systems in order to explore the properties of precipitation that drive streamflow?

Q3: Based on potential precipitation changes, what trends might we see in streamflow in the future?

The following sections examine the components and influencing factors related to the above three questions. They first present the methodology tools identified for answering the three questions in a robust manner, followed by the specific study areas on which this thesis is focusing. First, non-stationary extreme value theory is presented in the context of hydrological applications. Second, stochastic precipitation modeling methods are described. Third, we overview the components relevant for modeling future changes in streamflow. For each part of the study, the level of uncertainty of results is explored.

1.4 Methodological framework

1.4.1 Methodology for hydrological extremes trend detection: Extreme Value Theory in a nonstationary context

Using statistical representations of natural phenomena allows for accurately describing pertinent characteristics, including the frequency and distribution of values. They can be used to take into account a variety of processes across different scales and extract the resulting signals that emerge.

In the standard version of a statistical distribution, parameters have one fixed value (stationary distribution). However, a time-dependent component can be added to the parameter to make it non-stationary over time. The coefficient(s) of the time-dependent component(s) can give insight into the trends over time.

The advantage of using a statistical distribution to represent data is that one can then make an estimation of the probability of an event of a given magnitude occurring (François et al., 2019 and references therein). In the context of hydrology, this principle is represented by the notion of a return period. An event that has a return period of 10 years means that during any given year, the event has a probability of 1/10 or 10% of occurring. The magnitude of the event that has a 10-year return period is referred to as the 10-year return level. It is possible for the said event to occur more than once within 10 years, as there is a 10% chance of it occurring during any given year. Return levels are commonly used for the design of structures for flood protection and hydroelectricity.

Many statistical distributions exist that have differing properties. However, many are designed to be fit primarily based on the average or central tendency values of a given data set. Although central values may be well-represented by such distributions, very small or very large values - often simply considered outliers - are not. The "tail behavior" of a given distribution (how it treats very small and/or very large values) may not be representative of the actual extremes in the data set. This can be problematic when one wants to specifically evaluate the behavior of extremes.

Extreme Value Theory proposes statistical distributions designed specifically to handle rare values. They include parameters for the general behavior (e.g. central tendency and spread) of extreme values, as well as a parame-

ter that governs specifically the tail behavior, or how the rarest of the rare values relate to the rest of the distribution. As with other distributions, a time-dependent component can be added to a given parameter in order to evaluate potential non-stationarity.

The two main distributions used in the present thesis are the Generalized Extreme Value (GEV) distribution and Peaks Over Threshold (POT) distribution (see e.g. Coles et al., 2001). The GEV represents the distribution of a subset of the original data formed by extracting the maximum value of each interval of a set length. In the context of hydrology, this is commonly the annual flood peak. The POT distribution is used to represent a subset of values above a defined threshold. This can be used for representing extreme precipitation. The distributions within the context of Extreme Value Theory are used in the present PhD thesis in order to evaluate extreme hydroclimatological events and their evolution.

Chapter 2 presents the methodology and results for how GEV distributions with non-stationary parameters are used to model changes in hydrological extremes in the West African Sahel.

1.4.2 Methodology for flood drivers modeling: Precipitation as a main driver of Sahelian hydrological extremes

When modeling natural systems, one would ideally be able to explicitly represent all relevant processes and their interactions. However, due a combination of the complexity of the processes, the feasibility to model them (and their interactions) mathematically, the lack of current understanding of said processes, and limitations in computing power, it is not possible to precisely and accurately model all processes at all scales in a fully deterministic/mechanistic way.

The limitations of deterministic modeling are especially true when studying complex phenomena such as precipitation and the processes it generates. Modeling becomes increasingly more uncertain over time as slight differences in initial states can lead to greatly different outputs Lorenz (1963). The uncertainty of deterministic models is regularly confirmed by new and more complex atmospheric models and simulations (see e.g. McWilliams, 2019; Judt, 2018).

Stochastic models provide a solution for producing realistic replications

of natural processes. The stochastic modeling approach is particularly useful for precipitation and the resulting processes it generates as there is a strong random element.

In the previous section, approaches were described for stochastically modeling the value of a variable at one point. However, there are instances where modeling both the distribution of values at a single point and the distribution of those values in space is important. This is the case with precipitation, where values at one point are related to values at another point. As precipitation is considered one of the main drivers of hydrological processes in the Sahel, the second part of the PhD thesis focuses on how to accurately represent precipitation for use in impact studies.

The field of geostatistics has developed methods for stochastically model a variable such as precipitation in space. Two main elements are required: the marginal distribution of the variable (e.g. the statistical distribution that represents the magnitudes of all values), and the spatial covariance structure. The spatial covariance structure (commonly the variogram) represents the relationship between values at two different points - if they are likely to be both large or both small - and how much the correlation decreases with distance. This type of structure is relevant to precipitation modeling as precipitation at one point is generally correlated with precipitation at a nearby point.

Methods have been developed to generate fields in two-dimensional space based on Gaussian marginal distributions and a known covariance structure. These are known as Gaussian random fields. Precipitation, however, is generally not well-represented by a Gaussian (normal) distribution. For one, rain fields commonly have areas of no rainfall interspersed with areas where it is actively raining. Gaussian fields do not account for this accumulation of zero values. For another, the positive values of precipitation generally do not follow a symmetric normal distribution, but rather have an abundance of small values with some extremes.

In order to transform the Gaussian random field into a random field with a non-Gaussian distribution, a process called anamorphosis is applied. The magnitudes of the values in the Gaussian field are transformed from the normal distribution to the selected marginal distribution for the precipitation.

The above elements can be integrated into a stochastic precipitation model or stochastic precipitation generator. A stochastic precipitation model aims to simulate precipitation in a way where the statistical properties of the original precipitation data used to calibrate the model are maintained. This allows for several advantageous possibilities: the generation of precipitation

scenarios that are much longer than the original data series; the production of realistic rain scenarios at points where no measurements have been recorded; the exploration of variability; and the testing of parameters to see which variable is most significant for impact studies.

The parameters of the marginal distribution can also be given temporal covariates so that they can vary over the course of the season, or over different years.

Chapter 3 presents the study on how an existing stochastic precipitation generator has been improved, implemented, and evaluated to model storm precipitation in the West African Sahel.

1.4.3 Methodology for hydrological projection: Modeling chain from global climate model to river basin outlet

Understanding how hydrological extremes have changed in the past brings additional questions. How might hydrological extremes change in the future? More specifically, how might hydrological extremes change in response to changes in drivers such as precipitation?

Climate change has been studied extensively over the past several decades. Some elements, such as global temperature, are well-researched. There is general consensus that global temperature is currently increasing (Intergovernmental Panel on Climate Change, 2018; Rogelj et al., 2016) and will continue to increase over the next century, but with a magnitude that varies depending to the trajectory of GHG emissions. This has a ripple effect on other earth processes. One notable potential impact for the water cycle is the Clausius-Clapeyron relation, which states that the water holding capacity of the atmosphere increases with increasing temperature. This would allow for an increase in atmospheric moisture over time. Theoretically, the increase in atmospheric water holding capacity means that there could be less frequent precipitation events, but when they happen they are greater in magnitude (Trenberth et al., 2003; Trenberth, 2011). This is known as an intensification of the water cycle. Other changes in precipitation properties are possible, including changes in the spatial structure of storms, the frequency of precipitation events, and the distribution of precipitation over the Earth.

Climate change is studied using global climate models (GCMs). GCMs are a set of multidimensional equations representing Earth system processes.

The GCM is divided up into horizontal grids across the earth surface, and vertical layers as well. Each grid has associated parameters and ways in which they interact with the grids around them, based on known dynamic and thermodynamic properties of the atmosphere. In this way, the effects on climate (temperature, precipitation, etc) of changing certain factors such as atmospheric composition (i.e. from greenhouse gas emissions) are studied.

Due to computational limitations, the grid sizes of climate models are much larger than the scale needed to study hydrological impacts. Many processes are not explicitly represented in a dynamic, deterministic way, but are parameterized in the GCM. To resolve this problem, regional climate models (RCMs) are developed. They model only one part of the Earth's surface, and are commonly initiated and forced by a GCM simulation. Grid sizes for RCMs is generally much smaller than those of GCMs, and can approach scales that can be used for hydrological impact studies.

Up until recent times, however, most all climate models (even smaller-scale regional ones) do not model convective processes. As nearly all rainfall in the West African Sahel is generated by convective storms, inaccurate representation of convection leads to inaccurate representation of rainfall properties, even if the scale is appropriately small (Jenkins et al., 2002). One notable advance for Africa is the RCM CP4-Africa (Stratton et al., 2018), which resolves convection at a small enough grid scale for representing mesoscale convective systems.

An additional problem due to the heavy calculation costs of GCMs/RCMs is the fact that limited scenarios are produced. A stochastic rainfall generator such as that described in the previous section may be used to generate additional scenarios with lower calculation demands. After the above issues are all sufficiently addressed, the question remains of how precipitation changes may impact local hydrology. To answer the question of hydrological impacts, one may use a hydrological model. Hydrological modeling, as with climate modeling, aims to represent the most important processes depending on the problem being addressed. For this present thesis, the main question is how the discharge at the outlet of a river basin is changing. The type of model selected for the study is a distributed physically-based model of a Sahelian river basin (Quantin et al., 2017). This type of model has subbasins that each have specific parameters governing infiltration and runoff amounts according to the Hortonian flow commonly found in the Sahel. Precipitation fields are input into the model at the subbasins, and the model transforms it into the amount of discharge at the outlet.

Chapter 4 presents a modeling chain combining convection-permitting precipitation projections from the RCM CP4; a stochastic rainfall simulator to generate additional precipitation scenarios; and a hydrological model designed specifically for the Sahelian region. It shows how the modeling chain can be used to better understand the potential impacts of future climate change on local hydrology.

1.5 Study areas

1.5.1 Study area for trends in extreme streamflow in West Africa

To understand the trends in extreme streamflow over the contrasting sub-regions of West Africa, river discharge time series are evaluated for several stations in the Sahelian part of the Niger River basin and several stations in the Sudano-Guinean part of the Senegal River basin.

The Niger River has its headwaters in the Fouta Djallon area located in the Sudano-Guinean zone south of the Sahel, which features higher amounts of precipitation. The river passes through the inner Niger Delta before reaching the Sahelian zone of Southwest Niger.

Within the Sahelian area of the Niger River are three tributaries located on the right bank: the Sirba, the Dargol, and the Gorouol. Although the Niger River is perennial due to its sources located in a greener part of Africa, the Sahelian tributaries are ephemeral and only flow under the presence of precipitation during the rainy season. Their discharge quantities are highly susceptible to changes in precipitation.

The resulting flow of the Niger River after the confluence with its Sahelian tributaries is greatly impacted by local precipitation, notably at the Nigerien capital of Niamey. The Niger River at Niamey therefore has two flood peaks: an initial flood peak during the core of the rainy season in August/September (termed the "Red Flood" due to the presence of reddish sediments from local Sahelian runoff), and a second flood peak a few months later once the rainy season contributions from the upstream Guinean zone arrive at Niamey ("Guinean flood"). Although historically the Guinean flood peak levels at Niamey were greater than the levels produced by the local Sahelian floods, in recent years the Sahelian flood peaks exceed the Guinean flood peaks (Descroix et al., 2012).

Trends are also evaluated for the largely Sudano-Guinean subbasins of the Senegal River. The Senegal River also has its headwaters in Fouta Djallon. Unlike the Niger River, most of the contributing parts of the Senegal River are located south of the Sahel with higher rates of precipitation. The Senegal River outlets into the Atlantic Ocean.

For the first part of the thesis, four Sahelian data sets for the Niger River and seven Sudano-Guinean data sets for the Senegal River are evaluated.

1.5.2 Study area for high-resolution precipitation modeling

The second part of the thesis focuses more specifically on the Sahelian area of the Niger River. The data set used to develop the stochastic rainfall simulator is the set of 30 five-minute rain gauges from the AMMA-CATCH data collection site near Niamey, Niger. The rain gauges cover an appropriate area for studying the spatial structure of MCSs. At five minutes, the data set allows for the evaluation of MCSs at sub-event time scales. Data is available since 1990.

1.5.3 Study area for modeling chain for hydrological projections

The third part of the thesis uses the Dargol River basin as a test area for implementing a modeling chain for generating hydrological projections. Like the other Sahelian tributaries of the Niger River, the Dargol is ephemeral and only flows during the rainy season due to local precipitation inputs. The Dargol River has a drainage area of approximately 7600 km², which makes it a suitable size for use of Stochastorm outputs based on the mesoscale AMMA-CATCH Niger data. It is located sufficiently near to the AMMA-CATCH rain gauges to have a comparable (although not identical) climate.

1.6 Summary of thesis objectives

The present thesis seeks to explore the interface between surface hydrology and its influencing factors. It aims to better understand how hydrological changes - in particular floods - are related to changes in the larger global water

cycle, and also better understand how floods can affect and are affected by human societies.

The following three chapters answer the three main questions of this PhD thesis. First, extreme value theory is used to evaluate trends in hydrological extremes in the West African Sahel. Second, precipitation characteristics in the Sahel are analyzed and modeled with a stochastic precipitation generator. Finally, the potential future changes in Sahelian hydrology are evaluated for a mesoscale test river basin using a modeling chain that incorporates a convection-permitting RCM, the stochastic precipitation generator previously evaluated, and a hydrological model.

Although West Africa (and particularly the right bank Sahelian tributaries of the Niger river upstream of Niamey) is used as a test region, the following analysis has the broader goal of developing a methodology that can be applied more widely in the field of hydrology.

1.7 Thesis outline

The main results of the thesis are presented in the following three chapters. Chapter 2 presents the regional study of trends in extreme streamflow in West Africa. Primary results have already been published in *Journal of Hydrology*. Chapter 3 contains the study on the stochastic precipitation simulator *Stochastorm*. Chapter 4 presents the modeling chain developed for hydrological projections in the Sahel. The results in chapters 3 and 4 will be submitted for publication shortly, one article for each chapter.

The three articles were developed in collaboration with other researchers, both within my research group and as a part of international collaborations. My specific contributions are detailed at the beginning of each chapter.

Chapter 5 presents conclusions based on the findings in chapters 2-4. It also presents future work identified for the continuation of the research found in this thesis, notably the implementation of attribution methods in order to identify and quantify the causes of changes in extreme streamflow in West Africa.

Chapter 2

Trend detection of hydrological extremes in West Africa

2.1 Introduction to article 1

Before projecting hydrological changes into the future or evaluating the causes of their evolution, it is pertinent to first characterize hydrological changes in recorded history. A trend must be proven to exist at a given level of significance. The following article presents the results evaluating the evolution of extremes in portions of the Niger and Senegal river basins. Primary objectives were determining whether extremes were stationary or non-stationary; developing extreme value theory-based models to represent non-stationarity when found; comparing results in two distinct hydroclimatic zones; and evaluating the impact of the results on return levels. The return levels are of particular significance, as they can inform the design of hydraulic structures in the study regions. Return levels can also indicate the probability of an event of a given magnitude that may impact local populations and infrastructure.

The following chapter presents the results related to the evolution of trends in hydrological extremes, represented by the annual streamflow maxima, in West Africa. The chapter primarily consists of an article published on the subject in the *Journal of Hydrology* in 2018 (Wilcox et al., 2018).

2.1.1 Personal contributions

General methodological approach

For this study, I have carried out the data preprocessing, numerical developments, and computations needed to obtain the results. I also generated the associated figures for the paper.

Among these points, one of my primary contributions was to develop and implement the methodology for the non-stationary extreme value models. I tested several model types before selecting multiple linear segments as appropriate models (using non-linear segments did not significantly improve the representation of the data). I contributed to the development of the model selecting process by noting that the likelihood ratio test would not be theoretically valid for comparing the non-stationary models as it only tests the addition of specific parameter(s). We instead proposed the two-step model selection process described in the article, first selecting using AIC then using the likelihood ratio test to validate the selection of parameters.

Besides developing the main methods used for the article, I invested much time in data preparation and sensitivity testing of results. Appendix A contains some of this work as supplementary material for the article. The analyses include a presentation and evaluation of the hydrological data series from which the final data selection was made. Controlling errors and inconsistencies in the data is essential as the quality of an analysis is limited by the quality of the data used. Study sites and available data are presented, and the hydrological data is evaluated and filtered based on data quality criteria. The data evaluation and selection is followed by a sample of sensitivity testing results. Much of the sensitivity testing was also linked to data quality issues.

Numerical implementation

I used R software to program the following elements:

- Data processing and quality control
- Stationary GEVs
- Development of twelve model covariate options
- Optimization of non-stationary GEVs

- Model selection procedure
- Calculation of confidence intervals

The R packages `evd`, `ismev`, and `extRemes` were heavily used during the evaluation of trends in extremes. I explored the following modifications to the functionalities proposed:

- Combining the capacities of functions from different packages (e.g., one package allows you to fix the value of a parameter but not to use covariates, another allows for covariates but not declaring the value of a parameter, I combined the two features).
- After I investigated the source code, we determined that the confidence interval functions found in the `extRemes` package was not suitable for the purpose of our study.

Article writing, conferences, and collaborations

I wrote the first draft of the paper, and integrated all the feedback from the coauthors. I conducted the modification and submission of the article to the *Journal of Hydrology*. I was actively involved in the editing and review processes along with my coauthors.

I participated actively in the collaboration with Senegalese researcher Ansoumana Bodian, including a visit to Senegal in 2016.

Appendix A also includes a follow-up to the *Journal of Hydrology* article as part of a collaboration with researchers in the ANADIA 2.0 Niger project. The project had updated the rating curves for the Sirba River, which showed that the outdated rating curves produced significant inaccuracies in the time series. I updated the NSGEV analysis for the Sirba River and contributed my results and interpretation to an article on flood hazard evaluation.

Results were also presented at the 2016 FRIENDS conference in Dakar, Senegal; at the "Niger River Days" meeting in Toulouse, France in 2017; and at the AGU 2017 General Assembly in New Orleans.

2.2 Article: Trends in hydrological extremes in the Senegal and Niger Rivers

Abstract In recent years, West Africa has witnessed an increasing number of damaging floods that raise the question of a possible intensification of the hydrological hazards in the region. In this study, the evolution of extreme floods, represented by the annual maxima of daily discharge (AMAX), is analyzed over the period 1950-2015 for seven tributaries in the Sudano-Guinean part of the Senegal River basin and four data sets in the Sahelian part of the Niger River basin. Non-stationary Generalized Extreme Value (NS-GEV) distributions including twelve models with time-dependent parameters plus a stationary GEV are applied to AMAX series. An original methodology is proposed for comparing GEV models and selecting the best for use. The stationary GEV is rejected for all stations, demonstrating the significant non-stationarity of extreme discharge values in West Africa over the past six decades. The model of best fit most commonly selected is a double-linear model for the central tendency parameter (μ), with the dispersion parameter (σ) modeled as either stationary, linear, or a double-linear. Change points in double-linear models are relatively consistent for the Senegal basin, with stations switching from a decreasing streamflow trend to an increasing streamflow trend in the early 1980s. In the Niger basin the trend in μ is generally positive since the 1970s with an increase in slope after the change point, but the change point location is less consistent. The recent increasing trends in extreme discharges are reflected in an especially marked increase in return level magnitudes since the 1980s in the studied Sahelian rivers. The rate of the increase indicated by the study results raises urgent considerations for stakeholders and engineers who are in charge of river basin management and hydraulic works sizing.

Authors Catherine Wilcox, Théo Vischel, Gérémy Panthou, Ansoumana Bodian, Juliette Blanchet, Luc Descroix, Guillaume Quantin, Claire Cassé, Bachir Tanimoun, Soungalo Kone

2.3 Introduction

River floods are one of the deadliest natural hazards in the world. They produce major damages on infrastructure, lead to economic losses, and favor

water-borne diseases. In order to better understand such floods, hydrologists have long focused on assessing the rare (large in magnitude) river discharge values, represented by the tails of underlying statistical distributions (Gumbel, 1957). The primary aim, besides theoretical understanding, is to provide practical tools for flood risk management and civil engineering structure design. The main challenge for practical applications is estimating return levels for high return periods (typically 10, 50, or 100 years). The more the return period is larger than the length of the series, the greater the challenge of estimating the tail of the distribution.

Extreme Value Distributions (EVDs) are statistical tools designed for the study of such rare values (see e.g. Coles et al., 2001; Katz et al., 2002). For several decades, the main challenge when applying EVDs was to have a proper estimation of the tail (heavy, light, or bounded). The focus was then on developing robust estimation procedures (Regional Frequency Analysis – Hosking and Wallis, 1997; GRADEX and adaptation – Guillot, 1993; Paquet et al., 2013; Bayesian inference – Coles and Tawn, 1996 among many other developments) and then applying them to the longest hydrological series available (Koutsoyiannis, 2004). The stationarity assumption reigned during this “old hydrological world” (Milly et al., 2008).

However, both increases and decreases of extreme discharges have been reported via the evaluation of historical series around the world (e.g. Kundzewicz et al., 2005a; Bower, 2010; Condon et al., 2015). A main challenge of hydrological extremes thus concerns the validity of the stationarity assumption and the implications of its rejection. Ongoing global changes are expected to increase flood hazard mainly through the intensification of the hydrological cycle due to global warming (Hirabayashi et al., 2013; Arnell and Gosling, 2016) and the degradation of land surfaces due to anthropic pressure (Brath et al., 2006; Elmer et al., 2012). Other factors also tend to reduce flood hazards, including negative precipitation trends found in drying regions and flood protection structures such as dams. While some regions witness resulting changes in flood frequency, in other regions, no changes have been detected (Villarini et al., 2009). This could be a result of either the absence of substantial changes in drivers that could trigger/influence flood trends or competing phenomena that act in opposite ways. It could also be due to the use of non-robust methodology to detect concrete changes in the EVD of discharge. The last case necessitates improved methods able to detect trends in series characterized by low signal to noise ratio.

While numerous studies on flood hazard evolution have been undertaken

for developed countries, less has been done in the developing world. This is the case in particular over the tropics (Kundzewicz et al., 2005b) which contain two thirds of the developing countries, including the poorest. Populations living in the tropics are notoriously vulnerable to climate hazards, including droughts and floods that can occur within the same year at a given place. Global changes are expected to strongly impact flood risks in the tropics with studies already reporting significant increases in the frequency of rainfall extremes (Allan et al., 2010; O’Gorman, 2012; Asadieh and Krakauer, 2015), land use/cover changes (Lambin et al., 2003; Erb et al., 2016), rapid rates of urbanization (Di Baldassarre et al., 2010), and increasing vulnerability of populations due to very high demographic growth; the population of the least developed countries is expected to double from now to 2050 (Population-Reference-Bureau, 2016). The strong internal variability of tropical climates, the lack of long-term hydrological observations, and the large uncertainty of climate projections in the tropics challenge the scientific community to provide reliable and relevant information to stakeholders so they can define suitable flood risk management strategies.

West Africa is one of the most critical tropical regions for examining hydrological non-stationarities as it is a region in which the issues described above are exacerbated. West Africa is known for having strong precipitation variability, especially at the decadal level (Nicholson, 2013b). It underwent a devastating and long-lasting drought that abruptly started in the late 1960s and persisted through the 1970s and 1980s (Lamb, 1983; Le Barbé and Lebel, 1997; Nicholson, 2000; Camberlin et al., 2002; Le Barbé et al., 2002; L’Hote et al., 2002; Dai et al., 2004; Panthou et al., 2014; Bodian et al., 2011, 2016b). At the regional scale, this led to a decline in the flow of large rivers that was proportionally greater than the decrease in rainfall (Lebel et al., 2003; Andersen and Golitzen, 2005; Mahé and Paturel, 2009).

At the subregional scale however, two diametrically opposed hydrological behaviors were observed (Descroix et al., 2018). In the Sudano-Guinean subregion of West Africa (south of 12°N), a decrease in river flow was observed for small to regional scale catchments (Mahé et al., 2005; Descroix et al., 2009) until the 1970s and 1980s (Diop et al., 2017). The decrease in flow was attributed to a gradual drying up of the groundwater and thus a gradual decrease in the base flow of the rivers (Mahé et al., 2000; Mahé and Paturel, 2009). In the Sahelian region (belt between roughly 12°N and 16°N), runoff coefficients and runoff volumes increased despite the drought. This phenomenon – the so-called “Sahelian paradox” – was understood to

have been caused by a change in surface conditions (Albergel, 1987; Descroix et al., 2009; Aich et al., 2015; Cassé et al., 2016). Droughts played a role in increasing surface crust and decreasing vegetation (Gal et al., 2017), which consequently increased runoff coefficients and counterbalanced the effects of drought (Boulain et al., 2009). Anthropogenic changes (including land use change) appear to be a major factor in some basins (Seguis et al., 2004; Li et al., 2007; Leblanc et al., 2008; Gal et al., 2017). Other factors such as an increase in the density of the drainage network may have played a role in the increase of flow (e.g. Favreau et al., 2009; Gal et al., 2017).

Since the early 1990s, both total rainfall and streamflow amounts have increased compared to the drought decades of the 1970s and 1980s, though they remain lower than in previous pre-drought decades (Lebel and Ali, 2009; Mahé and Paturel, 2009; Panthou et al., 2014; Tarhule et al., 2015; Diop et al., 2017). In the Sahel, the increase was accompanied by higher interannual variability (Ali and Lebel, 2009; Panthou et al., 2014) and overall persistence of drought conditions under certain indices (L'Hote et al., 2002; Ozer et al., 2009). Of note is the increase in the intensity of rainfall during recent years (Ly et al., 2013; Panthou et al., 2014; Sanogo et al., 2015; Taylor et al., 2017). During the same period, an increase in the number and magnitude of extensive floods has been reported (Tarhule, 2005; Tschakert et al., 2010; Samimi et al., 2012; Sighomnou et al., 2013; Cassé and Gosset, 2015), causing extensive fatalities, damages, and population displacement. From the mean hydrographs of the Niger River at Niamey plotted for six decades from 1951 to 2010, Descroix et al., 2012 and Sighomnou et al., 2013 illustrated a strong increase in the intensity of the summer flood peak of the Sahelian tributaries during the 2000s, while the flood peaks coming from the remote Guinean tributaries and arriving at Niamey later in the year at Niamey were as low as in the 1970s. They also noted successive discharge records produced by Sahelian floods in 2010 and 2012, exceeding the Guinean flood.

The strong current and projected demographic growth in West Africa (Population-Reference-Bureau, 2016) is likely to increase the exposure of populations to floods, both from intensive and unplanned human settlements in flood-prone areas (Di Baldassarre et al., 2010), and from human-induced changes in land cover which affect runoff. Changes in hydrological extremes consequentially are particularly pressing for decision makers in West Africa, as the statistical tools used for infrastructure design have not been updated since the 1970s (Amani and Paturel, 2017). An improved quantitative understanding of how extreme flows are changing over time in the region has

generated an urgent demand to design and manage structures such as dams and dikes and, as a result, aid in risk mitigation, as well as the development of hydroelectric energy and irrigation systems.

However there is still very little literature on quantifying extreme flow changes in West Africa. For Sudano-Guinean regions, Nka et al., 2015 found a breakpoint (decrease) in the series of annual maxima during the drought period for the Falémé branch of the Senegal River at Fadougou. When only a more recent time period is considered (since 1970), no significant trends were found in the Sudano-Guinean catchments, including the Falémé. Bodian et al., 2013 explored trends in annual maximum daily discharge (AMAX) values on the Bafing tributary of the Senegal River (Bafing Makana and Daka Saidou stations). They found that high points in the series occurred during the pre-drought period (1967 and 1955), whereas the minima of the AMAX occurred in 1984. Diop et al., 2017 found that extreme highs in the Bafing Makana series decreased by 18% over the series and especially since 1971, while extreme lows stayed stable. Aich et al., 2016a analyzed time series of AMAX values at several stations along the Niger River. They found that changes in AMAX series followed the decadal variability of mean annual precipitation over Guinean and Benue-area catchments (a wet period during 1950s and 1960s, followed by a dry period during 1970s and 1980s, and values close to the long-term mean after), while the floods produced by Sahelian tributaries have recorded a monotonic increase since the beginning of the 1970s. Nka et al., 2015 found positive trends in the extreme values of three Sahelian catchments studied (Dargol River at Kakassi, the Gorouol River at Koriziena, and the Goudebo River at Falagontou). They also found significant (Mann-Kendall test) increases in extreme values in both AMAX series and peak-over-threshold (POT) series for the Dargol River at Kakassi. Breaks in AMAX were detected in 1987, and for POT in 1993. Mean extreme values were found to be greater (twice as high) during the later subperiods.

The aim of this paper is to detect and quantify trends in extreme hydrological values in West Africa. AMAX is used to represent extreme flow in the study. Discharge series are analyzed in tributaries of the Niger and the Senegal rivers, two catchments that reflect two differing hydrological and climatic processes of the Sahelian and the Sudano-Guinean West Africa. The temporal evolution of the AMAX series is assessed by exploring different Generalized Extreme Value (GEV) models that range from a stationary GEV (S-GEV) to more complex non-stationary GEV (NS-GEV) models. The following study proposes an original methodology for identifying the

most significant model to represent the evolution of extremes for a particular data series. Notably, the retained model is accompanied by significance levels and estimates of uncertainty. The retained model is used to compute time-varying frequencies of extreme flows. These changes are represented by the evolution of flow return levels over the last fifty to sixty years. Our results thus have implications for operational applications, as the design and operation of hydraulic structures depend on the magnitude of a flood event at a given return period.

2.4 Region of study and data

2.4.1 West African hydro-climatic features

The climate of West Africa is controlled by the West African Monsoon. The rainfall belt roughly follows the seasonal migration of the position of the Intertropical Convergence Zone (ITCZ). During the boreal winter (December-February), the rainfall belt is located over the Gulf of Guinea at around 4°N . It moves northward during the spring and reaches its northernmost position during boreal summer (June-September). At the regional scale, it implies that the hydro-eco-climatic features vary along a roughly north/south gradient. The mean annual rainfall amount decreases from south to north, ranging from over 1500 mm near the southern Guinean coast ($\approx 5^{\circ}\text{N}$) to less than 250 mm over the lower Saharan desert limit ($> 18^{\circ}\text{N}$).

The Sudano-Guinean and Sahelian regions are distinguished by their mean annual rainfall: the Sudano-Guinean region extends between the 1300 mm and 750 mm isohyetal lines and the Sahel between 750 mm and 250 mm. The regions have different seasonal rainfall cycles during the monsoon period (bimodal for the Sudano-Guinean region and unimodal signal for the Sahel), but are both characterized by a main rainfall peak in boreal summer and a dry season in boreal winter. The two regions are also differentiated by their respective vegetation: dense vegetation featuring tree savannah, woodland, and tropical forest for the Sudano-Guinean region (Bodian et al., 2016a); dry savannah and sparse bush in the Sahel.

These contrasts influence the dominant hydrological processes characterizing the two regions. The Sahelian hydrology is distinguished by the prevalence of Hortonian overland flow (Horton, 1933). In the event of precipitation, runoff is produced once the infiltration capacity of the soil is reached. As a

consequence, runoff production is driven by the hydro-dynamic properties of soils at the surface. The excess rainfall then runs off into the drainage network. Groundwater flow plays a minor role in the contribution to streamflow, if any. Due to this, river basins located in the Sahelian region are more sensitive to changes in fine-scale rainfall intensity (Vischel and Lebel, 2007). To the south, on the other hand, the Sudano-Guinean catchments have primarily Hewlettian hydrological processes (Cappus, 1960; Hewlett, 1961; Hewlett and Hibbert, 1967). Both surface and subsurface flow contribute to streamflow due to the elevated hydraulic conductivity of soils (Descroix et al., 2009). Under the same climatic evolution, river basins in the Sudano-Guinean zone may be less responsive to changes in rainfall intensity than in Sahelian river basins (Gascon et al., 2015).

2.4.2 Study catchments and datasets

Our analysis of changes in extreme flows is based on data available on two contrasted hydro-systems in West Africa: the upper reaches of the Senegal River located within the Sudano-Guinean region, and the middle reaches of the Niger River located within the Sahelian region. Table 2.1 overviews the data selection for the study, and Figure 2.1 displays a map of their locations.

Table 2.1: Annual maxima (AMAX) data used in the study.

Subbasin	Station	Area (km ²)	Years	Gaps	Missing years
Senegal River					
Bafing	Bafing Makana	21290	1961-2015	0.00%	None
Bafing	Daka Saidou	15700	1954-2015	4.84%	1956, 1958, 2009
Bakoye	Oualia	84700	1955-2015	1.64%	1982
Falémé	Gourbassi	17100	1954-2015	1.61%	2013
Falémé	Kidira	28900	1951-2015	23.10%	1960, 1963, 1965-68, 1970, 1972-73, 1978, 1980-82, 1986, 2010
Senegal	Kayes	157400	1951-2015	3.08%	2011, 2013
Senegal	Bakel	218000	1950-2015	1.52%	2009
Niger River					
Niger	Sahelian Niger River	125000	1953-2012	0.00%	None
Dargol	Kakassi	6940	1957-2015	16.90%	1961, 1989, 1994, 1996-97, 1999, 2000, 2002, 2004-05
Sirba	Garbe Kourou	38750	1956-2015	10.00%	1959, 1960-61, 2000, 2004-05
Gorouol	Alcongui	44850	1957-2015	16.90%	1960, 1990, 1993, 1996-99, 2001, 2004-05

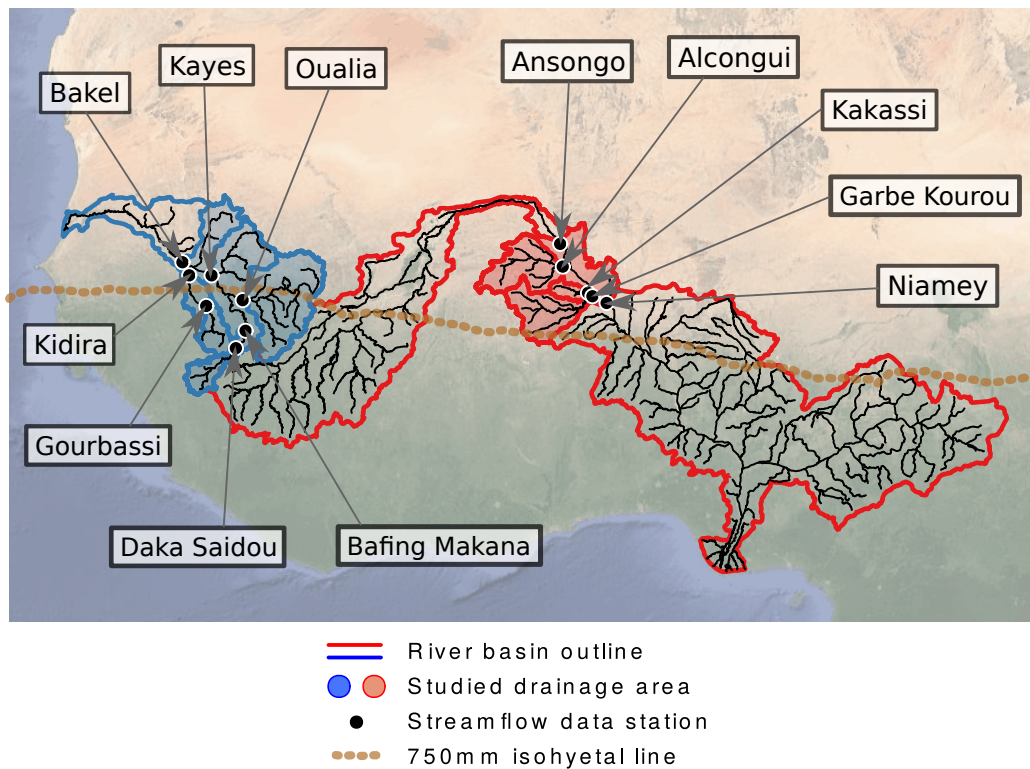


Figure 2.1: Map of stations used in the study with their respective drainage basins (Boyer et al., 2006; Kahle and Wickham, 2013).

Sudanian tributaries of the Senegal River

The second largest river in West Africa is the Senegal River. The Senegal River drains a basin of approximately 300,000 km² (Rochette et al., 1974), found within the borders of four countries which are (from upstream to downstream): Guinea, Mali, Senegal, and Mauritania. It is formed by the confluence of three affluents that take their sources from the Fouta Djallon highlands in Guinea: the Bafing, the Bakoye, and the Falémé. Due to the delayed contribution of groundwater, the annual flood peak occurs a few weeks later than in Sahelian Niger (Figure 2.2), whose seasonal hydrological signal follows that of precipitation more closely.

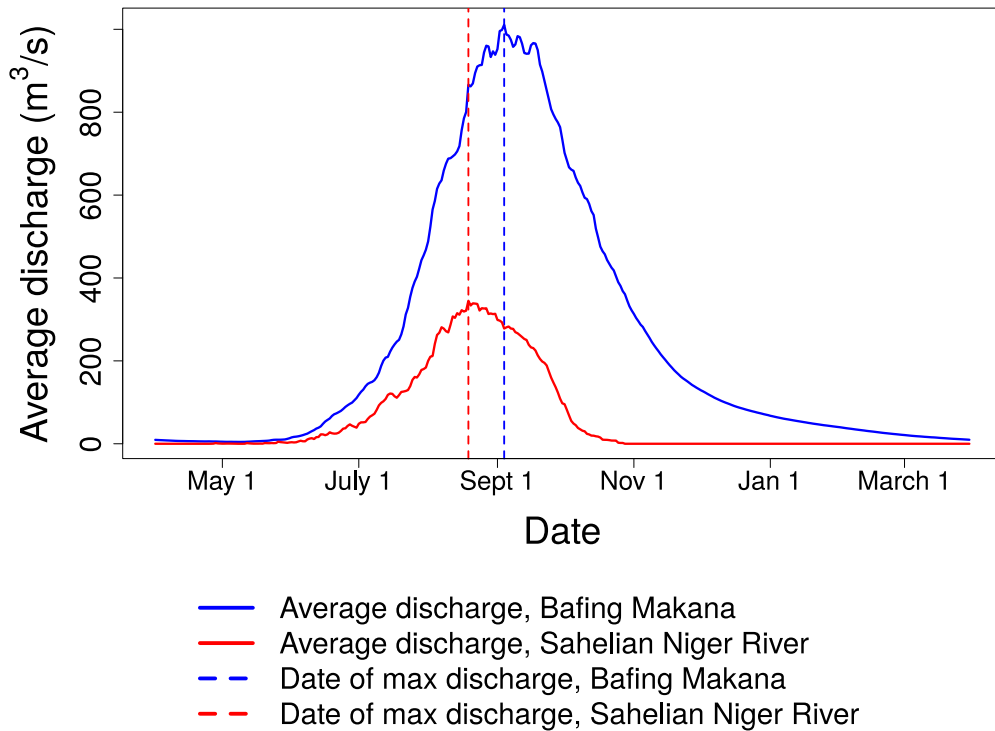


Figure 2.2: Average seasonal signal for the Bafing Makana station in the Senegal River basin (blue) and the Sahelian Niger River (red). Period of record: 1961-2012. The flood peak has a smoother descent and occurs a few weeks later in the Senegal River basin due to the contribution of groundwater.

Seven stations whose major contributions come from within the Sudano-Guinean region are analyzed for the Senegal River (including the Bafing, Falémé, and Bakoye affluents), covering a total drainage area of 218,000 km². Globally from upstream to downstream, the stations are as follows: The Bafing at Daka Saidou (1954-2015, 15,700 km²) and Bafing Makana (1961-2015, 21,290 km²); the Falémé at Gourbassi (1954-2015, 17,100 km²) and Kidira (1951-2015, 28,900 km²); the Bakoye at Oualia (1955-2015, 84,700 km²), and the Senegal at Kayes (1951-2015, 157,400 km²) and Bakel (1950-2015, 218,000 km²). The last two (Kayes and Bakel) are located downstream of the Manantali dam whose construction was completed in 1988. The Bakel station's catchment area includes those of all other stations studied, and represents the quantity of water that flows into the downstream valley.

Sahelian tributaries of the Niger River

With a drainage area of 2,170,500 km², the Niger is the largest river in West Africa, although only around 1,400,000 km² of its surface is estimated to effectively contribute runoff to the Niger River (Tarhule et al., 2015). It originates in the Fouta Djallon highlands in Guinea (Andersen and Golitzen, 2005). After spreading to form an inland delta in Mali, it reconverges and continues its course through the Sahelian region in Niger, crossing Benin and Nigeria before arriving at its outlet in the Gulf of Guinea. For the present study, analysis within the Niger basin focuses on the drainage area responsible for the Sahelian floods of the Niger River (Descroix et al., 2012; Cassé et al., 2016) that discharges its flows downstream of Ansongo and upstream of Niamey (Figure 2.1), an effective drainage area of 125,000 km². An aggregated data set extracted from the difference between the Niger River streamflow series at Niamey and Ansongo during the local Sahelian rainy season (1953-2012 – see Cassé et al., 2016, for more details) represents this area for the subsequent analysis. This data series is hereafter referred to as the Sahelian Niger River (SNR) series. Figure 2.2 shows the average seasonal signal of the SNR series.

The left bank of the Niger River within this catchment is largely endorheic. It only contributes to the Niger River during heavy rain events which generate small rivers that sporadically reach the main Niger River bed, although some evidence suggests that endorheic rupture is increasing in recent years (Mamadou et al., 2015).

The right bank of the Niamey-Ansongo reach consists of three major catchments: the Gorouol, the Sirba, and the Dargol, which together cover a total area of 90,540 km². Three data series are studied for these catchments: the Gorouol at Alcongui (1957-2015, 44,850 km²), the Sirba at Garbe Kourou (1956-2015, 38,750 km²), and the Dargol at Kakassi (1957-2015, 6,940 km²). All three rivers are intermittent and only flow during the rainy season, following the general pattern seen in Figure 2.2.

2.5 Theoretical framework and methodology

Extreme value distributions (EVDs) applied in a non-stationary context comprise some of the recent robust methods proposed for the detection of non-stationarity (Olsen et al., 1998; Cunderlik and Burn, 2003; Re and Barros,

2009; Marty and Blanchet, 2012; Park et al., 2011; Beguería et al., 2011; Panthou et al., 2013; Blanchet et al., 2016). Besides performing detection, EVDs also permit the quantification of trends and the evaluation of uncertainty. The principle of these methods is based on fitting EVDs both in stationary mode (stationary parameters) and in non-stationary mode (time-dependent parameters). The performance of the fitted models is then compared based on the capacity to accurately describe the data sample (goodness of fit) and the complexity of the model (parsimony). By searching for the most suitable temporal functions of parameter evolution, one can obtain an indication of the shape of the non-stationarity. The retained non-stationary model features vectors of parameters that best describe the data series in a statistically significant manner.

2.5.1 Selection of extreme discharge values

Extreme values can be defined as probabilistically rare occurrences, or values that are exceptionally large (or small) in magnitude. Extreme values can be extracted from a time series by two main approaches: by taking the maximum value within a given period, or by considering all values above a determined threshold. In this study – as in many climate and hydrological studies (see previous paragraph for examples) – extremes are defined as the maximum value of each year. A year is considered a long enough period for the extraction of maximum values for use in the subsequent analysis (Coles et al., 2001). At each station, the analyzed data series is formed by the annual maxima of daily discharge (AMAX).

The selected AMAX values were controlled for data quality. All eleven series span at least fifty years, which provides sufficient data points for the calibration of a statistical distribution. Data quality evaluation was focused on peak flow months. As demonstrated by West Africa’s consistent seasonal signal (Figure 2.2), the local rainfall-generated flood peak occurs on average within the months of August and September in both the Sahelian and Sudano-Guinean zones. Missing values before and after these months are unlikely to have an effect on the quality of the extreme flow data. On the other hand, a missing value during the peak streamflow months may have been the AMAX for that year. Identifying an incorrect data point as an extreme value would have an impact on the analysis.

With the potential impact of data quality in mind, the data series were evaluated. For the stations in the Senegal River basin, the year was removed

from the series if any daily streamflow value was missing during the months of August and September. For stations in the Niger River basin, the hydrographs were viewed year by year. If values were missing near the flood peak, the year was removed. Years were also removed where recording errors that could affect flood peaks were perceived (for example, for one year it seemed that $100 \text{ m}^3/\text{s}$ were added to all values).

Figure 2.3 displays a sample of the AMAX data used, from the Bafing Makana station for the Senegal River (Figure 2.3a) and SNR series for the Niger River (Figure 2.3b). One can note that although there appears to be some trend, there is also a high degree of variability. The AMAX values at the Bafing Makana station started decreasing in magnitude in the 1960s and started increasing in approximately the 1980s. This visual trend was also found for the other Senegal stations. In Sahelian Niger, however, the increase appears to have begun earlier, during the drought years of the 1970s.

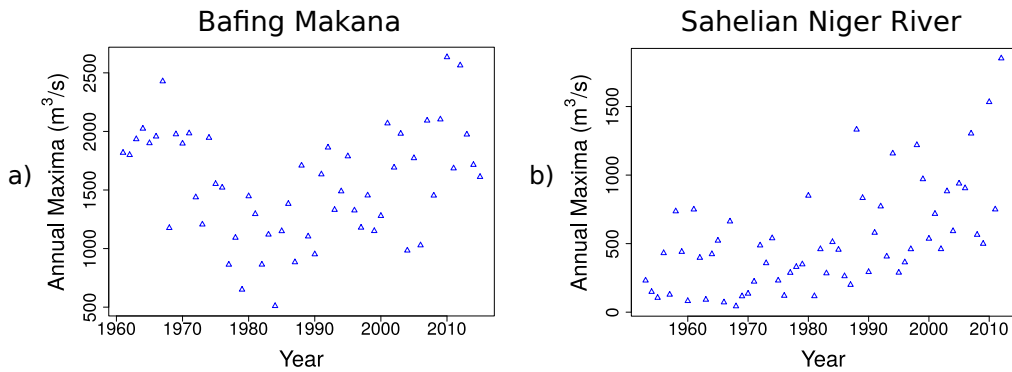


Figure 2.3: Sample AMAX data from the Bafing Makana station in the Senegal River basin (a) and the Sahelian Niger River series (b).

2.5.2 Formulation of statistical models

GEV distribution

A suitable statistical function used to represent the distribution of a random variable (Y) defined by block maxima is the GEV distribution (Coles et al., 2001), written as:

$$F_{GEV}(y; \mu, \sigma, \xi) = \exp \left\{ - \left[1 + \xi \left(\frac{y - \mu}{\sigma} \right) \right]^{-\frac{1}{\xi}} \right\} \text{ for } 1 + \xi \left(\frac{y - \mu}{\sigma} \right) > 0 \quad (2.1)$$

where μ is the location parameter (a measure of central tendency), σ the scale parameter (a measure of dispersion), ξ the shape parameter (a measure of tail behavior), and y the value at which the GEV is to be evaluated.

The GEV distribution is fitted on AMAX series (y_i) with constant parameters (S-GEV, Equation 2.2) and various forms of time (t in years)-varying parameters (NS-GEV, Equation 2.3):

$$Y \sim \text{GEV}(\mu, \sigma, \xi) \quad (2.2)$$

$$Y \sim \text{GEV} \{ \mu(t), \sigma(t), \xi(t) \} \quad (2.3)$$

Identifying appropriate temporal functions for GEV parameters

The implementation of one NS-GEV model requires choosing the general form of the appropriate temporal function for each GEV parameters. As there is no theoretical model for the time-dependent function, it must be assigned a priori. In order to determine a range of suitable functions, an initial exploration of trends is done by fitting S-GEV distributions in moving windows over the study periods. A window size of 15-years has been selected as a compromise between having sufficient data to fit the GEV and highlighting potential parameter evolution. Due to the difficulty in estimation, the parameter ξ was first calibrated using the entire data sample, then kept stationary while μ and σ change with each window.

Figure 2.4 displays an example of the moving window for μ (2.4a) and σ (2.4b) for the Bafing Makana station. For this station, both parameters are characterized by a v-shaped pattern which is more distinct for μ than σ . Based on the moving window analysis for the 11 different stations, it was identified that μ and σ can be qualitatively described by one single or several connected linear segments. For all stations it was visually observed that changes in μ were more clearly defined than changes in σ . One can note here that the moving window method allows for qualitatively assessing the overall trends in GEV parameters. However, unlike NS-GEVs, the moving window does not allow for the quantification of the trend, nor its significance.

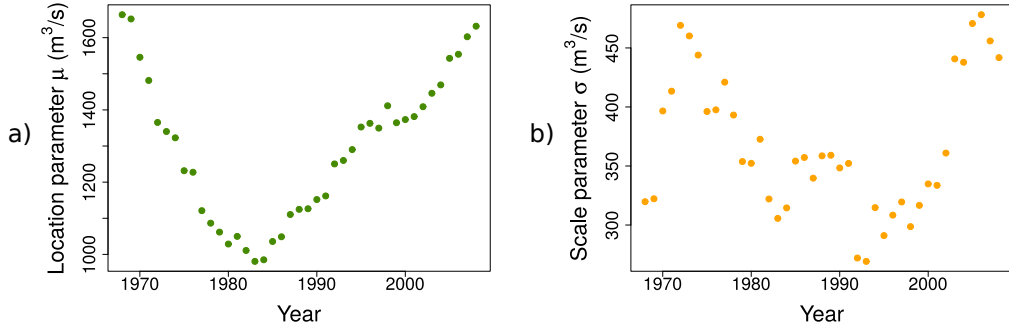


Figure 2.4: Moving window estimates for the GEV distribution parameters μ (a) and σ (b) for the Bafing Makana station. The points represent the center of the fifteen-year window over which the parameters were estimated.

Formulation of GEV parameter temporal functions

According to the qualitative analysis derived from the moving window GEV, several temporal patterns with varying complexity were identified to describe the GEV parameters. Linear, double-linear (with one breakpoint), and triple-linear (with two breakpoints) temporal functions were considered for μ , σ , or both. In the case of both parameters varying, μ and σ were permitted to vary independently. As with the moving window, ξ was kept constant; the difficulty in estimating the ξ parameter supports the choice in keeping it constant, as additional complexity would increase the uncertainty. A non-linear (polynomial) model was also considered initially, but showed no improvement over the multilinear models.

To represent this non-stationarity mathematically, we introduce the function $\eta(t)$, where η represents either μ or σ and t is a time-dependent covariate. $\eta(t)$ takes on different forms depending on the trend model:

Stationary parameter model:

$$\eta(t) = \eta_0 \quad (2.4)$$

This parameter model has only one degree of freedom, η_0 .

Single-linear trend:

$$\eta(t) = \eta_0 + \eta_1 \times t \quad (2.5)$$

In this case $\eta(t)$ has two degrees of freedom : η_0 and η_1 , and thus one additional degrees of freedom in comparison with a stationary parameter.

Double-linear trend:

$$\eta(t) = \eta_0 + \eta_1 \times (t - t_1) \text{ for } t \leq t_1 \quad (2.6)$$

$$\eta(t) = \eta_0 + \eta_2 \times (t - t_1) \text{ for } t_1 < t \quad (2.7)$$

t_1 represents the breakpoint in time (year index) where the two linear segments join (i.e. where the slope of the linear model changes). In this case $\eta(t)$ has four degrees of freedom: η_0, η_1, η_2 and t_1 , meaning three additional degrees of freedom in comparison with a stationary parameter model.

Triple-linear trend:

$$\eta(t) = \eta_0 + \eta_1 \times (t - t_1) \text{ for } t \leq t_1 \quad (2.8)$$

$$\eta(t) = \eta_0 + \eta_2 \times (t - t_1) \text{ for } t_1 < t \leq t_2 \quad (2.9)$$

$$\eta(t) = \eta_0 + \eta_2 \times (t_2 - t_1) + \eta_3 \times (t - t_2) \text{ for } t_2 < t \quad (2.10)$$

In this case, $\eta(t)$ has six degrees of freedom : $\eta_0, \eta_1, \eta_2, \eta_3, t_1, t_2$.

A total of 13 different GEV models are considered: one with all parameters stationary (S-GEV) and 12 NS-GEV models that combine the above parameter trend models in Equation 2.4–2.10 for μ and σ . They are reported in Figure 2.5, classified according to their degrees of freedom.



















Degrees of freedom	3	4	5	6	7	8	9
Models							
μ							
σ							
							

Figure 2.5: Covariate models tested for GEV distributions.

2.5.3 Model fitting

For S-GEV, the parameters are directly fitted using maximum likelihood estimation (MLE). In the NS-GEV scenario, for each temporal function (linear, multi-linear), the following procedure is performed:

1. If the formulation includes one or two breakpoints, the year of each breakpoint t_i is defined before estimating the other parameters η_i :
 - In order to limit border effects, the breakpoint(s) must be positioned not earlier than 10 years after the beginning of the series and no later than ten year before the end. Likewise, two successive breakpoints must be separated by at least 10 years.
 - The breakpoints are defined independently for $\mu(t)$ and $\sigma(t)$, and can be at a different point in time (though not necessarily).
2. At each defined breakpoint, the parameters η_i are estimated according to the formulations of $\eta(t)$ in Equations 2.4–2.10 using MLE.
3. Repeat steps 1 and 2 until all possible breakpoint dates have been tested.
4. Retain the model that gives the maximum likelihood among the different breakpoint dates tested in steps 1 to 3.

2.5.4 Selection of the best GEV model

A more complex model may provide better fit, but not to a degree that merits additional parameterization. The selection of the best model is done by comparing the maximum likelihood obtained by the 13 different GEV models per station and evaluating their significance. The selection process consists of two steps: First, an initial best model is selected via the Akaike Information Criterion (AIC – Akaike, 1974). Then, the model choice is validated via a Likelihood Ratio Test (LRT – Coles et al., 2001). According to Kim et al., 2017, AIC and LRT are both suitable for evaluating non-stationary representations of hydrological data. AIC in particular is robust with small data sets.

The AIC balances model fit against model complexity in the following equation:

$$\text{AIC} = 2k - 2 \log(L) \quad (2.11)$$

where k is the number of parameters in the model and L is the maximum likelihood value associated with the model. The model with the lowest AIC value is selected.

The LRT is a test between two models that must be “nested”; the simpler model is contained within the more complex models. While AIC compares all models globally, LRT validates the addition or subtraction of specific parameters. The likelihood ratio test (LRT) is performed by comparing the following statistic to the χ^2 distribution:

$$D = 2 \times \{\log [L(M_1)] - \log [L(M_0)]\} \quad (2.12)$$

where $\log[L]$ is the maximum value of the log likelihood of model M and M_0 is nested in M_1 . If D exceeds the α -quantile of the χ^2 distribution with n degrees of freedom, with n the difference in the number of parameters between the two models (additional degrees of freedom), then the more complex model is accepted at level α .

For this study, AIC is first used to find an initial model of best fit for each station. The model selection via AIC is then validated using LRTs. All models that are nested within the model selected via AIC are tested in pairs with the selected model using the LRT with $\alpha = 0.10$. This confirms that the added complexity is significant. More complex models that have the AIC selection as a nested model are likewise tested in pairs against the AIC selection using the LRT to validate the exclusion of additional parameters.

Note that the inclusion of the stationary GEV model in the comparison allows for the evaluation of the presence of a non-zero trend, accompanied by a significance level. If the selected model is an NS-GEV, then the stationary hypothesis is rejected.

2.5.5 Return level evaluation

The use of a parametric distribution for representing the data allows for the estimation of return levels r_T corresponding to return period T . The return level r_T is exceeded with a probability p in a given year where $p = 1/T$. The return levels can be calculated as follows:

$$r_T = \mu - \frac{\sigma}{\xi} \left\{ 1 - [-\log(1 - p)]^{-\xi} \right\} \quad (2.13)$$

For non-stationary models, the corresponding value of μ and σ for the NS-GEV are inserted in Equation 2.13 at each time step in order to obtain the non-stationary return levels for a given p .

A comparison of the relative evolution of return levels was conducted using normalized return level values for each station. The normalization was conducted by dividing the values of the non-stationary return levels by the value r_T calculated under the stationary assumption (S-GEV).

$$r_{T,normalized} = \frac{r_T(NS-GEV)}{r_T(S-GEV)} \quad (2.14)$$

2.5.6 Uncertainty assessment

Confidence intervals for model parameters were determined via nonparametric bootstrapping (Efron, 1979; Efron and Tibshirani, 1994; Davison and Hinkley, 1997). While approximate confidence intervals can be calculated via approximation to the normal distribution, the approximation becomes less valid for the parameter ξ and for values at the tail of the distribution (high return periods). Thus, bootstrapping was selected as providing a more accurate representation of the uncertainty.

For each station, a data sample of equal length to the original series was extracted via resampling. An NS-GEV of the same model type and with the same breakpoint as the selected NS-GEV for the station was calibrated on the sample. This was repeated 500 times for each station. Samples were discarded if their NS-GEVs had a ξ value greater than 1 or less than -1, or if there were errors while estimating the NS-GEV and associated uncertainties, likely due to particularly skewed samples (same values selected many times, extreme values overselected, etc). Confidence intervals for the percentiles of interest were then calculated at each time step of the data series.

In the methodology used for this study, the breakpoints were fixed before performing MLE to estimate the NS-GEV parameters. The uncertainty evaluation methods detailed above assume that the uncertainty in breakpoint estimation is negligible compared to the uncertainty in the estimation of the other NS-GEV parameters (uncertainty of the η_i). This assumption is explored further in section 2.7.3.

2.6 Results

2.6.1 Selected GEV model

Table 2.2 shows the model of best fit that was selected for each station with a p-value (α) of 0.10 used in the LRT. One can note that for all stations, an NS-GEV model always fit the series of AMAX better than the stationary GEV model.

Table 2.2: Model selection, GEV analysis results, and associated confidence intervals (CI).












Subbasin	Station	GEV model	Breakpoints	ξ	ξ , 95% CI
Senegal River					
Bafing	Bafing Makana		1983 μ	-0.33	(-0.88, -0.12)
Bafing	Daka Saidou		1980 μ 2000 σ	-0.15	(-0.72, 0.51)
Bakoye	Oualia		1983 μ 1994 σ	-0.15	(-0.37, 0.48)
Falémé	Gourbassi		1983 μ	-0.06	(-0.41, 0.14)
Falémé	Kidira		1984 μ 1995 σ	-0.03	(-0.69, 0.49)
Senegal	Kayes		1984 μ	-0.03	(-0.40, 0.18)
Senegal	Bakel		1984 μ	-0.13	(-0.71, 0.05)
Niger River					
Niger	Sahelian Niger River		1968 μ	0.37	(-0.17, 0.87)
Dargol	Kakassi		1990 μ	0.14	(-0.17, 0.48)
Gorouol	Alcongui			-0.08	(-0.50, 0.28)
Sirba	Garbe Kourou		1997 μ 1977 σ	0.18	(-0.20, 0.70)

Figure 2.6 visualizes an example of these models, with moving window parameter values (circles) and selected NS-GEV model μ values (line). Con-

confidence intervals for μ are shown with dashed lines. One can see that the selected models follow the general trends seen in the moving window parameter estimation of μ .

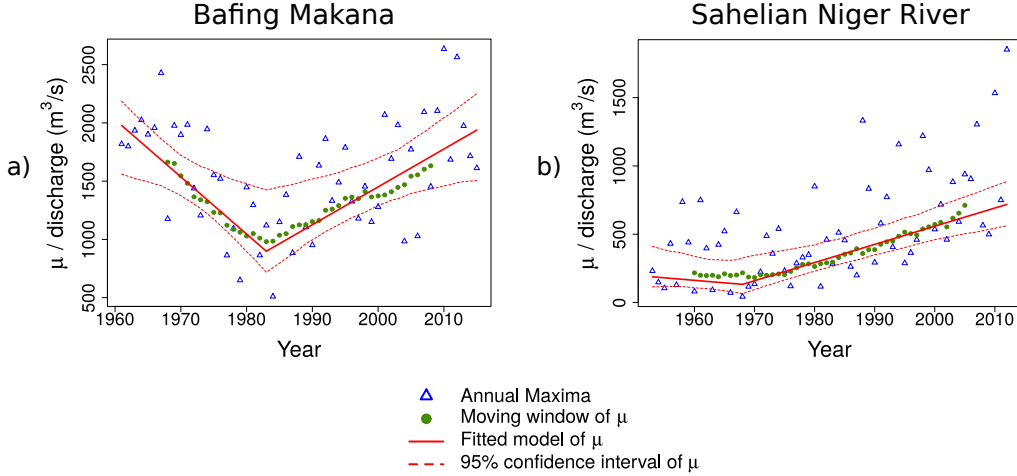


Figure 2.6: NS-GEV model for the Bafing Makana station (a) and SNR data series (b) with raw AMAX values (triangles), moving window estimates (circles), μ evolution for the NS-GEV model (solid line), and 95% confidence intervals for μ for the NS-GEV model (dashed lines).

A double linear model was selected for μ for all stations, with the exception of the Alcongui station in the Gorouol basin which was best represented by a linear model for μ (although a double linear model would have been accepted at $\alpha = 0.15$). The selection of a double linear model indicates that the slope of the trend for μ differed significantly between two subperiods of the time series.

In the Senegal River basin, significant breakpoints were consistently found for μ between 1980 and 1984 for all stations. The slope of the central tendency was negative (decreasing trend) during the period up until the early-mid 1980s, then became positive through the modern period. The changes in μ were less rapid in all stations during the latter period. Kayes and Bakel (the two stations downstream of the Manantali Dam) showed the least relative increase of all stations. Of the stations in the Senegal River basin, the Daka Saidou, Kidira, and Oualia stations demonstrated significant non-stationarity in the scale parameter (σ). All non-stationarity σ models were double linear.

Daka Saidou's breakpoint for σ was in 2000, while Kidira and Oualia both occurred in the 1990s (1995 and 1994 respectively). This reflects the general decrease throughout the majority of the time period under study then rapid increase in variability seen in the moving window for σ during the 1990s at these stations.

For the Sahelian stations in the Niger River, all stations showed an increasing trend starting as early as the 1970s. However, the specific model characteristics were less homogeneous between the different stations than for the Senegal River stations. Although all models were double linear for μ , breakpoints for μ were found in the 1990 for the Dargol (at Kakassi) and 1997 for the Sirba (at Garbe Kourou). The slope of the trend was positive for both subperiods for these two stations, with a greater (more rapidly increasing) slope during the more recent period. For the SNR data series, the slope was gradually decreasing during the earlier period of record up until 1968, then increasing at a higher absolute magnitude during the more recent period. The Gorouol series (at Alcongui) was linearly increasing throughout the period for μ . The SNR and Sirba, series showed significant trends in the σ parameter. For the SNR series, the change in σ was determined to be linearly increasing. For the Sirba, the model for σ was double linear with a breakpoint in 1977. The models closely follow the moving window estimates.

2.6.2 Extreme discharge tails behavior

Table 2.2 also shows the most likely ξ values for each distribution. A heavy-tailed GEV distribution ($\xi > 0$) indicates that larger values are possible (and more probable than if $\xi = 0$). $\xi < 0$ means that the distribution is bounded; rare values will approach but not exceed a maximum threshold.

For the Senegal River, all ξ values were either close to zero (Gumbel distribution, unbounded but not heavy-tailed) or negative (Weibull distribution). Almost all ξ values for the Sahelian Niger basin stations were positive (Frechet distribution), which means the distribution of the values is heavy-tailed without an upper bound. The exception was the Gorouol station at Alcongui, which had a slightly negative ξ value (Weibull distribution, bounded). However, the 95% confidence intervals for ξ for all stations in both river basins included both positive values and negative values, with the exception of the Bafing Makana station where the interval was entirely in the negative range (Weibull distribution).

2.6.3 Return level estimates of selected models

The main practical advantage provided by the NS-GEV models is the ability to estimate return levels from the fitted distribution. This is illustrated in Figure 2.7 where 2, 10, and 100-year return levels are plotted with their 90% confidence intervals for the Bafing Makana and Dargol stations. Return levels in the Senegal basin followed the general pattern of Bafing Makana, first decreasing below the stationary level then increasing again. Return levels for the stations studied in the Niger River started increasing earlier than for the Senegal River.

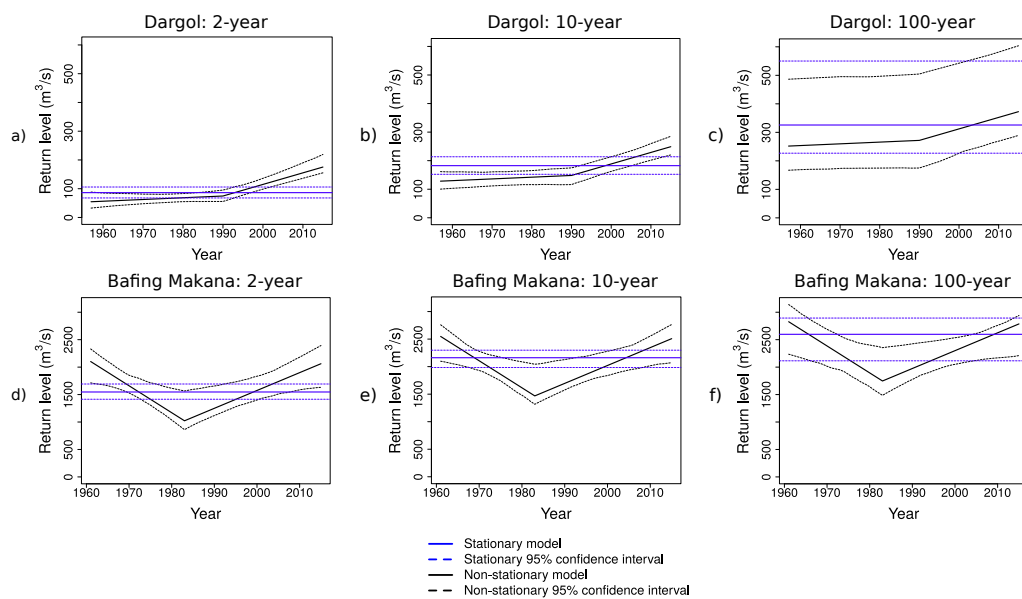


Figure 2.7: 2-year, 10-year, and 100-year return level values for the Dargol (a-c) and Bafing Makana (d-f) stations, with the NS-GEV values compared to the stationary model. Note that the 95% confidence interval for the NS-GEV return level completely exceeds the confidence interval for the stationary model for the 2-year return level, but for the 100-year return level the confidence intervals of the stationary model and the NS-GEV largely overlap.

Note the increase in the size of the confidence level with the longer return periods. For shorter (2 and 5-year) return periods, the confidence intervals for the non-stationary model were more likely to be distinctly higher than those of the stationary model. Especially at 10-year and longer return levels, the

confidence intervals of the stationary and non-stationary models increasingly overlap. Figure 2.8 demonstrates this separation and overlap between the confidence intervals of the stationary model and the chosen NS-GEV model for each station over time. The shades on the graph indicate up to which degree of confidence (80%-99%) the NS-GEV model and S-GEV model return level confidence intervals are disjoint, with the color indicating whether the NS-GEV confidence interval was centered higher (red) or lower (blue) than the confidence interval of the S-GEV model.

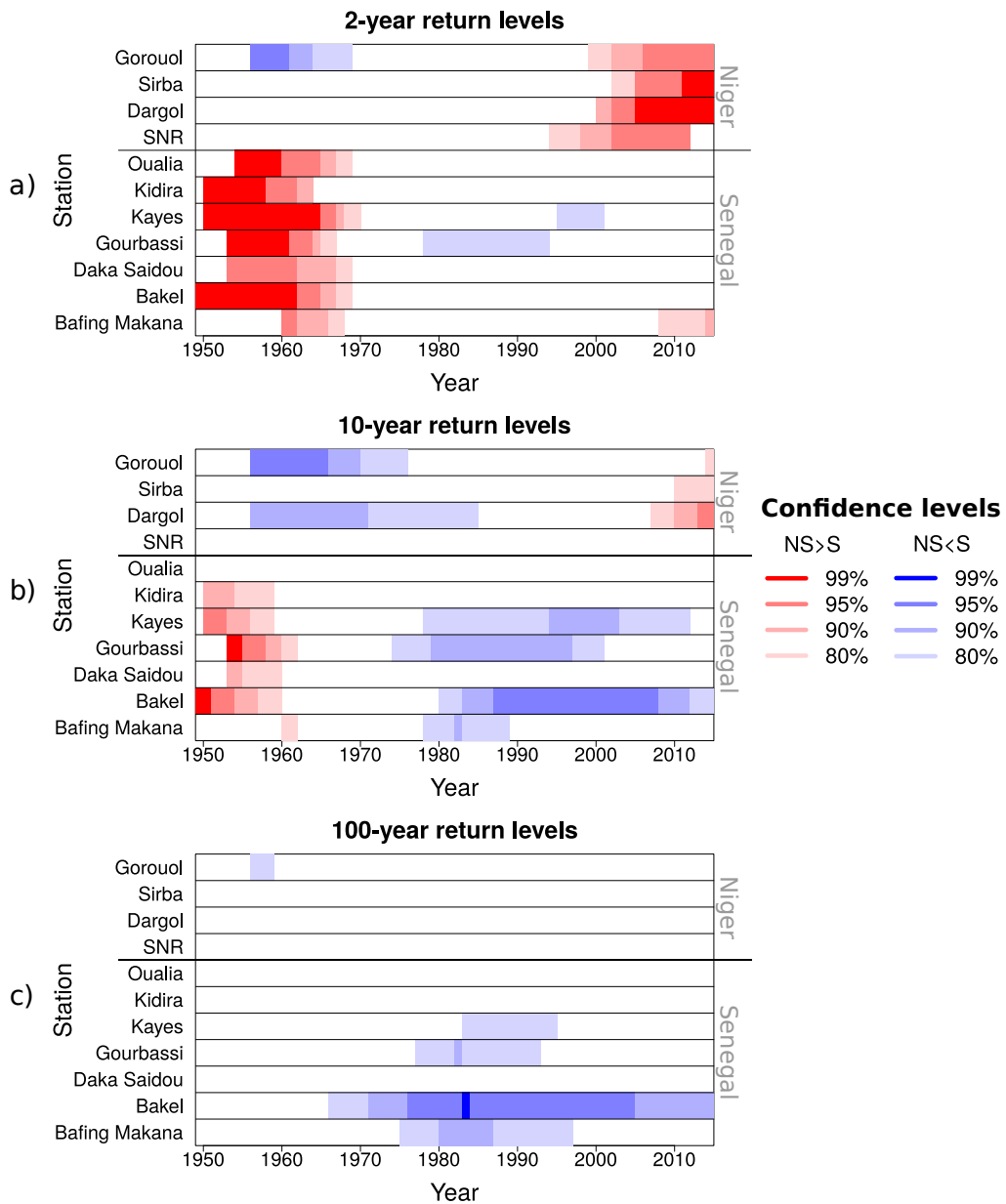


Figure 2.8: Significance of the separation between NS-GEV and S-GEV models over time by station for 2-year (a), 10-year (b), and 100-year (c) return levels. The separation is measured by the overlap between the confidence intervals of the model. Red indicates that the NS-GEV was significantly higher than the S-GEV (lower bound of the NS-GEV confidence interval greater than the upper bound of the S-GEV confidence interval at a given level of confidence), whereas blue indicates that the NS-GEV was significantly lower than the S-GEV (upper bound of the NS-GEV confidence interval less than the lower bound of the S-GEV confidence interval at a given level of confidence). The shade indicates the confidence level at which the intervals are disjoint at that point in time, ranging from 80%-99%.

One can note from Figure 2.8 that all of the Senegal stations were significantly above the S-GEV at the beginning of the record. For the 2-year return levels (2.8a), only Bafing Makana in Senegal was higher than its corresponding S-GEV at the end of the data record. The uncertainty increases with longer return periods, with none of the NS-GEVs significantly higher than the S-GEV at the end of the record for 25-year return levels or greater. NS-GEV return levels for the Oualia, Kidira, Gourbassi, and Daka Saidou stations were at approximately the stationary return level at the end of the study period or below the stationary level for longer return periods. Overall, the return levels of stations in the Senegal basin spend much of the period of record significantly below the S-GEV. One can note that the difference persists into the modern period for the Bakel data series, one of the stations affected by the Manantali Dam.

For the stations in the Niger River, at the most modern data points, the 90% confidence intervals surrounding the 2 and 5-year return levels globally surpassed the confidence intervals of the stationary return values. For the Sirba and Dargol, this separation existed also at the 99% confidence level, and at the 95% confidence level for the Gorouol. The exception was the SNR series whose lower non-stationary 90% confidence bound was slightly within the upper confidence bound of the stationary value for 5-year return levels.

Figure 2.9 compares the 2 and 5-year return level changes between all stations, with values normalized by each station's stationary return level (i.e. the return level estimated using the stationary GEV model, Equation 2.14). The separation in terms of return level evolution between the stations in the Senegal and Niger river basins is especially clear for the two-year return levels. The two-year return levels of the Senegal River stations (blue) start at around 1.5 times the stationary return level ($y\text{-axis} = 1$), reduce to as low as 0.5 during the 1980s, then increase throughout the modern period. Bakel and Kayes, the two Senegal stations affected by the Manantali Dam, have notably lower relative increases in return level values. These two stations reached to near the stationary return level value at the end of the study period, whereas the other stations all exceeded it and reaches values between 1 and 1.5 times the stationary return level. This shows the influence of the dam on trends in maximum values; one can hypothesize that without the influence of the dam, the stations Bakel and Kayes would have more closely followed the trend of the other stations that are located either upstream of the dam or on other tributaries of the Senegal River.

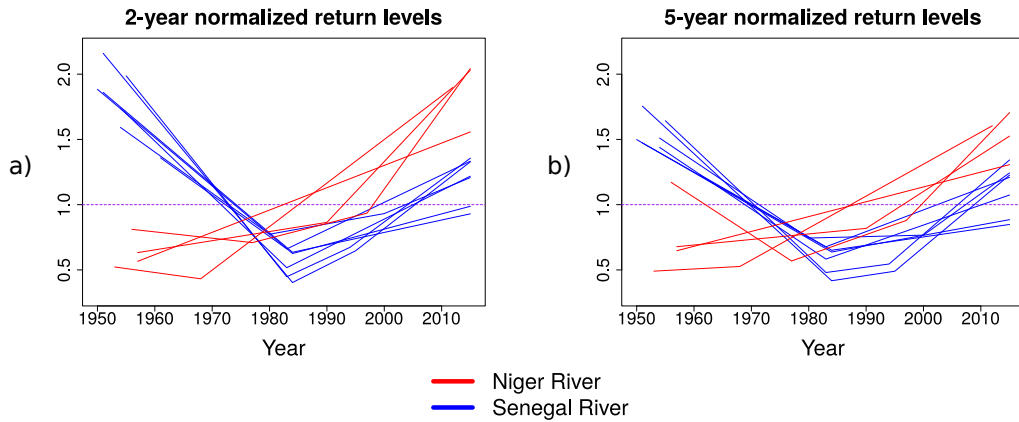


Figure 2.9: Normalized two-year (a) and 5-year (b) return levels for all stations. The red lines represent Sahelian stations, and the blue lines represent Sudano-Guinean stations.

For the Niger River stations (red), all stations started below the stationary 2-year return level and ended well above it. For most of stations the 2-year non-stationary return levels move from less than 0.7 to more than 1.5 times the stationary return level, meaning a doubling discharge for a two-year return period in roughly 50 years. The SNR series in particular tripled its relative value over the study period.

As for the five-year return levels, the regional separation becomes less clear due to the greater influence of the scale parameter at higher return levels. However, the relative decreases and increases by region remained similar. Bakel and Kayes remain relatively lower than the other Senegal stations.

2.6.4 Scale effects of drainage area

The absolute magnitude of the increase in μ was directly correlated with the size of the drainage area of a given station. However, no correlation was found in the relation between the relative increase in μ and the drainage area. For the Sahelian Niger, a moderate correlation (Pearson's $\rho = 0.6$) was found between drainage area and return level for return periods of 25 years or longer. The trend was more evident in the Senegal basin; when the stations Bakel and Kayes were removed, the correlation was greater than 0.6 for return periods of 5 years and longer. A similar correlation ($\rho \approx 0.6$) was

found between drainage area and the ξ parameter in both regions. The two-year return levels demonstrated little to no correlation with drainage area ($\rho = 0.25$). Given the limited number of data points, it is difficult to draw conclusions based on these results.

2.7 Discussion

2.7.1 Comparison of results with literature

The above results confirm the rising trend in extreme streamflow values since the 1970s and 1980s, previously found in other studies (Cassé and Gosset, 2015; Nka et al., 2015; Aich et al., 2016a).

The trends found in the Guinean stations in the Senegal River basin in this study followed the trends found in Aich et al., 2016a for the Guinean stations in the Niger River basin. In both studies a decreasing trend was found until approximately the mid-1980s, followed by an increasing trend. Results are overall consistent with Nka et al., 2015's findings that extreme discharge is reduced in recent years compared to what it was several decades ago. The models in the present study also detected a moderate increase in recent years, whereas in Nka et al., 2015 there was no significant trend since the 1970s.

The relatively lower trends at the Kayes and Bakel stations can be explained by the construction of the Manantali Dam upstream in 1988, which would have controlled many of the larger flows. This is in agreement with the results in Faye, 2015, which showed that monthly flow coefficients at Bakel were lower for peak season months in the period after dam construction than they were before dam construction. At the stations of Bafing Makana, Oualia, and Kidira, flow coefficients were higher for peak months when comparing the same time periods.

The breakpoint found at 1990 in the NS-GEV for the Dargol at Kakassi falls in between the breakpoints found by Nka et al., 2015 at 1987 (for AMAX) and 1993 (for peak over threshold values). For Sahelian stations, Aich et al., 2016a found a decreasing trend until the 1970s followed by an increasing trend. The initial decrease was found only in the SNR and Gorouol series, but all Sahelian stations tested show an increase since the 1970s. A breakpoint was found in the mid 1970s for the Sirba and early 1970s for the Gorouol, which is roughly consistent with the results in the present study.

The shifts in trends found in the SNR series (1968) and Gorouol series (1972) falls at the same point in time as the general climate shift in the late 1960s, as well as the mean discharge breakpoint identified in Tarhule et al., 2015. However, whereas the climate and mean streamflow shifts decreased after the break, the SNR series (and likewise all series for the Sahelian Niger) went from a low or negative slope to a positive slope. This is reflective of the well-documented Sahelian paradox (Albergel, 1987; Descroix et al., 2018) where locally-generated streamflow in the Sahel began increasing during the drought period, in spite of an overall reduction in rainfall.

2.7.2 Evaluation of the parameter ξ

In addition to the difference in timing and magnitude of trends between the Sudano-Guinean and Sahelian regions, differences in the shape parameter ξ were also found. The fact that the NS-GEVs for Sudano-Guinean stations were generally Weibull or Gumbel ($\xi \leq 0$) and Sahelian stations were generally Frechet ($\xi > 0$) could be due to the differences in hydrological functioning.

In the Sudano-Guinean region, the flow type is Hewlettian and groundwater plays a greater role. A larger portion of the precipitation first infiltrates and contributes to river discharge at a later time, smoothing out the high spatio-temporal variability of fine-scale rainfall intensities. Flood generation is thus sensitive to both the initial conditions of the basin (groundwater storage, subsurface water, etc) and the amount of rainfall accumulated over the basin. In the Sahel, streamflow is driven by Hortonian processes (local precipitation-generated runoff) and therefore is sensitive to the intensity of rainfall at small scales. The role of initial conditions seems to be smaller in comparison to factors such as the area affected by high intensities over a short time period. These differences in the spatio-temporal scale of the processes primarily responsible for flood generation in the two regions could explain in part the differences in the tail behavior of extreme discharges between the two regions. Indeed, it is observed that rainfall at fine spatio-temporal scales (Sahelian flood generation) has heavy tail behavior (Koutsoyiannis, 2004; Panthou et al., 2012), while rainfall averaged over larger spatio-temporal scales (Sudano-Guinean flood generation) is expected to have bounded tail behavior.

This said, great care must be taken in drawing conclusions from results for ξ as the confidence intervals are large (Table 2.2) and include both pos-

itive (Frechet) and negative (Weibull) values for almost all stations. The confidence intervals themselves seem to indicate a difference in tail behavior between the two regions; the lower bounds of the 95% confidence intervals for ξ in the Senegal catchments are much lower than the lower bounds in the Sahelian Niger catchments (with the exception of the Gorouol), and the upper bounds are generally lower in the Senegal basin as well (though less universally). However, due to the great overlap between the confidence intervals, it is difficult to draw conclusions with a high level of certitude.

2.7.3 Sensitivity analyses: robustness of the results

Sensitivity of the model selection process to the different tests and the p-value threshold chosen for the LRT

For three out of the eleven data series, the additional application of the LRT test modified the model selection. In all three cases, the model became simpler: the scale parameter (σ) for Bakel became stationary, the location parameter of Kayes became double linear instead of triple linear, and the Gorouol model became simple linear for μ instead of double linear.

For ten out of the eleven data series, the model selection did not change with an increase in LRT test stringency, with the p-value equaling 0.05. The only change with the stricter requirement were that σ became stationary for the SNR series

With less strict criteria ($\alpha = 0.15$), the results more closely approximated the initial AIC selection results. σ was modeled as linear non-stationary for the Bakel station, instead of the stationary model for σ selected at the $\alpha = 0.10$ significance level. The Gorouol station became double linear for μ and stationary for σ . The Kayes station NS-GEV at the p-value of 0.15 was a double linear model for μ and a simple linear model for σ . The general trends (strongly positive over the past few decades for μ and return levels) did not change with the choice of the model.

Of note at the $\alpha = 0.15$ significance level is the triple-linear model selected for μ for Kayes. The Kayes station's flow has clearly been regulated by the installation of the Manantali dam in 1988, which may have resulted in three distinct phases over the study period rather than two.

Sensitivity of the model parameters to optimization methodology

The choice of MLE parameter optimization method did not have a significant impact on model parameter results, nor on model selection results. Optimization methods tested were Nelder-Mead (Nelder and Mead, 1965), BFGS (Shanno, 1970), conjugate gradients (Fletcher and Reeves, 1964), L-BFGS-B (Byrd et al., 1995), and simulated annealing (Bélisle, 1992). However, the boundary limit between breakpoints and the edge of the data series did have an impact on the selection of the breakpoint. This could be of interest as the main breakpoint in the early-mid 1980s in Senegal was less than ten years before the construction of the Manantali dam. As a triple-linear model with a distance between breakpoints of one decade was almost selected (initial AIC model selection) for the Kayes station which is downstream of the dam, the limitation could have had an impact on model selection.

Additional sources of uncertainty

One source of uncertainty lies in the accuracy of the rating curves for each of the stations in this study (Jalbert et al., 2011; Morlot et al., 2014). Rating curves in regions subject to sedimentation such as the Sahelian Niger River basin risk being nonstationary in time. Rating curves may also be less accurate for extreme values if measurements of flow of comparable magnitude were not used in the rating curve calibration. Although some stations (notably Kidira, Bakel, Daka Saidou, and Niamey) included such large values, this was not the case for all stations.

However, rating curve uncertainties, while possibly influencing the specific magnitudes of results, are highly unlikely to be the cause of the consistent trends detected and thus do not alter the conclusions of the present study. Trend detection was conducted using a regional approach with two large river basins within the region and several stations within each river basin. The regional approach makes the methods robust and smooths the effect of uncertainty related to rating curves.

One can also question the influence of the choice of breakpoint on the uncertainty of the results. Sensitivity testing was performed with the Bafing Makana and SNR series over a breakpoint range of five years before and after the breakpoint of the selected model. The spread of the 95% confidence interval of the selected model (one fixed breakpoint) was compared with the spread of the global confidence interval obtained from the range of

breakpoints. The area within the global confidence interval but outside the selected model’s confidence interval is due to breakpoint uncertainty. Based on this, the contribution of breakpoint estimation uncertainty to the overall uncertainty is on average 13% for Bafing Makana and 15% for SNR for a breakpoint range of plus and minus five years from the selected breakpoint. It was thus verified that the primary source of uncertainty comes from the GEV calibration process performed in step 2 of subsection 2.5.3 (uncertainty of the η_i) and not from uncertainty about the position of the breakpoint.

2.8 Conclusions and implications

The preceding analysis proposed a selection of NS-GEV models for hydrological annual maxima in West Africa. In all cases, the NS-GEV model was significantly more representative of the data series than the stationary GEV model. The trend is positive since the 1970s for the Sahelian stations and the mid-1980s in the Sudano-Guinean stations, with both regions demonstrating an intensification of the hydrological signal. Certain parameters and return levels, notably the μ parameter and the 2 and 5-year return levels, surpass the values expected with a stationary model with a high level of confidence at certain stations.

The results improve over other studies by providing the underlying statistical distributions for the non-stationary data series, confidence intervals on parameter values, return level estimates, and a model selection process with robust criteria. It also compares two subregions, and notably includes an extracted data series for the cumulative Sahelian red flood inputs to the Niger River. Although West Africa is used as a test region, these analyses can be applied to hydrological time series elsewhere in the world.

The methods used in this paper have some limitations. First, only parametric models that were preselected as potential best models are evaluated, thus eliminating a large range of other potential models. Second, the study only consider breakpoints that are transitions from one linear slope magnitude to another, not abrupt shifts. Furthermore, uncertainty is high (which reflects the current reality). The uncertainty is especially high for the ξ parameter, which represents the rarest of the AMAX values and is also the most difficult parameter to estimate precisely. The methods also require a certain level of expertise for use and interpretation. Additionally, the estimated uncertainties do not take into account the uncertainty in the estimation of

streamflow via rating curves, which could have a significant impact on the accuracy of extreme values (Jalbert et al., 2011; Morlot et al., 2014).

However, the methods proposed in the present study are advantageous for several reasons. It is possible to use other trend and breakpoint detection methods, but many of these tests assume that the data is normally distributed (which is not the case with extremes) and thus will not be robust with data sets consisting of extreme values. Classic breakpoint detection tests (such as the Pettitt test) may work but do not provide an estimate of the magnitude of the trend. They also do not permit the estimation of return levels, which is a significant advantage of the methods based on fitting probability distributions proposed in this paper. The power of classical trend and breakpoint tests to reject the null hypothesis when applied to extreme value series is also known to be lower than when applying tests specific to GEVs. Moreover, even if some expertise is required to use them, the R packages used in this study are freely available (Heffernan et al., 2016).

The results for the return level estimates indicate that if the stationary model were to be used, it would underestimate the current return levels in the Sahelian reaches of the Niger River. For example, the non-stationary ten-year return level for the SNR series in 2012 is $600 \text{ m}^3 \text{ s}^{-1}$ larger than the value estimated from a stationary model. For all four data series in the Sahelian Niger, at the end of the data record (2012-2015), the non-stationary 2-year return level exceeds the 5-year stationary return level, indicating an increase in frequency of events of greater magnitude.

The nonstationarity of the return levels has direct implications for hydraulic works construction and river basin management. In both Sahelian and Sudanian areas, the identified increase of 2 to 10-year return levels is important for small structures and might have contributed to the increasing number of damaged and destroyed bridges and roads reported over the last decades (Amani and Paturel, 2017). In the Senegal basin, an accurate estimation of higher return level values (for return periods greater than 25 years) is needed not only for the management of existing dams such as the ones at Manantali, Diama and Félou, but also for the construction of additional structures such as spillways and the hydroelectric dams planned by the Organization for the Valorization of the Senegal River (in French, OMVS, see Bonneau, 2001). As the region surrounding Niamey in the Niger Basin continues to be threatened by severe flooding, accurate return level estimates are required in order to ensure that flood protection systems can protect against a given flood. In all of the above cases, if a stationary model is used, it risks

overestimating or underestimating the magnitude of river discharge.

Uncertainty remains high for longer return periods. This is largely tied to the size and variability of the data set; estimating a 100-year return level based on only 60 years of data forcibly has a high level of uncertainty. The uncertainty of longer return levels is closely tied to the ξ parameter, which governs tail behavior and is notoriously challenging to estimate, especially with limited data. As more data is collected, uncertainty will decrease and the ability to more precisely estimate return levels for longer return periods will likely improve, provided that the data is represented by a model that best suits its trends.

One way to improve the estimation of ξ and as a result the estimation of return levels for longer periods would be to apply a regionalized approach incorporating data sets within the same region that are believed to have similar tail behavior. With the use of additional data, the estimation becomes more robust and the level of certainty increases. An example of how a regionalized approach may be used to calculate the ξ parameter may be found in Sun et al. (2015).

Uncertainty may also be reduced with a greater understanding of flood drivers. Much speculation and study has occurred in attempt to determine the causes of the changes in flood peaks in the West Africa (Seguis et al., 2004; Leblanc et al., 2008; d'Orgeval et al., 2008; Descroix et al., 2009, 2012, 2018; Aich et al., 2015; Cassé and Gosset, 2015; Cassé et al., 2016). In addition to climate changes, West Africa has undergone extensive land cover changes (Loireau, 1998; Anyamba and Tucker, 2005; Descroix et al., 2009) including a considerable increase in the percentage of cultivated area from the 1950s-2000s (Cappelaere et al., 2009).

Whereas much of the “Sahelian Paradox” during the drought can be attributed to land use/land cover changes, in recent years changes in river discharge seems to correlate more with changes in precipitation. Case in point, the regional trends found in this study follow those found for mean non-zero rainfall in Senegal and the central Sahel in Blanchet et al., 2018. The issue is complex; for example, in the present study the Sirba basin streamflow did not increase as much as that of the Dargol and Gorouol, yet it both receives more rainfall (500 mm as opposed to 400 mm annually) and had increased runoff coefficients, most likely due to the impacts of agriculture (Descroix et al., 2012). Land use and climate also have impacts at different scales (Blöschl et al., 2007). On a larger scale, teleconnections between climate processes and local hydrology may provide insight into the evolution of AMAX behav-

ior. One may, for example, use a climate indice linked to ENSO in place of a temporal covariate (Sun et al., 2015).

An improved understanding of the attributed causes of trends in extremes would give guidelines for the projection of pertinent results into the future. Such an approach would require coupling NS-GEV models with projected climate and land use changes. Factors to be taken take into account are both climate projections at the scale of hydrological processes and socio-economic scenarios that allow for the estimation of the anthropic pressure on the soil and the resulting changes in hydrodynamic parameters. Projection of model results into the future, however, must be done with caution due to the potential of future shifts in trends and decadal variability not accounted for in the climate and land use trends.

We recommend that those dimensioning hydraulic works seriously consider the possibility that hydrological extremes are increasing, as this is the current evidence available. This is especially pertinent for the coming decade over which evidence supports an increasing frequency of extreme rainfall and ongoing hydrological intensification (Taylor et al., 2017; Panthou et al., 2018). With this in mind, we recommend that stakeholders design structures with a shorter design life span (10-20 years) with the assumption that extremes will most probably increase. Such structures include flumes, small urban hydraulic structures, pumps, levees, and smaller dams. For longer-life structures such as large dams and spillways, they should continue to consider all factors, including the possibility that the trend may change and decrease again. Despite the potential impacts of projected land use changes and the ongoing warming of the Sahara that triggers intense rainfall events, the decadal variability of climate in the region is also likely to continue.

In spite of the uncertainties, the present study concludes within a strict level of confidence that hydrological extremes are currently increasing, and although uncertainty about the magnitude of this increase is high, it is more concrete and certain than speculation about an unknown future. The trends are consistent for all stations within each watershed despite flow uncertainties. We advise that stakeholders place importance on the possibility of greater and more frequent flood magnitudes, especially while designing smaller structures but also for larger structures. We further recommend that they take causal factors into account, although more studies are needed in order to understand the mechanisms of flood drivers.

Acknowledgements

The research leading to these results has received funding from the NERC/DFID Future Climate For Africa program under the AMMA-2050 project, grant NE/M020428/1. This work was also supported by the French national program EC2CO-LEFE "Recent evolution of hydro-climatic hazards in the Sahel: detection and attribution." Ansoumana Bodian benefited from a grant received from the French Embassy in Senegal which financed exchanges with other researchers. We warmly acknowledge the Niger Basin Authority (ABN) and the Organisation pour la Mise en Valeur du Fleuve Sénégal (OMVS) for providing the Niger River and Senegal River discharge data.

Chapter 3

Precipitation modeling and scenario generation

3.1 Introduction to article 2

Several drivers could have provoked a change in the statistical characteristics of extreme streamflow. One potential key driver of hydrological extremes is an increase in precipitation, especially in the Sahel region where hydrological processes are dominated by Hortonian overland flow. The impact of precipitation is particularly high for the rainfed ephemeral tributaries of the Niger River in the Sahelian zone: the Sirba, Dargol, and Gorouol. A change in precipitation could impact local streamflow.

Long-term hydrological changes in the region are expected to be driven by changes in soil surface properties and precipitation regimes, both with impacts at fine scales. To understand the impacts, one must accordingly make use of fine-scale physically-based models.

Daily rainfall series are available within the subbasins of the Sahelian tributary, but the network density, length of the time series, and resolution of the time step are not appropriate for forcing physically-based hydrological models. This is due to the time scale of processes that govern the partitioning of the water. The same considerations are also true for other impact studies and models (e.g. in agronomy and ecology).

A rainfall simulator can generate scenarios at sufficiently high spatiotemporal resolutions for hydrological impact studies. It can be used to provide realistic simulated data series at points where there are no in-situ measure-

ments, and to produce scenarios for testing hypotheses about how changes in precipitation affect hydrology.

In the following article, a stochastic precipitation simulator was improved and tested using the 30 rain gauges of the AMMA-CATCH Niger data set, located near to Niamey, Niger, within the Sahelian climate zone. The article is currently in the process of exchanging between coauthors, and the results being refined before submission.

3.1.1 Personal contributions

Acquiring proficiency in the use of a precipitation model and its recent developments

In this part of my thesis, I inherited a rainfall simulator that has been developed over the course of over 20 years. I received it in its most recent state after the work of Claire Aly, which was primarily a) modeling both large convective systems and smaller events in order to account for the 10% of annual cumulative values that the previous simulator versions were missing, b) explicitly modeling extreme values above a certain threshold for large storms, c) incorporating the use of censored likelihood for model parameter estimation, and d) modifying the spatial storm structure used in the model. She also developed a method of temporal disaggregation that simulated maximum event intensities at five minutes from a gamma distribution by class of cumulative event rainfall. The changes and the simulator as a whole were consolidated into an R package at this stage.

Model and data evaluation

As the first besides C. Aly to use the R package and the associated new changes, my role was to master the use of the simulator and test its implementation. I used the tools contained within the package and my own personal additions to validate C. Aly's findings. I compared simulator parameters and outputs between different data sets. I developed my own scripts and functions that combined the different calibration and simulation steps into a smooth workflow.

Minor improvements that I made mostly consisted of ensuring that the code would be applicable to a wide range of precipitation data sets other than the initial data used for development. I also divided simulation functions

into smaller steps in order to test and evaluate results at each step of the simulation process.

A preliminary analysis of AMMA-CATCH rainfall data was also conducted and can be found in Appendix B.

New developments: Temporal disaggregation approach

The most major modification to the simulator in which I participated was the development of the temporal disaggregation methodology. The initial version of the simulator linked the maximum event intensity to the cumulative event rainfall via a linear relationship. This, however, does not represent the natural variability in intensities, and commonly produces simulated events that are unrealistically strong.

As previously mentioned, C. Aly proposed a method that instead linked maximum intensities to cumulative precipitation via a gamma distribution divided into different classes. We decided to instead explore a continuous beta distribution with upper and lower bounds in order to constrain maximum intensities into a somewhat realistic range while still representing the variability in intensities. The four parameters of the beta distribution all depended on the value of cumulative event precipitation as a covariate. My role was to identify suitable upper and lower bounds and develop the code for implementing the beta distribution method into the simulator, including the choice of parameter covariates.

Article writing and conferences

The following article presents the changes developed by both C. Aly and myself, with guidance from other members of the research team. My primary role for the article was to create the first complete draft by proposing the initial introduction and framework for the paper, assembling and developing the text for the methodology, producing the figures and tables, and incorporating coauthor remarks. Results were presented at the EGU 2019 General Assembly.

3.2 Stochastorm: A stochastic rainfall simulator for the intertropical zone

Abstract Stochastic rainfall generators aim to reproduce the main statistical features of rainfall occurrence and intensity at small spatial and temporal scales. Used to simulate long-term synthetic rainfall series, they are recognized as suitable for use with impact analysis in the fields of water, agricultural, and ecological management.

While many stochastic rainfall generators have been developed in the last decades and applied in regions with contrasted climates, only a few of them have been developed and used in intertropical regions. The largely convection-driven rainfall in the intertropical belt presents properties that need to be specifically considered and included in stochastic rainfall generators. These include (i) a strong rainfall intermittency, (ii) high variability of intensities within storms, (iii) strong spatiotemporal correlation of intensities, and (iv) a marked seasonality that affects the statistical properties of storms (i.e. occurrence, intensity). In addition, intertropical storms are among the most powerful on Earth, and an intensification of the most extreme ones is already observed in some regions, tied to global warming.

In this paper, improvements for an existing statistico-dynamic rainfall generator that models convective storm systems in the intertropical zone are presented. Notable improvements include (i) the ability to model the occurrence of precipitation events via a model based on the distribution of the inter-event time parameter, (ii) an improved temporal disaggregation scheme that better represents the rainfall distribution at all sub-event scales, and (iii) the use of covariates that reflect seasonal changes in precipitation occurrence and marginal distribution parameters. Extreme values are explicitly considered in the distribution of storm event intensities. In this study, the simulator is implemented in the Sahelian region, specifically in southwest Niger. The simulator is calibrated and the simulations validated using 28 years of 5-minute precipitation data from the 30 rain gauge AMMA-CATCH network. The simulation is used to generate both large propagative systems and smaller local convective precipitation. Results show that the improvements in the simulator coherently represent the local climatology. The simulator can be used to generate scenarios for hydrological and agricultural impact studies with a more accurate representation of convective precipitation characteristics.

Authors Catherine Wilcox, Claire Aly, Théo Vischel, G er emy Panthou, Juliette Blanchet, Guillaume Quantin, Thierry Lebel

3.3 Introduction

Stochastic rainfall generators aim to simulate realistic rainfall series by reproducing key statistical features that characterize rainfall variability. Commonly modeled elements include rainfall occurrence, intensity, and dependence structures in time and/or space. As stochastic rainfall generators are suitable for generating long-term rainfall sequences at fine resolutions, they are useful in many applications: conducting risk assessment studies to estimate the return periods of very rare events (Evin et al., 2018; Arnaud et al., 2016); and assessment of rainfall estimation uncertainties and their propagation into impact models (Renard et al., 2011; Borgomeo et al., 2014), to name a few. These statistical models are complementary to physical atmospheric or climate models as they can be used in climate change impact studies as a means to downscale and disaggregate coarse-resolution climate model rainfall outputs (Wilks, 2010; S rup et al., 2016; Peres and Cancelliere, 2018). For these reasons, stochastic rainfall models are recognized as useful tools in numerous areas of environmental sciences for which rainfall is of major influence, for instance hydrology, agronomy, and ecology.

While many stochastic rainfall generators have been developed over the last decades (see Wilks and Wilby (1999); Ailliot et al. (2015); Vu et al. (2018); Loveridge and Rahman (2018) for a review) and applied in regions with contrasted climates, only a few of them have been used in intertropical regions. A first reason is that the tropics are sparsely-monitored regions, a factor which limits the possibility to infer the statistical parameters of stochastic rainfall generators, especially for rainfall properties at sub-daily scales. A second reason is that the intertropical belt presents specific rainfall characteristics that are rarely considered and included in stochastic rainfall generators. Precipitation events in the tropics are mainly, if not exclusively, due to convective storms. These storms can be very localized due to local convection processes, but mostly are long life cycle propagative convective systems sometimes referred to as mesoscale convective systems (MCS). They are largely driven by synoptic atmospheric processes that take place in regional climate systems such as seasonal monsoons.

One of the distinct properties of intertropical precipitation regimes and

storms is a markedly strong seasonality. The movement of the intertropical convergence zone (ITCZ) provokes strong trends on convective storm development and propagation. These dynamics generate strong seasonal signals that are generally consistent from one year to another, but that are also susceptible to evolve or cycle over time.

In addition, intertropical storms are some of the most powerful on the Earth (Zipser et al., 2006), and an intensification of the most extreme ones is already observed in some regions in the Tropics, tied to global warming (Taylor et al., 2017; Tan et al., 2015). MCSs have been shown to be associated with extreme rainfall events (Schumacher and Johnson, 2005). This underlines the need to specifically treat extreme intensities in rainfall generators in this region.

Given the nature of convective systems, tropical storms are characterized by a strong intermittency of rainfall, a high variability of intensities within storms, and a strong correlation of intensities in time and space. An appropriate rainfall generator for tropical storms would thus need to simulate spatio-temporal rain fields and not independent single site precipitation series.

Among the variety of stochastic rainfall generators, those aiming at simulating spatiotemporal rainfall fields are often divided in two classes: multi-site and random fields models. The first are an extension of single-site stochastic models over several distant locations (often corresponding to rain-gages). They are mainly based on non-parametric resampling methods, on parametric point processes based on the successive use of statistical rainfall occurrence and a statistical rainfall amount model, or on cluster point processes (Cowpertwait et al., 1996; Wilks, 1998). The second category focuses on continuously simulating (on regular grids) the spatial variability of rainfall. This family includes rain cell models (Féral et al., 2003), scale invariance models (Serinaldi, 2010; Lombardo et al., 2017; Raut et al., 2018) and meta-Gaussian random fields (Benoit and Mariethoz, 2017). The latter group of models - meta-Gaussian fields - is considered in this paper as a suitable method for modeling the spatiotemporal properties of convective storm systems in the intertropical zone.

Some promising developments in rain field modeling have been made in other regions. Peleg and Morin (2014)'s model produced both convective storm cells and areas of low-intensity rainfall. Oriani et al. (2017) and Singer and Michaelides (2017) conditioned their models' parameters on factors such as elevation and weather state. Lee (2018) improved methods of spatial cor-

relation for the copula method of modeling marginal distributions. Baxevani and Lennartsson (2015) and Bárdossy and Pegram (2016) developed Gaussian field precipitation models that are dependent on both space and time.

Regarding extreme events, Baxevani and Lennartsson (2015) and Evin et al. (2018) proposed modeling precipitation magnitudes with a gamma distribution for smaller values and a generalized pareto distribution (GPD) for larger values (for Baxevani and Lennartsson (2015), above a given threshold; for Evin et al. (2018), with a transition function as developed in Naveau et al. (2016)). Wilks (1999) evaluated various marginal distributions for their ability to reproduce extreme event characteristics.

A selection of stochastic rainfall generators have been developed and/or applied to modeling rain fields in the intertropical zone. Some, as in Cowden et al. (2008), provided stochastically generated series of rainfall amounts, but without a spatial structure, a potentially significant criteria for impact studies in the intertropical zone (Carney et al., 2008). Others provided only the occurrence of wet and dry days without rainfall amounts (Jimoh and Webster, 1999; Robertson et al., 2004). Several rain field simulations were developed for the intertropical zone based on the the Global Atmospheric Research Program Atlantic Tropical Experiment (GATE) dataset, including Valdes et al. (1990), Bell (1987), Ferraris et al 2003, and Over and Gupta (1994). The spatial structure of seasonal storms in Mexico City was evaluated in Bouvier et al. (2003).

A stochastic simulator developed for the Sahelian region of West Africa was initially presented in Lebel et al. (1998). Guillot and Lebel (1999a), Guillot and Lebel (1999b), and Balme et al. (2006) provided further developments for the spatial and temporal disaggregation respectively, and Onibon et al. (2004) proposed the Gibbs sampling method for the simulation of marginal distribution values. Vischel et al. (2009) explored point conditioning methods for the model. The above articles demonstrated that the precipitation model accurately reproduce both the spatial distribution and marginal distribution of precipitation events, an important characteristic for evaluating hydrological impacts (Troutman, 1983; Wilson et al., 1979). It also treated the problems of spatial and temporal disaggregation separately.

The rainfall simulator in its state for Vischel et al. (2009) did not take into account a few key variables, notably extreme values, the frequency of precipitation events, and the seasonal precipitation signal. The model also produced sub-event intensities that were stronger than those found in the record, an effect linked to the temporal disaggregation method. The choice of temporal

disaggregation method and the resulting synthetic hyetograph has direct impacts on simulated hydrological outputs (Lambourne and Stephenson, 1987).

Building on the rainfall simulator described in Vischel et al. (2009), this paper demonstrates recent advances in stochastically generating convective storm events. We propose an improved version named "Stochastorm" that models additional phenomena pertinent to the intertropical zone and relevant for driving impact models. Notable improvements in this paper include (i) the ability to model the occurrence of precipitation events via modeling the distribution of the inter-event time, (ii) the explicit consideration of extreme values in the distribution of storm event intensities, and (iii) an improved temporal-disaggregation scheme that better represents the rainfall distribution at all sub-event scales. The seasonality of the rainfall properties is taken into account by adding covariates that reflect seasonal changes in precipitation occurrence and marginal distribution parameters. In this study, the simulator is implemented in the Sahelian region, specifically over the AMMA-CATCH Observatory that covers an area of 10,000 km² in southwest Niger and provides 28 years of 5-minute precipitation data from the 30 recording rain gauges.

3.4 Stochastorm presentation

The principle of Stochastorm is to simulate a series of mesoscale convective rainfall events that have the same statistical characteristics as the general climatology of the study region. Factors considered include inter-event frequency, temporal intermittency, the magnitude and spatial coherence of cumulative event rainfall amounts, and the intensities at intra-event time steps.

3.4.1 Description of the previous version of the stochastic rainfall model

The following section describes the rainfall simulator (Lebel et al., 1998; Guillot and Lebel, 1999a; Vischel et al., 2009) in the state it was in before the most recent developments presented in Section 3.5.

Occurrence

The previous rainfall simulator did not explicitly model the moment in time that events occurred. It operated under the assumption that an event simulation meant that an MCS passed over the study/simulation window, but without assigning a specific time or date to the event. As rainfall occurrence is a major characteristic of a given rainfall regime, there is a need to simulate it in the rainfall generator.

Event-based rain fields

The stochastic simulation of event-based rain fields is achieved within the framework of meta-Gaussian random functions. It consists of deriving non-Gaussian random fields (in this study, rainfall fields at the event time scale) from Gaussian random fields by using an anamorphosis function (Guillot and Lebel, 1999a). Gaussian fields have well-known properties and can be generated more easily than spatial fields with other distributions (Emery, 2002). In the first version of the generator, Lebel et al. (1998) used the turning band method. Guillot and Lebel (1999b) implemented it with a nested anisotropic covariance function that was shown to be more appropriate to simulate the diversity of storms structures than in Lebel et al. (1998). Onibon et al. (2004) proposed to generate Gaussian fields by using the sequential method which, coupled with an acceptance-rejection algorithm, allows conditioning the simulations by surface average values.

The transformation/anamorphosis of Gaussian to non-Gaussian fields is the main difficulty of the meta-Gaussian framework. In particular, the appropriate spatial structure of the random Gaussian fields must be prescribed in order to reproduce the expected spatial structure and marginal distribution of the non-Gaussian fields after anamorphosis (see Section 2.2.3 for a more formal presentation). In case of discontinuous processes, like intermittent event-based rain fields which contain a mass of zero values in their marginal distribution, there is no analytical solution to assess the spatial structure function of Gaussian random fields (Guillot and Lebel, 1999a; Emery, 2002). While an empirical trial and error approach was used in the first version, Vischel et al. 2009 proposed to use a Gibbs sampling algorithm to assess the spatial structure function of Gaussian fields represented by a nested anisotropic variogram. The simulator as it was in Vischel et al. (2009) did not explicitly consider extreme values in the marginal distribution of cumulative event

rainfall.

Via the above methods, the marginal distribution and spatial structure of cumulative event rainfall amounts are obtained. The simulation outputs are punctual, with simulations recorded on locations determined by the user on a regular or irregular grid.

Temporal disaggregation

Temporal disaggregation, or simulating intensities at small time intervals within an event, is conducted with the aim of representing the physical properties of MCSs. This disaggregation is on a deterministic synthetic hyetograph of a convective storm which is here considered to consist of a symmetrical triangular peak representing the convective front of the storm, followed by a long stratiform trail of lower intensity (Figure 3.1). The hyetograph parameters (maximal intensity and duration) depend entirely on the total event rainfall via a relationship that evolved over the different model versions, the most recent being the relationship published in Balme et al. 2006. The temporal disaggregation also includes a model of MCS kinematics that consists of defining a field of hyetograph time of arrival based on prescribed MCS propagation speed and direction.

3.5 New developments and technical definitions

3.5.1 Season limits and intra-seasonal variability of parameters

Much of the intertropical zone characteristically has a wet season and a dry season. Start and end dates of the rainy season are modeled in Stochastorm with a separate normal distribution for each.

Several parameters in Stochastorm are permitted to evolve over time throughout the season according to the following equation:

$$param(t) = f_{param}(t, \theta_{param}) \quad (3.1)$$

where t is the time covariate, f_{param} the selected function for representing seasonality, and θ_{param} the vector of coefficients to be optimized for the function.

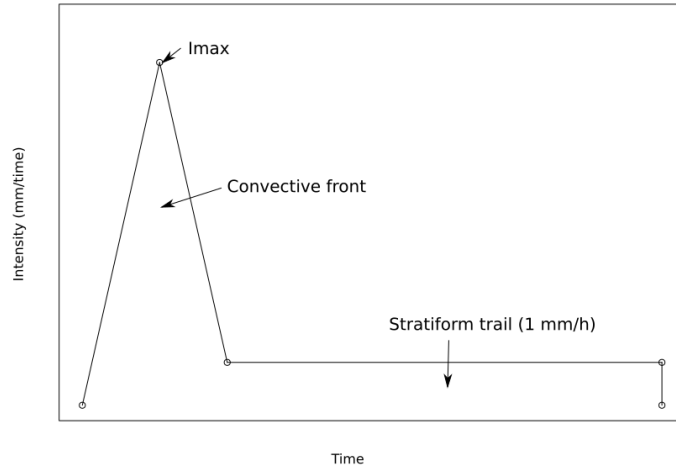


Figure 3.1: Standard hyetogram shape from Balme et al. (2006) implemented in Stochastorm, consisting of convective and stratiform parts.

The parameters obtained from calibrating the statistical distribution for a given variable in a moving window over the data are plotted. From these plots, the types of possible functions for seasonal covariates are estimated visually. Then, statistical distributions using the different possible seasonal covariates are calibrated over the entire data set. The covariate models are then compared using AIC and likelihood ratio tests. The choice of seasonal covariates may also be informed by knowledge about local climatology in the study region.

Hereafter, the symbol * is used to designate parameters that are permitted to vary in magnitude throughout the season.

Parameters are obtained by maximum likelihood estimation unless otherwise noted.

3.5.2 Event occurrence

The event occurrence in the new version Stochastorm is represented by the Inter-Event Time (IET), which here is defined as the time between the start times of two events.

The density of the gamma distribution is denoted $f_{\gamma}(x, b, k)$ with a scale

parameter $b > 0$ and a shape parameter $k > 0$ (equation 3.2).

$$f_\gamma(x, b, k) = \frac{1}{\Gamma(k)b^k} x^{k-1} e^{-\frac{x}{b}} \quad (3.2)$$

The gamma distribution could alternatively be formulated using mean (μ) and shape (k) parameters given the relationship $\mu = kb$.

The IET parameter is determined to follow a gamma distribution with x as the IET value, modeled using the time-varying scale ($*b_{IET}$) and shape ($*k_{IET}$) parameters.

3.5.3 Marginal distribution of cumulative event rainfall

The marginal distribution F_{cumul} of cumulative event rainfall at each station is defined by the probability of zero values, denoted by $*f_0$, and a combined distribution referred to as Gamma+GPD (F_γ, F_{GPD}).

$*f_0$ represents the proportion of zero values in a spatial rain field. $*f_0$ is assumed to be constant throughout the study region. It is fitted by least squares estimation.

Distribution of precipitation value magnitudes (F_γ, F_{GPD}) The magnitude of cumulative event precipitation is characterized with a two-part distribution similar to the approach used in Furrer and Katz (2008). Events with cumulative rainfall below a given threshold u are modeled by a gamma distribution for positive values as in equation 3.2 with a scale parameter $*b_{cumul}$ and a shape parameter $*k_{cumul}$. In order to explicitly represent the distribution of extreme rainfall values, over a certain threshold u the gamma distribution is replaced by a GPD distribution with a scale parameter σ_{GPD} and a shape parameter ξ_{GPD} . See Baxevani and Lennartsson (2015) for a similar approach.

Let Y be the random variable of rain at a given site, and F_γ and F_{GPD} be respectively the gamma and the GPD distributions. Then the marginal distribution F_{cumul} of cumulative rainfall can be written as

$$F_{cumul}(y) = \begin{cases} *f_0 + (1 - *f_0)F_\gamma(y, *b_{cumul}, *k_{cumul}) & \text{if } y < u, \\ f_u + (1 - f_u)F_{GPD}(y, \sigma_{GPD}, \xi_{GPD}) & \text{if } y \geq u, \end{cases} \quad (3.3)$$

where

$$f_u = {}^* f_0 + (1 - {}^* f_0)F_\gamma(u) \quad (3.4)$$

Since the gamma distribution only includes values below the threshold u , the gamma distribution is fitted by maximizing a censored likelihood (L^c) on positive data. Let y be the matrix $(y_{ij})_{i=1,\dots,N;j=1,\dots,K}$ of the data, where i is the station index, N the total number of stations, j the event index, and K the total number of events. The censored likelihood is then expressed as

$$L^c(y, {}^* b_{cumul}, {}^* k_{cumul}) = \prod_{0 < y_{ij} < u} f_\gamma(y_{ij}, {}^* b_{cumul}, {}^* k_{cumul}) \prod_{y_{ij} \geq u} [1 - F_\gamma(u, {}^* b_{cumul}, {}^* k_{cumul})] \quad (3.5)$$

where F_γ is the CDF of the gamma distribution and f_γ is the density.

In this study, the GPD is fitted by maximum likelihood estimation on values larger than u . The GPD does not have seasonal covariates.

3.5.4 Spatial dependency: Gaussian fields with censored likelihood

Transformation of data into censored Gaussian data As a prerequisite to determining the spatial covariance structure (see Section 3.4.1), the non-Gaussian measured rain fields are first transformed into the process H . H is a version of the Gaussian process G but censored below a certain limit due to the zero values within the rain field.

Let Φ denotes the $\mathcal{N}(0, 1)$ distribution. The following transformation is applied to the data for each event j ($j \in \{1, \dots, K\}$):

$$h_{ij} = \Phi^{-1}[F_{cumul_j}(y_{ij})] \quad (3.6)$$

where h is the Gaussian version of y . In this way, K (total number of events) realizations of a spatial process H are obtained. Note that for each event j , the Gaussian field realization h_j is censored below the Gaussian value c_{0_j} corresponding to 0mm in the observed rainfall field:

$$c_{0_j} = \Phi^{-1}[F_{cumul_j}(0)] \quad (3.7)$$

Note that the value c_{0_j} is different for each realization due to the temporal dependence of F_{cumul} on t .

Estimating the covariance function In order to simulate the process H , the covariance function ρ of the process G must first be estimated. The Gibbs sampling algorithm proposed in the last model version (Vischel et al., 2009) presented numerical convergence problems, especially for marginal distributions where the frequency of zero values is high. Here, we propose an alternative approach based on censored likelihood that is better suited to strong f_0 values.

Let g_{ij} denote the values of the realizations of the process G . Values of g_{ij} which exceed c_{0_j} are known. For the values that do not exceed c_{0_j} , it is known only that $g_{ij} \leq c_{0_j}$. For this reason, a classical likelihood calculation can not be used to fit the model on data. Instead, a censored version of the likelihood is required.

Let \mathcal{D}_j be the set of stations where it does rain during the j -th event.

$$\mathcal{D}_j = \{i \in \{1, N\} \text{ such that } g_{ij} > c_{0_j}\} \quad (3.8)$$

Let θ_ρ be the parameters of the covariance function ρ that is to be estimated. Assuming that events are independent from one another, the censored likelihood of θ_ρ is:

$$L^c(\theta_\rho) = \prod_j L_j^c(\theta_\rho) \quad (3.9)$$

If every g_{ij} is observed for the j -th event (i.e. if it rains at all stations for the event j), then

$$L_j^c(\theta_\rho) = f_{GP}(g_{1j} \dots g_{Nj}; \theta_\rho) \quad (3.10)$$

where f_{GP} is the density of the Gaussian process with covariance ρ .

If at least one station is censored (within c_0), the likelihood becomes:

$$L_j^c(\theta_\rho) = f_{GP}(\{g_{ij}\}_{i \in \mathcal{D}_j}; \theta_\rho) \Pr[\{G_{ij} \leq c_0(t_j)\}_{i \notin \mathcal{D}_j} | \{G_{ij} = g_{ij}\}_{i \in \mathcal{D}_j}; \theta_\rho] \quad (3.11)$$

The probabilities are the CDF of a Gaussian process because

$$\{G_{ij}\}_{i \notin D_j} | \{G_{ij} = g_{ij}\}_{i \in D_j}, \quad (3.12)$$

is Gaussian with mean and variance given by

$$\mu = \Sigma_{1,2} \Sigma_{2,2}^{-1} g_{D_j} \quad (3.13)$$

$$var = \Sigma_{1,1} - \Sigma_{1,2} \Sigma_{2,2}^{-1} \Sigma'_{1,2} \quad (3.14)$$

where g_{D_j} is the vector formed by the elements of \mathcal{D}_j and Σ is the covariance matrix of the vector $(g_{D_j}, g_{\overline{D_j}})$ with

$$\Sigma = \begin{pmatrix} \Sigma_{1,1} & \Sigma_{1,2} \\ \Sigma_{1,2} & \Sigma_{2,2} \end{pmatrix} \quad (3.15)$$

The covariance ρ can be modeled with a variety of possible functions. Two have been tested in this study (see Section 3.6.2).

3.5.5 Temporal disaggregation

The temporal disaggregation step takes the cumulative rainfall amounts and divides them into sub-event intensities. The arrival time of the storm at a given point is conducted as in previous versions of the model, with a predetermined propagation speed and direction based on empirical data.

In the methods used in this article, given the cumulative station rainfall P for the event, the only parameter to estimate stochastically is I_{max} . The other intensities are then calculated according to the synthetic hyetograph in Figure 3.1.

Two methods for determining the shape of the hyetograph via the relationship between the maximum (peak) intensity and the cumulative total rainfall at a station are compared and evaluated in this study:

- The height of the peak (maximum intensity, I_{max}) and the cumulative event rainfall are considered to have a linear relationship according to Equation (3.16), as in the previous version of the simulator (Balme et al., 2006).

$$I_{max} = 2.01P + 0.53 \quad (3.16)$$

- A four-parameter beta distribution with covariates relating I_{max} to P at a given station. This theoretically makes the relationship between the variables more flexible and more representative of the variability present within the natural system.

The four-parameter beta density function is defined as follows:

$$f_{Beta}(I_{max}, min, max, \alpha, \beta) = \frac{(I_{max} - min)^{\alpha-1} (max - I_{max})^{\beta-1}}{Beta(\alpha, \beta) (max - min)^{\alpha+\beta-1}} \quad (3.17)$$

where I_{max} is the maximum event rainfall intensity, min is the lower bound of the distribution, max is the upper bound of the distribution, and α and β the two shape parameters. All four parameters can potentially have the cumulative event rainfall as a covariate. See Section 3.6.2 for details on how the four-parameter beta distribution was implemented in the present study.

The effects of the choice of maximum intensity generation is discussed in Section 3.7.3.

3.5.6 Overview of calibration

Table 3.1 recapitulates the parameters required by the model.

Table 3.1: Overview of model parameters

Category	Object	Parameters
Season definition	Start date	Normal distribution $\mathcal{N}(\mu, \sigma)$
	End date	Normal distribution $\mathcal{N}(\mu, \sigma)$
Occurrence	IET	Gamma distribution $F_\gamma(b_{IET}, k_{IET})$
Event rainfield	Marginal distribution	$F_{cumul}(f_0, b_{cumul}, k_{cumul}, u, \sigma_{GPD}, \xi_{GPD})$
	Spatial structure	Covariance function (ρ) and parameters (θ_ρ)
Temporal disaggregation	Propagation	Speed and direction
	Relationship I_{max} / P	Linear or Beta distribution (min, max, α, β)

3.5.7 Simulation procedure

Once the parameters are obtained, the following simulation steps are conducted:

Simulation of event start times

1. Wet season start and season end dates are generated using the normal distributions calibrated in the occurrence model (Section 3.5.1).
2. Starting from the season start date simulated in the above step, dates of event starts are sequentially generated using the occurrence model of IET values (Section 3.5.2) until the end date of the season is exceeded. The last event is kept or discarded according to a Bernoulli distribution with $p=0.5$.

Simulation of cumulative event rainfall

3. One Gaussian field (marginal distribution $\sim \mathcal{N}(0, 1)$) is simulated per simulated event start.
4. The marginal distribution $\mathcal{N}(0, 1)$ of the Gaussian fields is transformed (anamorphosis) to the established event marginal distribution (gamma+GPD), using the values of the gamma distribution at the covariate t of the start date.

Temporal disaggregation

5. A speed and direction is determined for the event (see Sections 3.5.5 and 3.6.2 for details).
6. Cumulative event rainfall per station is disaggregated into the determined time step using the selected method for determining the I_{max} value of the hyetograph (see Section 3.5.5).

3.6 Application to Sahelian storms

3.6.1 Sahelian hydroclimatology

The Sahel is a band located roughly between the 250mm and 750mm isohyetal lines of the subsaharan precipitation gradient. Sahelian climate is driven by the West African Monsoon, which determines the magnitude and frequency of MCSs and dictates a pronounced seasonal signal for the region (Lebel et al., 2003; D'amato and Lebel, 1998). The rainy season extends approximately

from April to October, with peak rainfall months in July and August and little to no rainfall outside of the rainy season. The average cumulative amounts and variance of precipitation events are higher in the middle of the season, with a lower percentage of null values (i.e. more large storms in July-August) (Ali et al., 2003; Balme et al., 2006).

An important factor in the capability of precipitation simulations to replicate the interannual and seasonal variability in the intertropical zone is the number of events per year, and by deduction the time between events (event frequency). Numerous studies found that the number of events has a significant impact on cumulative annual rainfall in the Sahel (Ali et al., 2003; Le Barbé et al., 2002; Lebel and Ali, 2009). By placing generated rainfall events at the dates of recorded historical rainfall Vischel et al. (2009) found that much of the seasonal signal of rainfall amounts was driven by event frequency. The cumulative annual precipitation was also replicated to some extent.

The consideration of extreme storms is of particular importance in the Sahel. A recent increase in extreme precipitation values has been documented (Taylor et al., 2017; Panthou et al., 2014, 2018). Given the recent series of catastrophic floods in the region (Descroix et al., 2012; Sighomnou et al., 2013; Wilcox et al., 2018), it is important to understand if changes in extreme precipitation events are tied to changes in extreme hydrological events.

As large MCSs generate the majority of local streamflow, the consideration of certain precipitation variables is of particular importance for impact studies. Intensities at short durations have a particularly significant impact on runoff (Malam Abdou, 2014; Peugeot et al., 1997), as does the spatial variability of precipitation (Koren et al., 1999). However, a non-negligible portion (up to 10%) of cumulative annual precipitation originates from smaller, locally-generated rainfall events.

Data used: AMMA-CATCH network

The calibration and validation of the simulator is performed with a subset of the AMMA-CATCH network of recording rain gauges. AMMA-CATCH consists of eco-hydrological data collection at three mesoscale sites in West Africa. It is unique for the region in both its spatial density and the length of continuous data recording: since 1990 in Niger, 1999 in Benin, and 2002 in Mali. The data is freely available from the AMMA-CATCH data base.

Stochastorm was calibrated on the AMMA-CATCH study site located

in the Sahel near Niamey, Niger. The site features a set of 30 rain gauges located within a one square degree area, spread over a domain of 120 x 160 km². 28 years of data (1990-2017) at the five-minute time step formed the primary data set used in the development of Stochastorm. A map of data locations is found in Figure 3.2.

3.6.2 Model implementation

Event definitions

A rainfall event is considered to be distinct when it is separated in time from other series of precipitation; here, we define an event as being separated by at least 30 minutes of no precipitation at the station level, with at least one time step of no rain in the entire window of study.

The last version of the simulator in Vischel et al. (2009) only considered the most consistent rainfall events associated with the organized and propagative mesoscale convective systems. As a consequence the simulations were missing a portion of the annual cumulative rainfall associated with smaller and less propagative local convection events.

These small events are characterized by a strong intermittency (and thus a high frequency of zero value in the event rainfall marginal distribution) that, in practice, limits the possibility of convergence of the Gibbs sampling method to transform rainfall into Gaussian values in the anamorphosis process.

Here we benefit from the use of the censored likelihood approach that is much more efficient in handling large zero atomic values. While Vischel et al. (2009) only selected rainfall events covering at least 10/30 of the AMMA-CATCH Niger rain gage network, here we define events as having at least 2/30 (or an equivalent percentage) of the rain gauge network receive more than 1mm of cumulative rainfall.

Smaller events that did not meet the criterion were considered inconsequential; they may be due to erroneous data (for example a false tipping bucket), or precipitation that is too sparse to be organized into a storm. Measurements from events that were not considered in the study contributed less than 0.01% of the annual rainfall amount.

Categorization of large and small events Once the initial event subset was created, the events were then classed into "large" and "small" categories.

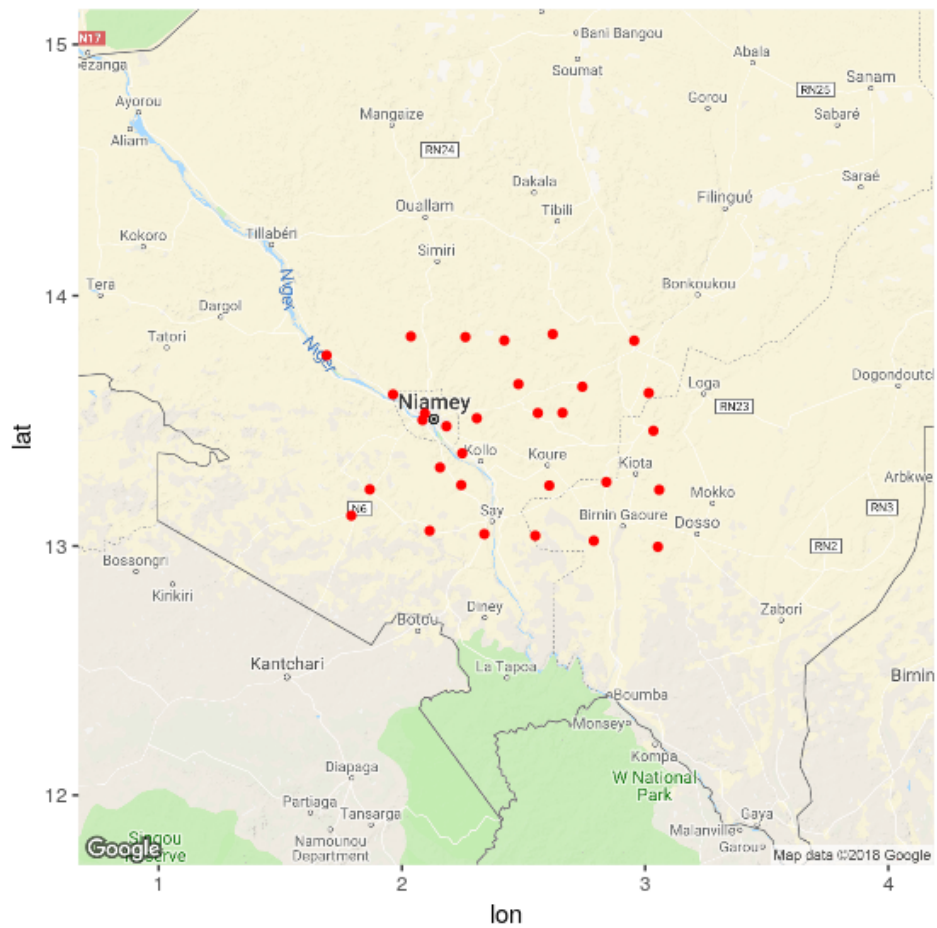


Figure 3.2: Location of rain gauge stations for the AMMA-CATCH network (red) near Niamey, Niger.

A large event has 30% or more of stations/data points registering rainfall. All other events were labeled as small.

The classification of events as large or small reflects the distinct physical properties of Sahelian storms. As shown by Mathon et al. (2002), large events are more likely to be associated with organized and propagative precipitation systems (MCS) while small events are more likely to be linked to local convective rainfall. Because of these physical distinctions, we decided to assign to each category (large/small) its own set of parameters (see Sections 3.6.2 and 3.6.2 for details).

The distribution of large and small events and the contribution of each to the total cumulative annual rainfall is shown in Figure 3.3.

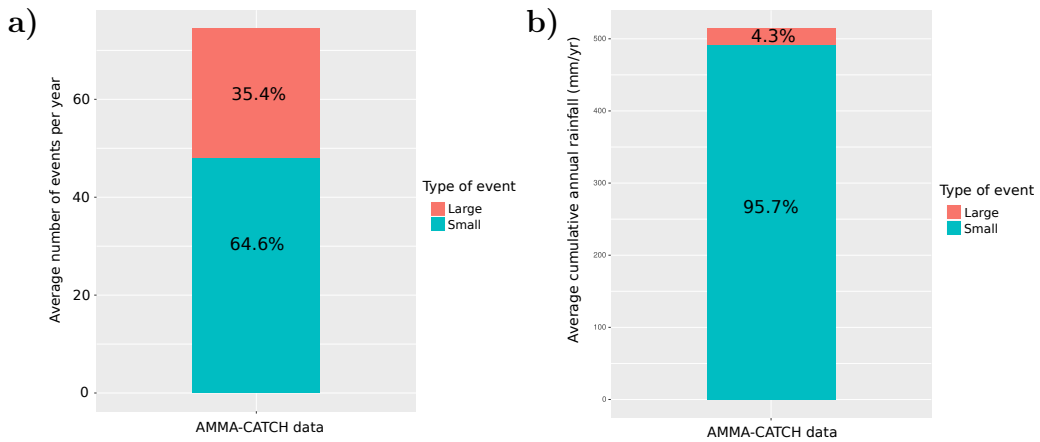


Figure 3.3: The relative contributions of large and small events to a) total events per year and b) total cumulative annual rainfall.

Season definition and occurrence

Only events occurring from April to October are considered, as this is the period of time during which localized precipitation-generated runoff is produced in the Sahel (precipitation events outside of this time frame are few and do not have a large impact on local hydrology, although they could have agricultural impacts).

The seasonal covariate t is defined as follows: For the central Sahel, the season is considered to go from the 1st of April ($t = 1$) to the 31st of October ($t = 215$). The seasonal covariate t is defined by a decimal number between 1 and 215. The integer digit of this decimal indicates the day in the season

of the event start and the decimal part corresponds to the hour and minutes of the event start.

For the Sahel, we would expect smaller IET values (i.e. more frequent storms) in the middle of the season (July-August).

Modeling the seasonal repartition of large and small events The distribution of large and small events (Section 3.6.2) throughout the season is modeled empirically with a Bernoulli distribution based on the input data. A spline is used to represent the proportion of small events throughout the season (Figure 3.4). The value of the spline at a given date provides the parameter of the Bernoulli distribution for events at that point in the season. For simulation, this Bernoulli distribution is used to randomly generate large and small event labels at each simulated event start day.

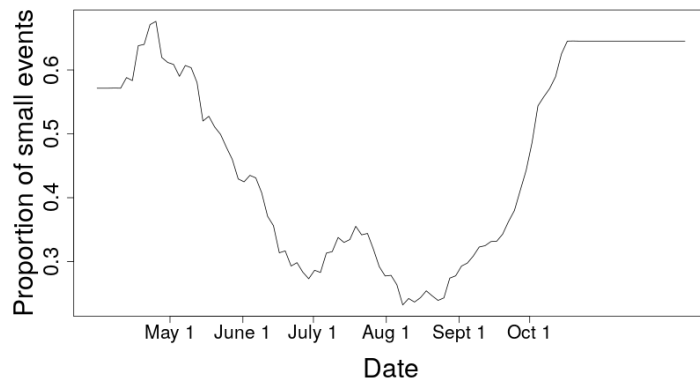


Figure 3.4: The proportion of small events throughout the season for the AMMA-CATCH 1990-2017 data set.

Marginal distributions of cumulative event rainfall

Each category (large/small) has its own set of associated parameters for the marginal distribution of cumulative event rainfall. Extremes are modeled only for large storms; the large storms are modeled with a gamma+GPD distribution as described in Section 3.5.3, whereas small events are modeled only by a gamma distribution.

In this study, the threshold u for the GPD distribution is fixed at 40 mm, approximately the quantile 0.97 as defined in Blanchet et al. (2018).

The GPD parameters are considered constant during the season, either because there is no detectable seasonality, or because the sampling effect due to the rarity of extreme events prevents the detection of a signal.

For the Sahel, we would expect marginal distribution parameters that produce larger cumulative event rainfall amounts with smaller f_0 values in the middle of the season.

Covariance functions used to model spatial dependency

The methods described in Section 3.5.4 are used to fit covariance functions on series of small and large events. There is one spatial dependency structure for small events and one spatial dependency structure for large events.

On small events, an isotropic exponential covariance function is fitted, given by:

$$\rho(d) = \exp\left(-\frac{\|d\|_{eucl}}{\phi}\right) \quad (3.18)$$

where $d = s_m - s_n$ is the difference between two sites s_m and s_n and $\|\cdot\|_{eucl}$ denotes specifically the Euclidean distance. ϕ is the range parameter, which controls the rate of decay as distance increases.

For large events, an anisotropic covariance defined by a sum of exponential functions is fitted, given by:

$$v * \exp\left(-\frac{\|h\|_{anis}}{\phi_1}\right) + (1 - v) * \exp\left(-\frac{\|h\|_{anis}}{\phi_2}\right) \quad (3.19)$$

where v is the proportion of the field variance associated with the first exponential, and ϕ_1 and ϕ_2 are the range parameters of the two structures.

$\|\cdot\|_{anis}$ denotes an anisotropic distance defined as:

$$\|h\|_{anis}^2 = \|s_m - s_n\|_{anis}^2 = (s_m - s_n)' M' M (s_m - s_n) \quad (3.20)$$

where

$$M = \begin{pmatrix} \cos \psi & \sin \psi \\ -a \sin \psi & a \cos \psi \end{pmatrix}$$

with $a > 1$ and $\psi \in [-\frac{\pi}{2}; \frac{\pi}{2}]$.

ψ is the angle between the x-axis and the major axis of the ellipse. a is the ratio of the major axis length on the minor axis length. With this distance, the level lines of the covariance function are elliptic.

Temporal disaggregation

The synthetic hyetograph (Figure 3.1) produced via the equations in Balme et al. (2006) was previously implemented in the Sahel. The present study focuses specifically on improving the estimation of the maximum intensity I_{max} of the synthetic hyetograph via the use of a four-parameter beta distribution.

An initial exploratory moving window analysis was conducted by calibrating beta distribution parameters on I_{max} by range of precipitation values from the recorded AMMA-CATCH data. The analysis revealed strong evidence of nonstationarity within the parameters, with parameters increasing at varying rates as precipitation increased. The four parameters of the beta distribution in Equation 3.17 were thus determined to depend on cumulative event precipitation. A function of best fit was determined for each parameter.

The beta distribution upper bound (max) was modeled using a two-part function (Figure 3.5). For a lower range of cumulative rainfall values, the total event rainfall was used as the value of max . For larger values, max was defined as a log function that must exceed two times the observed I_{max} values. The switch between the two types of bounds was identified as the intersection between the cumulative rainfall value and the log function. We consider this to be a reasonable limit as the highest max values are near the world record for five-minute precipitation intensities (Burt, 2007).

For the lower bound (min), linear segments that pass beneath the lowest observed values were used for smaller rainfall values, then extrapolated with a log function at the same point the log function starts for the max (Figure 3.5).

For the α and β parameters, a log function and an exponential function were chosen respectively to link their values with the covariate of cumulative event rainfall.

Lower and upper bounds of beta distribution

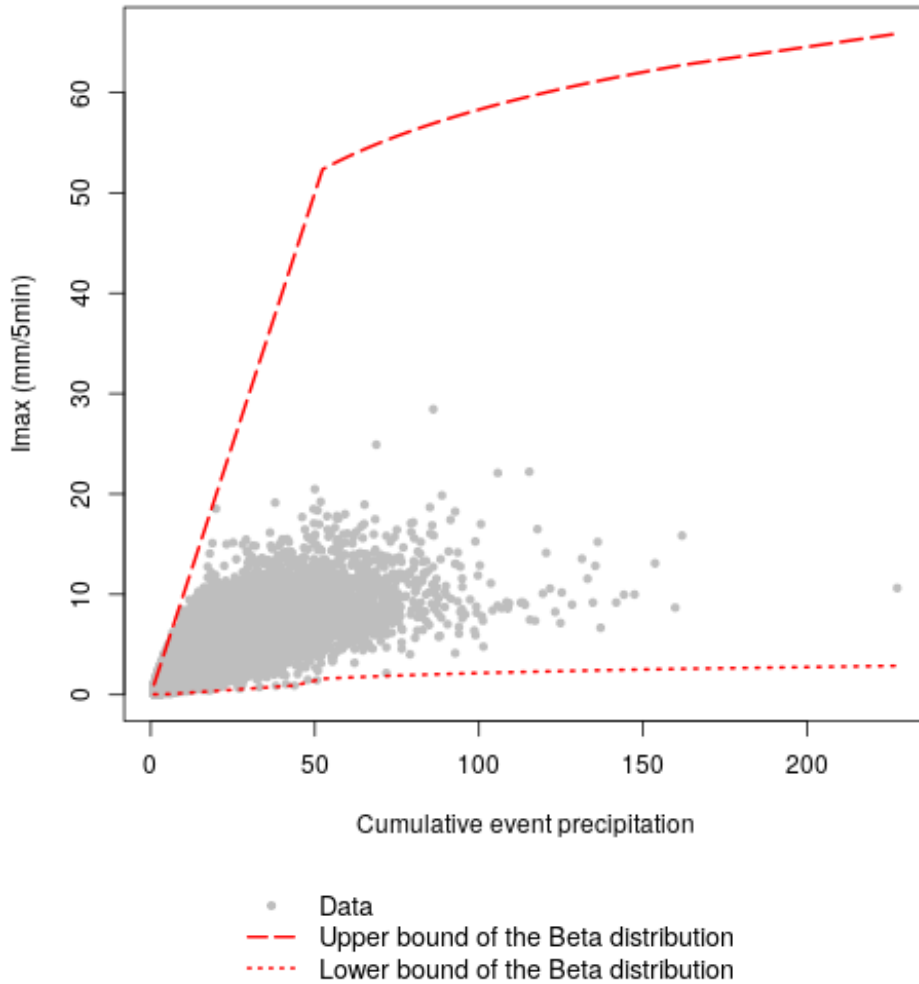


Figure 3.5: Upper and lower bounds of the underlying beta distribution used to model maximum intensity (I_{max}) with cumulative event rainfall as covariates for the beta distribution parameters.

Speed and direction are determined using an input database of measured data with speed, direction, and cumulative rainfall associated with each event. The recorded cumulative event rainfall (P_{tot}) closest to a given simulated cumulative rainfall amount is identified, and the associated speed

and direction are used for the simulated event as well. This approach resembles the selection of an analog event within the recorded data used in Chardon et al. (2014), for an example.

3.7 Evaluation of the model using AMMA-CATCH data (Sahel)

The parameters of the Stochastorm model was calibrated using the AMMA-CATCH 1990-2017 dataset. 30 simulations of 28 years were generated. The model allows for simulation at a choice of points; we chose to simulate only at the locations of the 30 AMMA-CATCH measurement stations in order to compare simulation results with the data.

The following sections describe the ability of the model simulations to reproduce both model parameters (i.e. whether simulated outputs reflect calibrated parameters) and observed characteristics of MCSs not directly prescribed in the model (whether simulated outputs are coherent with observations).

3.7.1 Event occurrence

Figure 3.6 displays the results for the simulation of the first and last day of the season. One can observe in Figure 3.6 that the both the model and simulations closely match the data, and that the first and last days of the season are well-represented by a normal distribution.

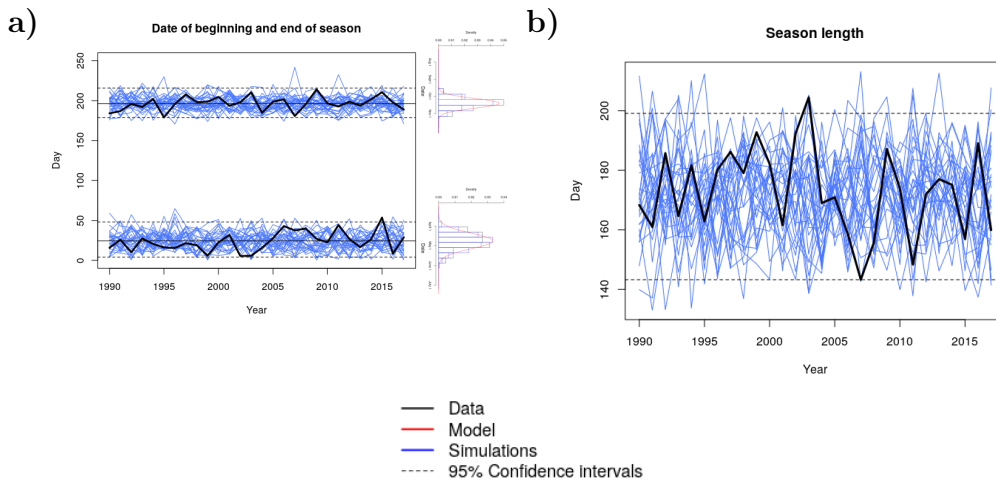


Figure 3.6: Distributions of beginning and end of season dates, with data, simulations, and model (a). Season length (b).

Results for the IET (Figure 3.7) also shows good coherence between the simulation outputs and the original calibration data. This means that storms were reproduced at a frequency which matched that of the recorded record, with more frequent storms (lower IET) in July-September and less frequent storms at the beginning and end of the season. The model parameters are well-reproduced in the simulations. The main difference is towards the end of the season, where the seasonal evolution in the simulations is less smooth and lower than the prescribed model parameters (although more similar to the data). This could be explained by the use of the Bernoulli law to decide whether or not to keep the final event of the season.

Of note is the coherence between the data, the length of the season, and the number of events per season (Figures 3.6 and 3.7). The simulations reflect the original data for the beginning and end date (Figure 3.6a). Note that although the season length was not explicitly parameterized in the Stochastorm model, simulations accurately represent the original data's season length (Figure 3.6b). Although the number of events per season was also not explicitly modeled, the number of simulated events generated from the IET parameter are representative of the data (Figure 3.7).

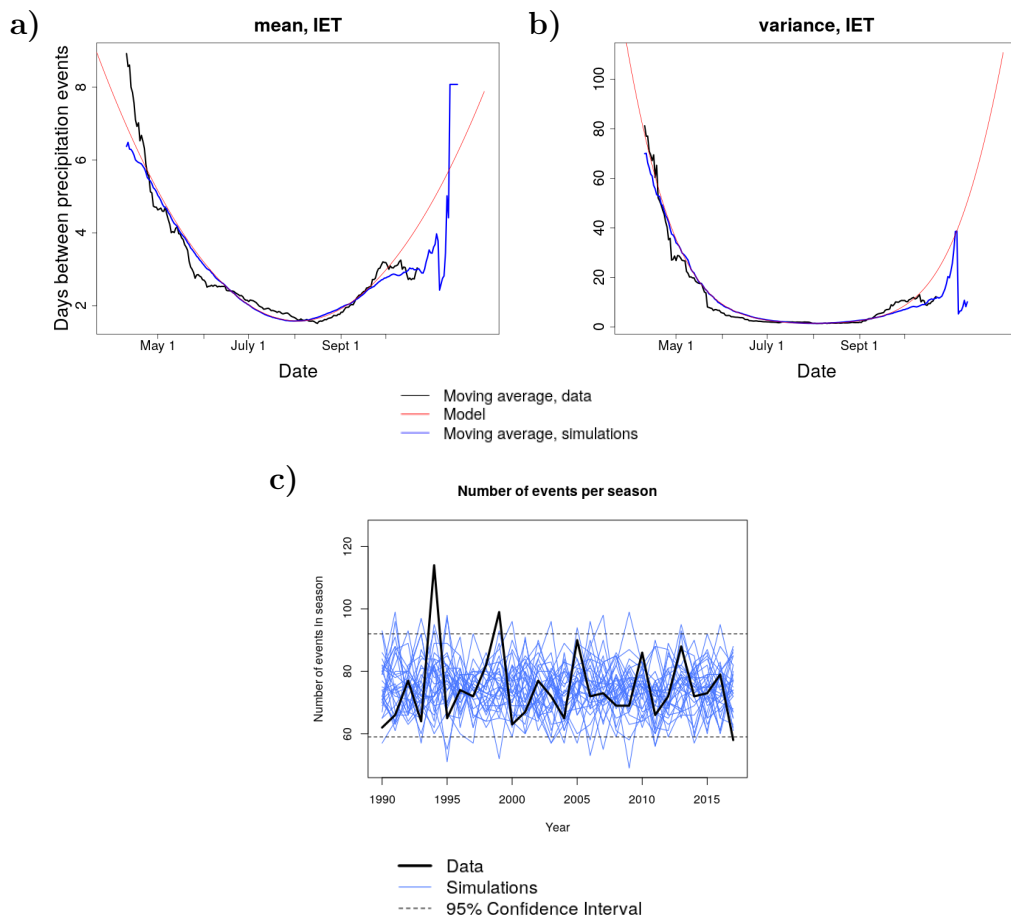


Figure 3.7: Results for the inter-event time (IET) (a,b) and number of precipitation events per season (c).

Confidence intervals for IET simulation results can be found in the annex, as well as Stochastorm parameters.

3.7.2 Event-based rain fields

The results for the spatial rain fields were also coherent. Figures 3.8a and 3.8b show the mean and variance of the cumulative event rainfall amounts and f_0 . The seasonal signal of mean values is well-represented, although the variance is underestimated during the core of the season.

Of particular note are the results for f_0 (Figure 3.8c). For the AMMA-

CATCH network, the simulations were conducted separately for large and small events. When the simulations are combined, the seasonal signal of f_0 in the data is accurately reproduced. The variability of the extension of the events is also well-simulated. This is a notable result coming from the ability to simulate both large and small events. The arbitrary simulation of only large events (imposed in the previous version of the model) hindered the capacity of the simulator to reproduce the distribution of f_0 found in the data. Inversely, figure 3.9 confirms that the overall frequency of event extension values (proportion of non-zero values) is also reproduced.

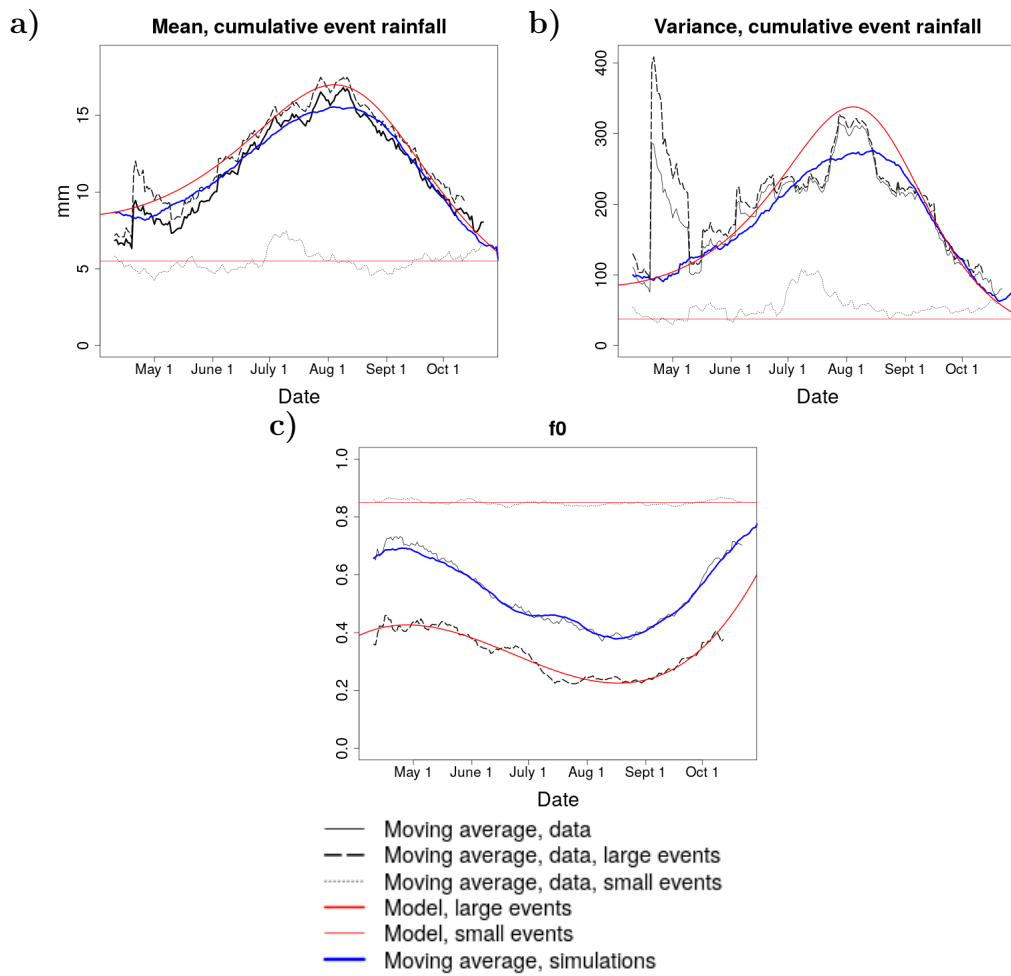


Figure 3.8: Results for cumulative event rainfall over the study area (30 stations/simulation points aggregated).

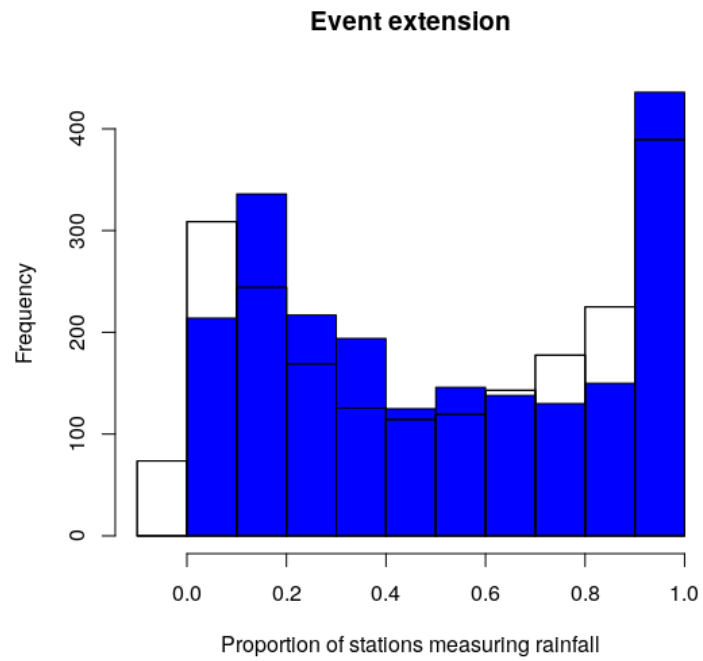


Figure 3.9: Distribution of the extension of events (proportion of stations measuring rainfall), with data in black and simulations in blue (30 stations/simulation points aggregated).

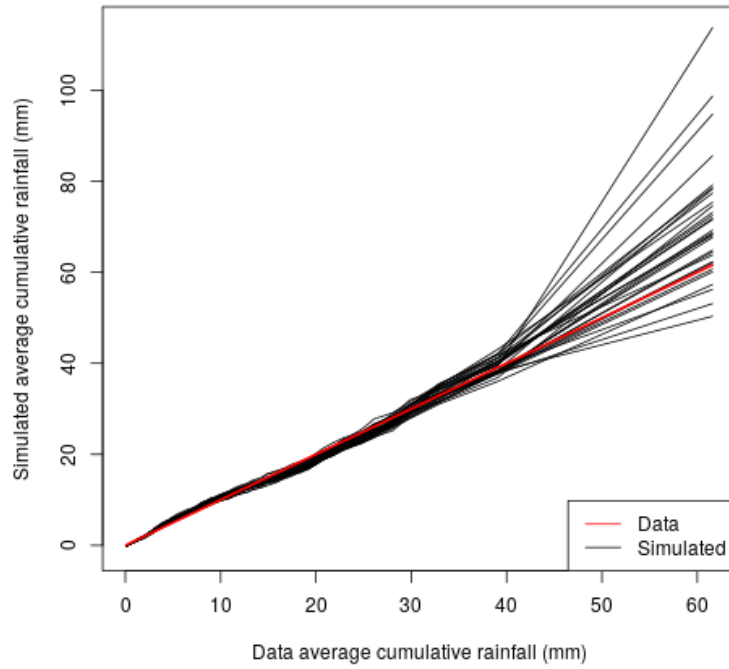


Figure 3.10: Results for the distribution of cumulative event rainfall over the study area (30 stations/simulation points aggregated).

Figure 3.10 shows the CDF of the cumulative event rainfall values. Figure 3.11 shows the results for the modeled spatial structure of precipitation.

Confidence intervals and Stochastorm parameters for the rain fields can be found in the appendices.

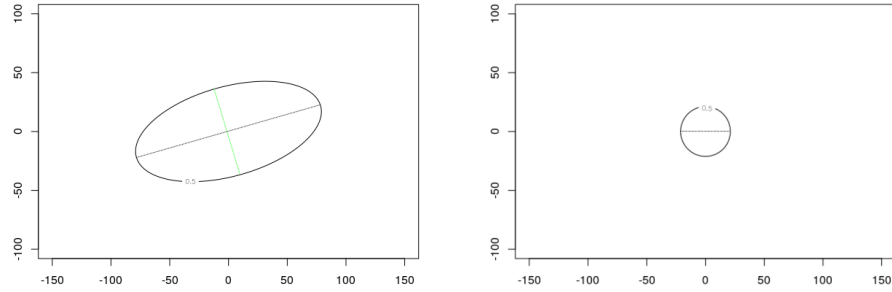


Figure 3.11: Results for the modeled covariance structure spatial structure for large events (left) and small events (right)

3.7.3 Temporal disaggregation

Figure 3.12 compares the maximum intensities generated from the two methods of temporal disaggregation with the data. One can note that the newly proposed method using a beta distribution to link the maximum intensity with the cumulative event rainfall more closely follows the data. There is a slight underestimation on average for larger cumulative precipitation values (Figure 3.12a), but this is much smaller in magnitude than the overestimation when using the previous method. The beta distribution method more realistically models the natural variability in maximum intensities (Figure 3.12b).

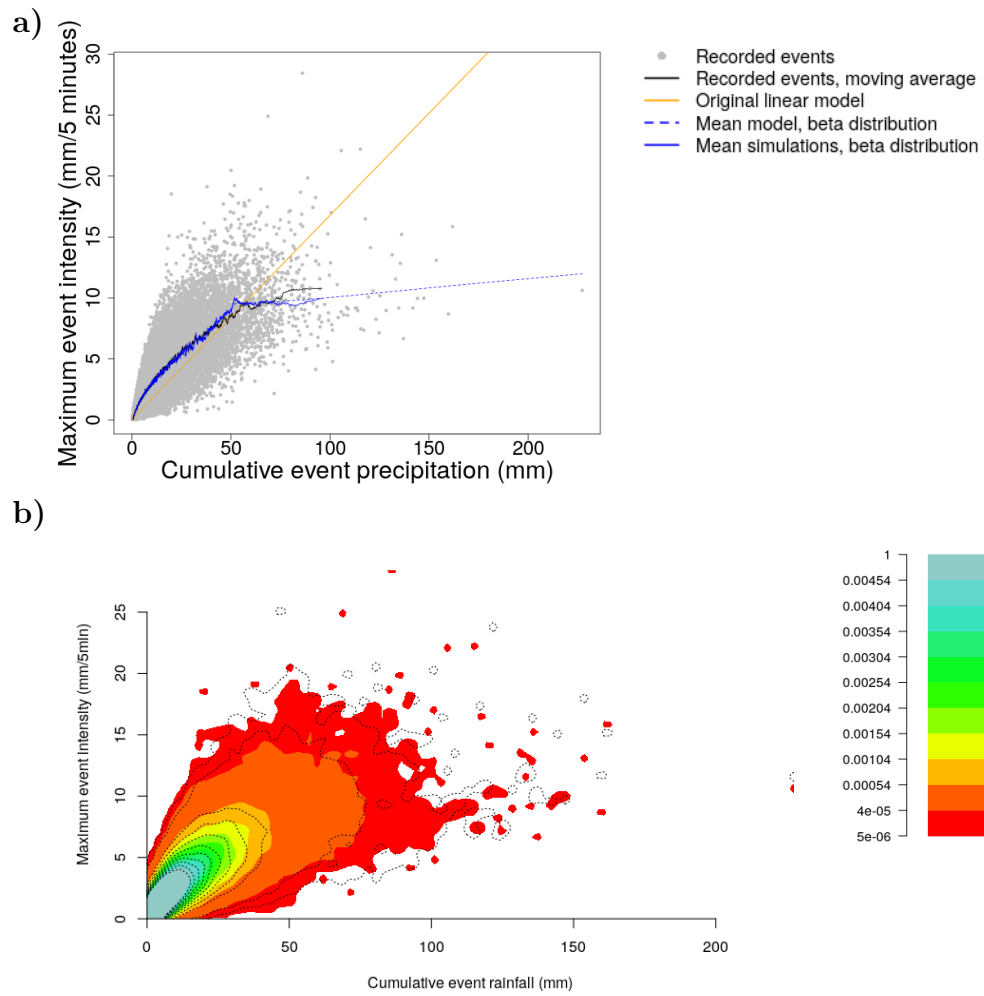


Figure 3.12: Top (a): Comparison of the effect of the choice of disaggregation method on maximum event intensity. Bottom (b): Comparison of maximum storm intensities simulated using the four-parameter beta distribution (black contours) with the original data (heat map).

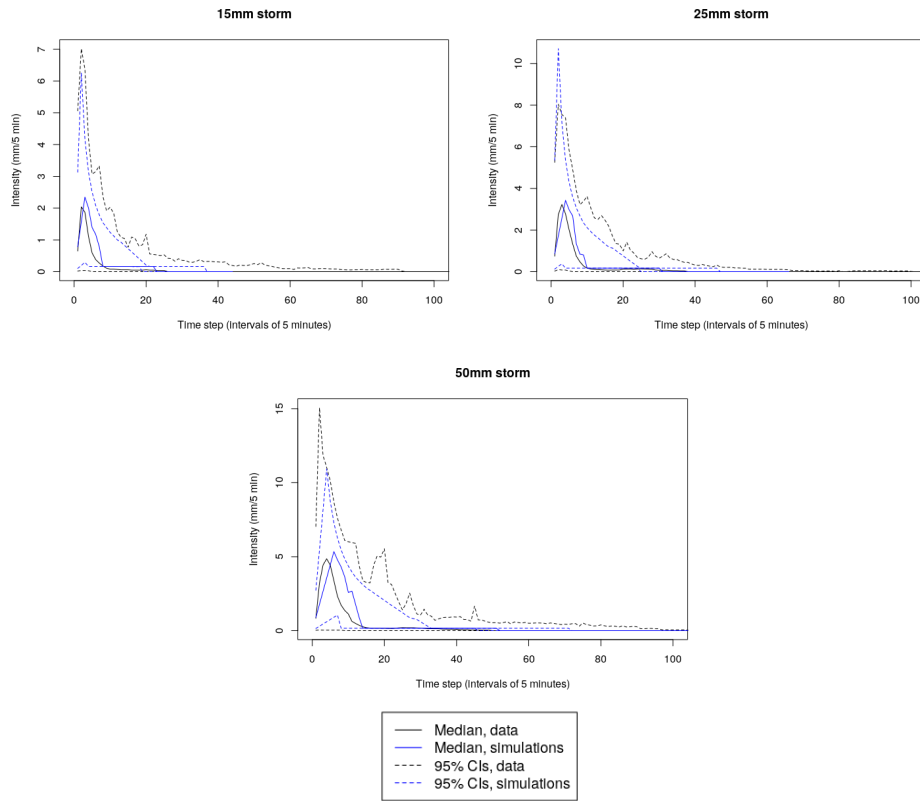


Figure 3.13: Measured and simulated hyetographs corresponding to storms of different cumulative precipitation magnitudes (15mm, 25mm, 50mm).

Figure 3.13 shows the hyetographs of events having a given cumulative precipitation value. Although only the peak event intensity was specifically generated, the magnitudes of other sub-event intensities were well-reproduced by the temporal disaggregation method using the synthetic hyetograph. Both the average hyetograph and the variability (confidence interval) associated with a given cumulative value were reproduced.

3.8 Conclusion

The above study presents the recent developments for the stochastic precipitation generator Stochastorm, a modeling and simulation tool that aims to replicate the properties of MCSs in the West African Sahel. The simulator

can generate long series of annual precipitation scenarios that have the same climatic variability as the input data.

Improvements include modeling of event occurrence dates via the inter-event time (IET) parameter and simulation of rainy season start and end dates. In addition, the model now features: added parameters for seasonality (seasonal covariates for occurrence and the marginal distribution); explicitly modeled extremes; and the use of censored likelihood to coherently transform Gaussian fields into the marginal distribution of the precipitation. Finally, the model uses a new method of temporal disaggregation using the four-parameter beta distribution to relate maximum event intensity to cumulative event precipitation. The new method is conceptually more coherent with the characteristics of convective rainfall than the linear model previously used.

Stochastorm was applied to the Sahel region of West Africa. Specific adaptations included the categorization of small and large events, with the ratio evolving throughout the season (more large events during the peak precipitation months).

Results had good coherence with data, closely following the seasonal signal and annual properties for both occurrence and magnitude of events. The spatial intermittency was also well-replicated, in spite of the division into small and large events for the Sahel.

Although the model was implemented in the Sahel, it is based on precipitation characteristics that are common to many intertropical regions, especially semi-arid ones. Stochastorm may be implementable in other regions provided that parameters can be tuned on locally observed data.

The simulation results have implications for the applications of hydrological modeling and agricultural modeling. The fact that simulation outputs are at fine scales with a coherent and representative spatial structure is promising for implementation in hydrological models (Li et al., 2017). A priority for future work is implementing the outputs of Stochastorm as the inputs which drive a hydrological model. In particular, Stochastorm can be calibrated on GCM outputs. The use of GCM as calibration data would allow Stochastorm to function as a statistical downscaling tool (Ferraris et al., 2003) that can translate the GCM into relevant information at hydrological scales.

The model is limited in its ability to handle long-term nonstationary, such as decadal trends. An example of ways to treat non-stationarity with stochastic weather generators can be found in Verdin et al. (2018). By incorporating nonstationary climate projections into the stochastic weather generator and coupling it with a hydrological model, one gains the capacity

to perform water resource projections (Borgomeo et al., 2014).

Appendix: Model parameters

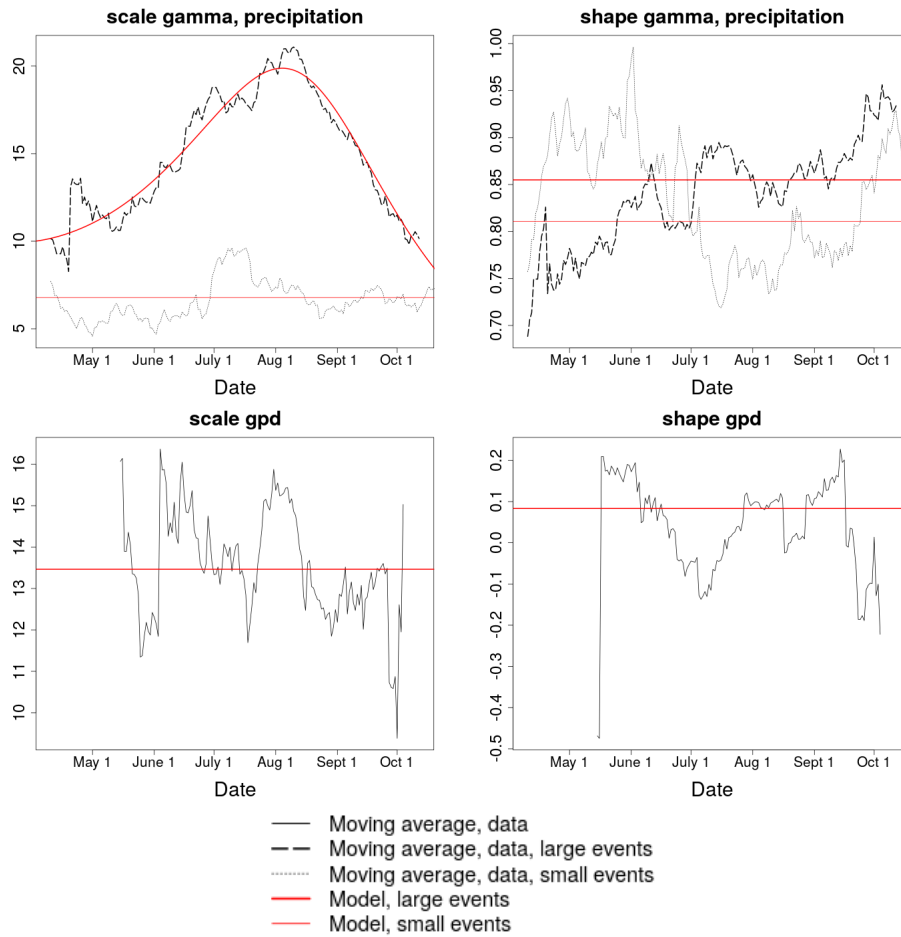


Figure 3.14: Model parameters for the gamma and GPD distributions of cumulative rainfall amounts for the AMMA-CATCH network.

Extra plot options (with confidence intervals)

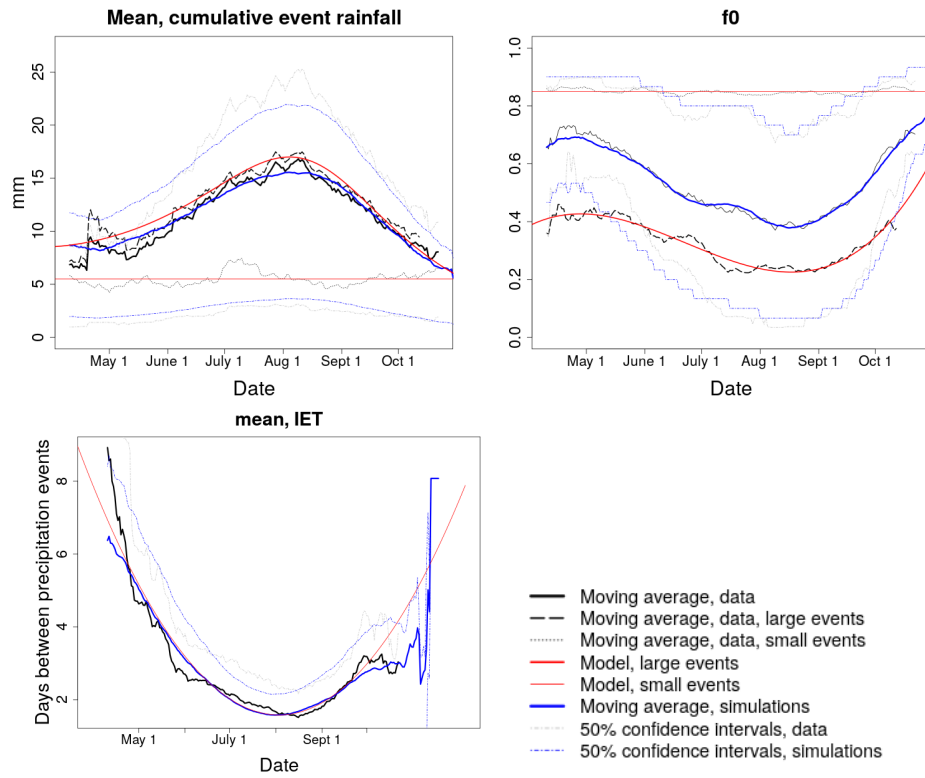


Figure 3.15: Summary plots with 50% confidence intervals. Note the good coherence between confidence intervals of data (gray) and simulations (blue).

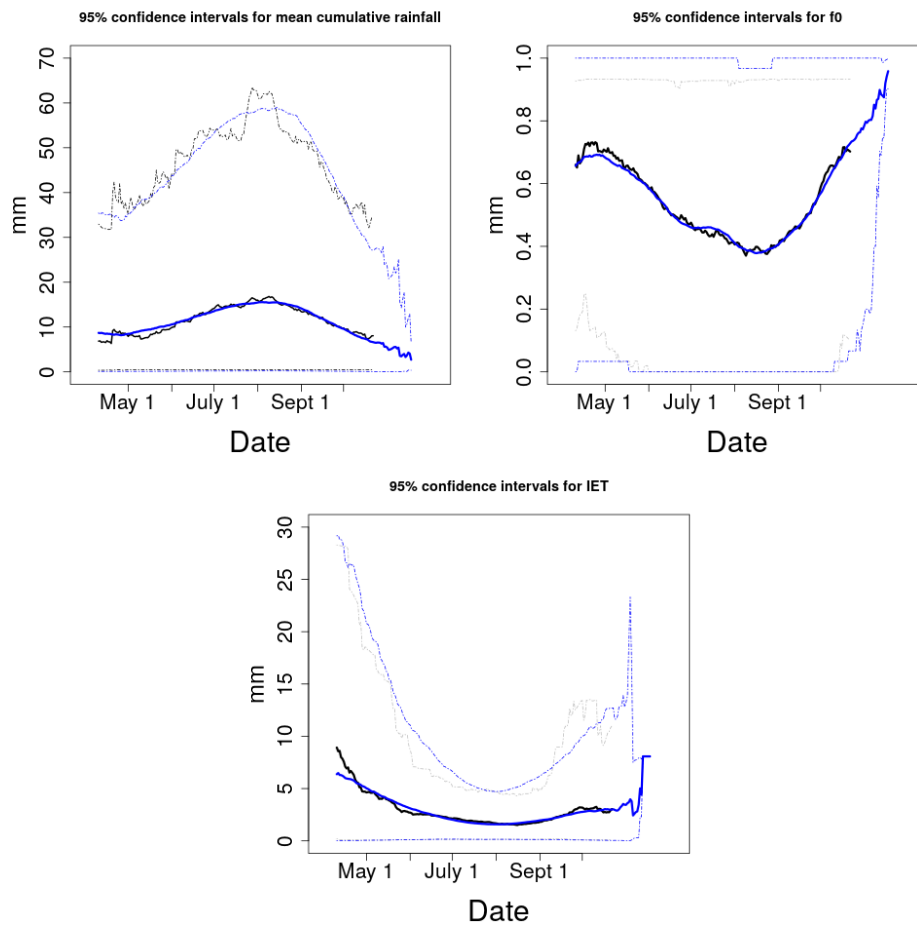


Figure 3.16: Plots with 95% confidence intervals. Note the good coherence between confidence intervals of data (gray) and simulations (blue).

Chapter 4

Modeling chain for using a convection-permitting regional climate model to drive hydrological projections

4.1 Introduction to article 3

A precipitation model is an essential part of modeling a hydroclimatic system. The next step is to pair the precipitation model with a hydrological model to create rainfall-runoff scenarios. A scenario of great interest is evaluating how river discharge might evolve in the future in response to climate change.

The following article presents a modeling chain for producing and evaluating climate change-driven hydrological projections. The precipitation projections come from the newly-released simulations from the RCM CP4-Africa (Stratton et al., 2018). CP4-Africa simulations are a promising advancement in climate modeling as they are the first large-scale RCM simulations (performed over ten years and a large region) that explicitly represent fine-scale 3D convective processes. This permits the representation of mesoscale convective systems (MCSs). The advancement is significant because MCSs are the primary source of precipitation in West Africa.

This is significant as precipitation in West Africa is primarily driven by convective processes.

CP4 is first compared with in-situ data then corrected for biases accord-

ingly. CP4 is then linked with the stochastic rainfall generator described in Chapter 3 to produce precipitation scenarios. Finally, the scenarios are used as inputs to a process-based hydrological model designed for the Sahelian region.

After establishing the methodology for the modeling chain, the primary goal of the paper was to use the modeling chain to create hydrological projections. Potential changes in river discharge in the future are simulated and evaluated.

4.1.1 Personal contributions

Data processing and evaluation

At the time I started work on this subject, only 3.5 years of CP4 data for the present had been previously analyzed by my team. I received a total of ten years of simulations from the present and ten years for a future period. I extracted events from the data, handling differences in formats and time stamps between CP4 and in-situ data sets.

Using the extended data set, I verified the analysis that had previously been conducted for the present. I then analyzed differences between present and future CP4 simulations. I tested a wide range of seasonal covariate models for Stochastorm parameters to determine which were the most suitable fit for CP4. I performed extensive comparisons of CP4 data with AMMA-CATCH in-situ data. I also extended the analysis to CP4 data over Ouagadougou, and compared the two sites.

Methodological contributions

Using Stochastorm, I produced all of the rain field scenarios for use in hydrological modeling. I developed my own scripts and functions that allowed me to modify and reproduce my work in a short amount of time.

At one point, we were unsure what the greatest source of bias in CP4 was. We noticed that hydrological modeling outputs driven by CP4 significantly underestimated observed values even after applying CDFt bias correction. I proposed an approach of replacing CP4-based parameters in Stochastorm with AMMA-CATCH-based parameters one by one. In this way we were able to identify that the proportion of zero values was a great source of error that needed to be corrected.

I coded and tested at least five different approaches for correcting the bias in the proportion of zero values and the magnitude of positive values for CP4. I also explored correcting the bias in the number of events.

Article writing, collaborations, and conferences

I wrote the article, conducted a review of relevant literature, and produced figures. I decided which of the extensive analysis I had conducted would be most relevant for the paper. I also incorporated feedback on key points in the article. The article will be submitted for publication after review from coauthors.

The work with CP4 was conducted as part of the international AMMA2050 project which aims to better understand the regional climate of West Africa, its evolution, and the impacts of its evolution. In the context of this project, my work on comparing CP4-Africa simulations with AMMA-CATCH data contributed to the recent paper Berthou et al. 2019. My work was also presented in several conferences: SWGEN (Berlin, 2018); GEWEX (Canmore, 2019) and at the EGU General Assembly in 2019.

4.2 Article: An original statistico-dynamical modeling chain for hydrological projections under future changes in convective rainfall

Abstract There is now evidence that global warming has contributed to the recent intensification of precipitation in some regions in Africa. The modification of the storm-scale dynamics can have major impacts on the hydrological cycle and related hydrological risks. However, storm features are not captured at the coarse resolutions of global climate models (GCMs). GCMs also parametrize convection; as convective processes generate nearly all precipitation in the tropics, this greatly limits their direct use for hydrological risk assessment and related decision making. While regional climate models (RCMs) offer the possibility to dynamically downscale GCMs at higher resolution, recent RCM implementations in Africa did not integrate explicit representations of convective processes. RCMs also tend to be

biased, and outputs are not at a small enough scale for use in hydrological applications. The newly-developed RCM CP4-Africa is unique in that it is the first convection-permitting model in the region to provide long-term precipitation outputs over a large domain. It is at a small enough spatial resolution (4.5km) for use in impact studies. Simulations currently exist for two 10-year periods: one in approximately the present period (1997-2006) and one in a future world under climate change (RCP8.5 forcing at the end of the 21st century). This study aims at providing a first evaluation of CP4-Africa for hydrological impact studies. An original modeling chain that integrates CP4-Africa precipitation simulations, bias correction methods, stochastic spatiotemporal disaggregation, and hydrological modeling is presented and applied to the intertropical zone in West Africa. CP4 outputs are bias corrected using an adaptation of the CDFt method, with 10 years of data from the AMMA-CATCH network in southwest Niger as the control set. CP4 present and future outputs are used to calibrate a stochastic rainfall simulator "Stochastorm," which is used both as an evaluation tool to compare present and future precipitation characteristics and to generate precipitation scenarios. Finally, the simulation outputs are used as inputs to a process-based hydrological model for the Sahelian region of West Africa. The future CP4 simulations display a moderate decrease in the number of events at the core of the season but a significant increase in the magnitude and variability of event rainfall, and in particular an increase in extreme events. Annual cumulative rainfall increases by 64%. Implementation of the modeling chain in a Sahelian test catchment showed that streamflow is projected to increase significantly under climate change for both annual volumes and peak discharge. Results show how RCMs can be combined with stochastic rainfall generators in order to evaluate the impact of climate change on hydrological processes.

Authors Catherine Wilcox, Théo Vischel, G  r  my Panthou, Guillaume Quantin, Phil Harris, Juliette Blanchet, Claire Aly, Chris Taylor, S  gol  ne Berthou, Jean-Pierre Vandervaere, Rachel Stratton

4.3 Introduction

The modern period has witnessed numerous global climate changes, notably an observed increase in surface temperatures produced by anthropogenic

green house gases emissions (Stocker et al., 2013). The warming trend is expected to continue; a total warming of 1.5 degrees C in average surface temperature since the beginning of the industrial era is already projected to occur over the coming decades, even if anthropogenic greenhouse gases are strictly limited (Millar et al., 2017). From a mid-term perspective, the intensity of the global temperature increase will likely be greater in magnitude (Rogelj et al., 2016; Steffen et al., 2018).

The global warming trends have provoked numerous local effects (Intergovernmental Panel on Climate Change, 2018). Not the least of these effects is the intensification of the hydroclimatic cycle, consisting of an increase in extreme events such as storms and floods (Hirabayashi et al., 2013; Giorgi et al., 2011; Trenberth, 1999). As global warming continues, the risk of local impacts from extreme hydrological events also increases (Mora et al., 2018; Arnell and Gosling, 2016). Besides extremes, other modifications of local climate regimes such as seasonality and rainfall frequency can affect agricultural production (Guan et al., 2015; Butt et al., 2005). Such hazards pose a serious threat to societies, economies, and the environment.

The threat of climate-related hazards is especially large in the intertropical zone (Allan et al., 2010; Zhang et al., 2007; Asadieh and Krakauer, 2015). The region has a particularly high regional sensitivity to global warming (Bathiany et al., 2018; Nyong and Niang-Diop, 2006) coupled with high vulnerability to climate change (Vincent, 2004) and limited adaptation capacity on average compared to countries in other regions (Shi et al., 2016). Studying how local impacts will change as a result of global climate modifications is pertinent in order to better characterize the hazards that societies may face. In such a context, increasing the resilience of populations to future potential hazards is an urgent question of equity. Impact studies are a necessary step for proposing adequate adaptation measures and strategies. In such complex systems, future evolutions and associated threats are not straightforward to project. Impact studies using numerical models can provide a promising study framework.

Projections based on global climate models (GCMs) are, thus far, the only way to understand of how the earth's climate may change in the future. They can indicate how large-scale phenomena such as average sea surface temperatures may change. However, it is more challenging to use them to estimate the evolution of smaller-scale climate-related hazards in the future. Hydrological hazards (storms, floods, drought) are produced by processes occurring at scales that are smaller than the grid sizes of GCMs. Often,

GCMs will output one value for a grid that covers a region containing a wide variety of hydroclimatic processes. The processes that govern floods are not dynamically modeled within the GCM parameters either, leading to misrepresentations in the projections.

A common solution to the scale issues of GCMs are regional climate models (RCMs). RCMs model smaller areas of the globe and thus can operate at a much smaller grid scale than GCMs, some at a scale that is directly useful for hydrological impact studies. However, up until now, few RCMs have included convective processes in their dynamic parameterization. This is a critical issue in the tropics, where the majority of precipitation is produced by convective rainfall. The rainfall is mainly generated by organized meso-scale convective systems (MCSs), for which resolving 3d convective processes is crucial to model their specific dynamics. The lack of inclusion of convective processes leads to an inaccurate representation of precipitation.

Studies specifically evaluating hydrological projections are also few, and largely not conducted specifically over the tropics. Several studies coupled climate model projections with global or large-scale regional hydrological models (Arnell and Gosling, 2016; Dairaku et al., 2008; Douville et al., 2002; Hagemann et al., 2011). They found that hydrological impacts varied widely by region and time of year. Salathé Jr et al. (2014), Wang and Wang (2019), Dibike and Coulibaly (2005), Wang et al. (2019), and Leong and Donner (2015) present evaluations of climate change impacts using a hydrological model calibrated for a specific local river basin. Wang and Wang 2019 specifically used a convection-permitting climate model to generate the hydrological projections (uncommon in the literature). Koutsoyiannis et al. (2007) and Cameron et al. (2000) found that projected future hydrological changes were within the boundaries of uncertainty for their study areas.

Krysanova et al. (2017) and Pechlivanidis et al. (2017) conducted robust analyses of multiple river basins (twelve and five respectively) by using five GCMs, four emissions scenarios, and multiple hydrological models per river (five and nine respectively). Pechlivanidis et al. (2017) found that climate change impacts were more severe near the end of the century, and greater in dry regions. Climate model uncertainty was greater than hydrological model uncertainty in dry regions.

A few studies specifically looked at extreme events and floods, including Pechlivanidis et al. (2017), Wang and Wang (2019), Salathé Jr et al. (2014), Arnell and Gosling (2016), Condon et al. (2015). Most showed that extreme events would increase in their respective study region(s).

Some studies did not make use of hydrological models, but instead directly used the water balance in climate models of precipitation-evaporation (Sun et al., 2011; Held and Soden, 2006) or used inference and statistical models to connect hydrological variables to climate variables (Li et al., 2016; Condon et al., 2015).

New RCMs that include convection offer promising possibilities for more accurately modeling and projecting future precipitation in tropical regions. The present study seeks to evaluate the capacity of simulations from the convection-permitting RCM CP4-Africa (Stratton et al., 2018) to correct many of the limitations associated with climate models and be used to evaluate projected hydrological impacts. CP4-Africa is one of the few climate models that generates climate simulations realized at a large regional scale and over a significantly long time period that also explicitly resolve convective processes. As convection is an important precipitation-driving process for the tropics, it means that storm generation and propagation can be more realistic than models which use a parametrized convection. CP4-Africa has a grid size of only 4.5 km, a suitable scale for hydrological impact studies. Currently, 10 years of CP4-generated precipitation for a present control period (1997-2006) and 10 years of projected precipitation on a future horizon (2090-2100) are available. The future projections give an idea of how precipitation over Africa may change over the coming century.

The study region selected for this site is the West African Sahel, in particular the Sahelian reaches of the Niger River. The region has experienced a significant increase in flood hazard (Wilcox et al., 2018) and associated flood damages (Fiorillo et al., 2018). Previous studies found that the ability of GCMs to accurately simulate precipitation over West Africa was highly variable depending on the model used, with an overall poor ability to simulate accurate rainfall volumes in the Sahel (Biasutti, 2013). The accurate simulation of precipitation is important given that studies showed runoff changes in the Sahel are highly sensitive to climatic changes (Aich et al., 2016b, 2014; Gerbaux et al., 2009).

Notably, changes in properties of monsoon storms are major drivers of hydrological regime changes (Lebel et al., 2003). Storms produce the great majority of rainfall in West Africa (Mathon et al., 2002); their occurrence, intensity and size within the monsoon season modulate the response of hydrosystems (Vischel et al., 2009, 2019). The relevance of impact studies thus primarily depends on the quality of input precipitation not only in term of accuracy but also in term of the space-time resolutions that they encompass

(Vischel and Lebel, 2007; Gascon et al., 2015).

Results of hydrological projections due to climate change in the region showed high uncertainty, including uncertainty on how surface temperature increases will impact the West African Monsoon (d’Orgeval et al., 2006). Models and associated impact studies disagree on whether climate conditions will become wetter or drier, in part due to model deficiencies, in part due to multiple competing mechanisms in the region (Druryan, 2011; Roudier et al., 2014; Gerbaux et al., 2009; Aich et al., 2016b, 2014). Great uncertainty exists also because of the limited consideration of scale issues in hydrological climate impact studies (Gerbaux et al., 2009; Roudier et al., 2014).

In this paper we present a modelling chain that aims to study the hydrological impact of climate change on West African catchments. The chain is an original attempt in West Africa to explicitly encompass the continuum of scales from global climate to local hydrological processes. It includes (i) dynamical downscaling of a GCM using CP4-Africa, (ii) a statistical bias correction method, (iii) a stochastic storm generator to reproduce CP4-based storm feature changes in an ensemble of rainfall stochastic scenarios at the suitable resolution for hydrological models, and (iv) a process-based hydrological model representing the dominant processes at play in the rainfall-runoff relationship in the Sahelian environment.

We first assess the potential of CP4-Africa to replicate the rainfall regime at the storm scale based on a high-resolution precipitation dataset unique in West Africa. Then, we use the modeling chain to explore potential hydrological impacts of future climate over a meso-scale Sahelian catchment.

Section 4.4 outlines the study region and the data used used. Section 4.5 provides an initial evaluation of CP4-Africa simulations. Section 4.6 presents bias removal methods and the different modeling elements. Section 4.7 presents study results. Section 4.8 presents study conclusions and perspectives.

4.4 Region and data

4.4.1 Study site: AMMA-CATCH network

In-situ precipitation data

The present study focuses on the Sahelian region of West Africa. The specific study region located in southwest Niger was selected due to the availability of

high-resolution in-situ data from the AMMA-CATCH network (Cappelaere et al., 2009; Lebel et al., 2009; Galle et al., 2016, 2018). AMMA-CATCH is an eco-hydrological data collection for West Africa with sites in Niger, Benin, and Mali/Senegal. It is the only observatory in West Africa that has sufficiently dense and lengthy in-situ observations to document the rainfall regime in the Sahel at the meso-scale.

The AMMA-CATCH precipitation gauge network in Niger is a set of thirty 5-minute tipping bucket rain gauges located within a one square degree area, spread over a domain of 120x160 km². Continuous five-minute data is available from 1990-2017.

For consistency in the comparison between CP4 and AMMA-CATCH, the rainfall simulator was calibrated using 10 years of data over the period 1997-2006. A map of AMMA-CATCH station locations is found in Figure 4.1.

Data preprocessing

The precipitation data for CP4 and AMMA-CATCH were both grouped into events according to the same criteria used in Wilcox et al. (in preparation): at least two out of thirty (or an equivalent percentage) of stations/grid points measuring 1mm of precipitation or more. Between events there is 30 minutes of no precipitation at a station plus an interval of no rain in the study window.

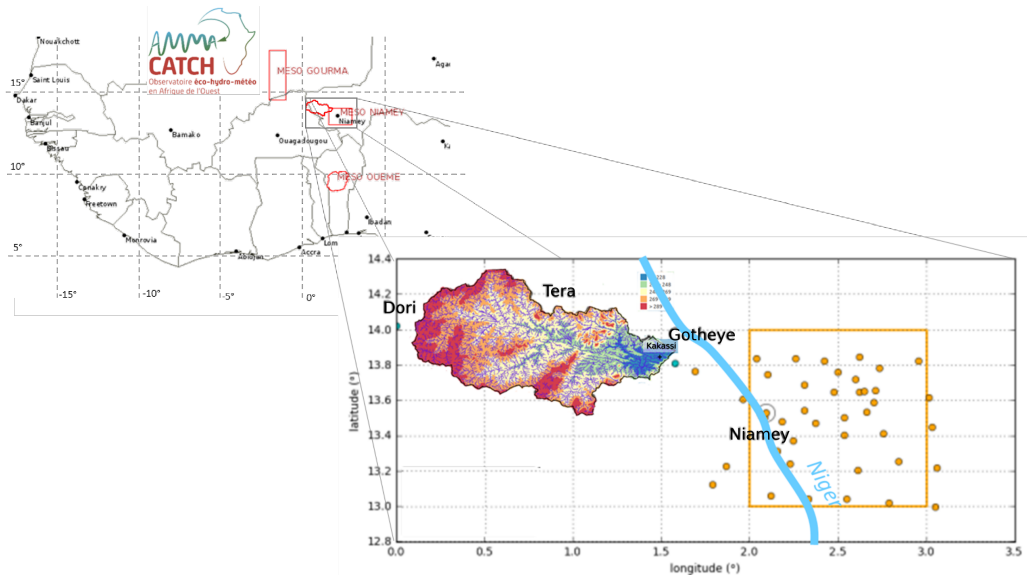


Figure 4.1: Location of rain gauge stations for the AMMA-CATCH network (orange box) and the Dargol River (west of the Niger River). CP4-Africa grid points were extracted over the AMMA-CATCH study site.

4.4.2 Convection-permitting regional climate model: CP4-Africa

Description

The primary data evaluated consists of precipitation outputs from the regional CP4 model over Africa (Stratton et al., 2018). The spatial scale of the gridded data is 4.5km. Intensities are generated at the 15-minute time step.

The CP4 data set used in the present study is comprised of 10 years of simulations from 1997-2006 and 10 years on a future horizon towards the end of the 21st century. Future projections were forced by the RCP8.5 climate scenario.

Data preprocessing

Grid points were extracted over the AMMA-CATCH study area. Precipitation events from CP4 were extracted according to the same criteria used with AMMA-CATCH data.

4.4.3 Hydrological study site and data

The river basin selected for hydrological model implementation is the Dargol River. The Dargol is a catchment with typical Sahelian features regarding watershed processes. It is a tributary of the Niger River and contributes to the increasing trend in recurrent floods in the Niamey region (Wilcox et al., 2018). Its size is compatible with that of mesoscale precipitation systems. The catchment area has a similar climatology to the nearby AMMA-CATCH Niger study site.

Streamflow data exists for the Dargol near the confluence with the Niger River (Kakassi station) (Table 2.1). Although there are some gaps in the data, there is sufficient information to estimate the average hydrological regime and its dispersion. This allows for the testing of a hydrological model's ability to replicate the regime.

As high-resolution subdaily precipitation data is not available within the catchment, the nearby AMMA-CATCH data will be used to study the rainfall-runoff relationship. The goal is not to precisely replicate or predict the data for a specific year, but to use the model to replicate the general hydrological regime and perform sensitivity tests.

4.5 CP4 rainfall: preliminary evaluation

An evaluation of CP4-Africa was already realized for West Africa by Stratton et al. (2018) and Berthou et al. (2019). Here we focus on the specific study zone used in this article and on the key characteristics for hydrological impacts, notably event occurrence, intensity, and size of the events. For all of these characteristics, we also consider their seasonality.

4.5.1 CP4 versus AMMA-CATCH

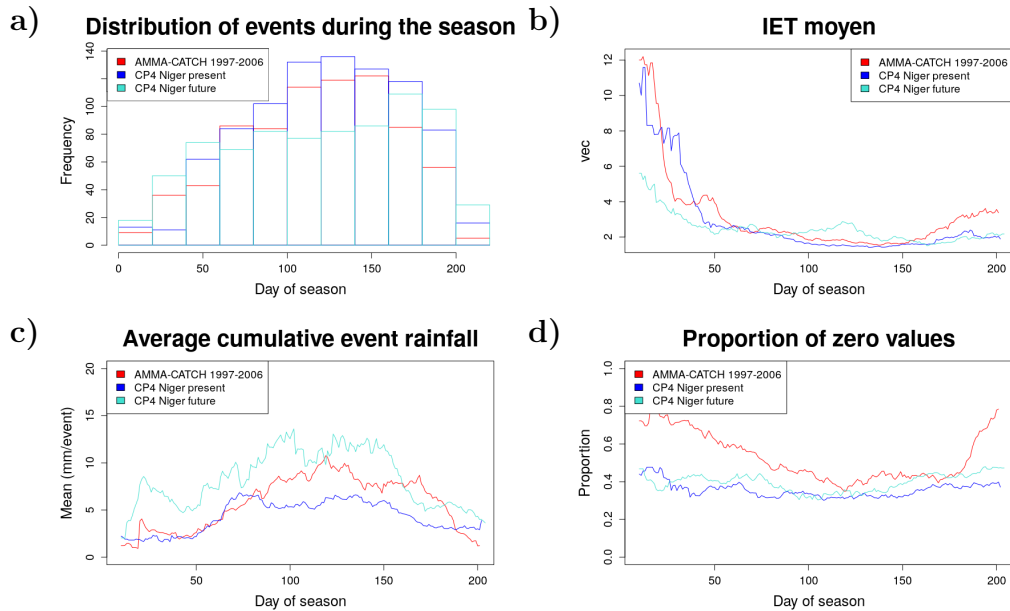


Figure 4.2: Initial comparison of AMMA-CATCH and CP4 data, including CP4 simulations for the recent past (1997-2006) and for a future horizon (2100). a) Distribution of the number of events throughout the season. b) Moving window of time between two precipitation events. c) Average cumulative event rainfall. d) Proportion of zero values.

The number of storms produced by CP4 is more than the number of events registered by AMMA-CATCH according to the event definition used in this study. In particular, CP4 produces too many small events. However, these events contribute a very small percentage of the annual cumulative precipitation. They are unlikely to have a large impact on local hydrology due to their small size and timing during the less rainy parts of the season. The frequency of larger events during the middle of the season when flooding is most likely to occur is well-replicated (Figure 4.2a). Likewise, the time between storm events throughout the season is generally well-replicated by CP4, with less time between storms during the middle of the season (Figure 4.2b).

The seasonal dynamics of the magnitude of precipitation per event also reflects that measured by AMMA-CATCH, and more generally the regional West African Monsoon developments. The season starts with generally sparse

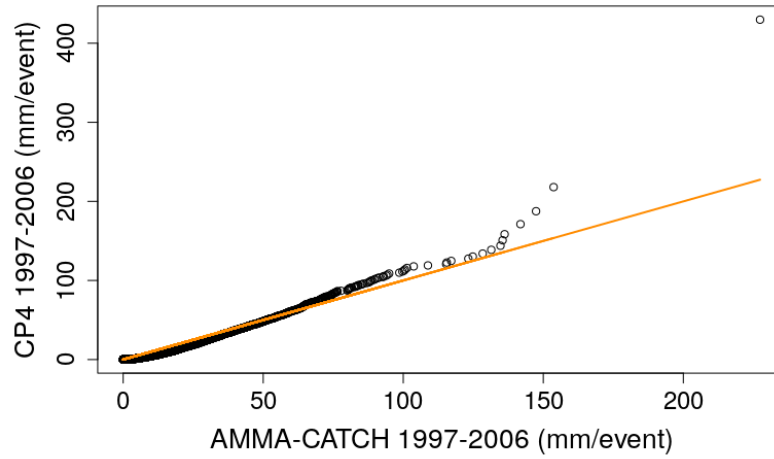
and low-intensity rainfall, then the magnitude of event intensity increases around June (Figure 4.2c). Rainfall levels remain higher during the peak rainfall months around August. This is promising, as it shows CP4's capacity to replicate natural climate phenomena in the region.

However, the average event rainfall produced by CP4 during the middle of the rainy season is significantly lower than that measured by AMMA-CATCH, especially in the middle of the rainy season (Figure 4.2c). The underestimation is amplified by the fact that there are more events during the middle of the rainy season, so the deficit is accumulated. The underestimation of precipitation magnitude is reflected in an underestimation of annual cumulative values.

At the same time, the proportion of zero values in CP4 is too low (Figure 4.2d). CP4 underestimates the proportion of zero values, a criteria considered representative of storm extension (e.g. storms in CP4 are too large in size). This is in part due to the excess of small values produced by CP4. These values are below the threshold of recordability by the AMMA-CATCH rain gauges (the lowest recorded precipitation at a station is 0.12mm).

CP4 underestimates moderate values (Figure 4.3a). On the other end of the spectrum, CP4 produces a few extreme values that exceed any event recorded within the AMMA-CATCH network. It was also observed that events produced by CP4 had a longer duration on average than those of AMMA-CATCH.

a)



b)

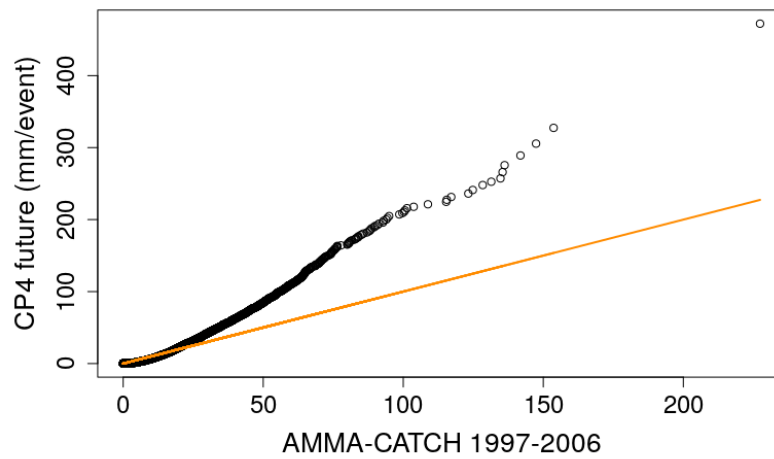


Figure 4.3: Comparison of quantiles between AMMA-CATCH data and CP4 simulations (present (a) and future (b)). CP4 underestimates moderate values but overestimates extremes. Future simulations project an increase in the magnitude of precipitation values.

4.5.2 CP4 present versus CP4 future projections

CP4 simulations project that the study region will have less events during the core of the rainy season (Figure 4.2a). Time between events are projected to

become shorter on average at the beginning of the season and longer during the middle of the season (Figure 4.2b). Average cumulative event rainfall are projected to increase significantly (Figure 4.2c, Figure 4.3b). The proportion of zero values is projected increase slightly (Figure 4.2d).

4.6 Methodology

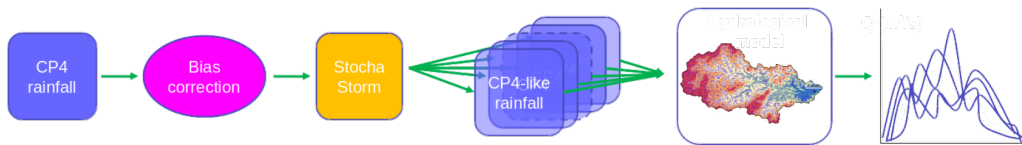


Figure 4.4: Elements of the modeling chain proposed for future hydrological projections: The RCM CP4 as input data; bias-correcting methods applied to correct CP4; The stochastic precipitation generator Stochastorm used to create multiple scenarios of CP4-like rain fields; the scenarios used as an input to a hydrological model; discharge outputs produced and evaluated.

The following section outlines the steps taken for using CP4 to evaluate hydrological impacts. Selected based on the preliminary rainfall comparison results (Section 4.5), bias correction methods are applied in order to correct inaccuracies in CP4. Next, CP4 is used to calibrate a stochastic precipitation generator. The generator is used to produce a set of CP4-like precipitation scenarios. The precipitation scenarios are then used as inputs to a hydrological model. An overview of the modeling chain is presented in Figure 4.4.

4.6.1 Bias correction methods

The goal of bias correction is to correct the characteristics of a data set so that they more accurately represent ground truth data. Based on the factors described in Section 4.5, we consider the most important biases to correct to be 1) the inaccuracies in the proportion of zero values and 2) the underestimation of precipitation magnitude. As the error is larger in the middle of the season, seasonality will be considered for the correction.

The main approach selected for bias correction in this study is the cumulative distribution function transform (CDFt) method (Michelangeli et al.,

2009). CDFt operates by mapping the quantiles in the CDFs of the biased simulations (CP4) with quantiles in the CDF in the reference data (AMMA-CATCH). CDFt was selected as it theoretically will correct both the excess of small values and the extremely high extremes produced by CP4. The calibrated transform function can be then applied to a new dataset, either at a new location or (as in this study) to future projections. CDFt has already been shown to be effective for precipitation in West Africa (Famien et al., 2018).

In addition, once a transform function has been calculated based on the reference data set, the same transform can be applied where there is no reference data. This includes different simulated areas of the model, or simulations of a different time period. In the current study, the transform function developed for correcting CP4 simulations for the present can then be applied to CP4 simulations for the future. See (Vrac et al., 2016; Vrac and Friederichs, 2015) for some examples on how CDFt has been adapted and implemented.

The four CDFt-based methods presented in Vrac et al. (2016) were tested as they specifically address the issues of correcting both the occurrence of null values and the magnitudes of positive values. The first method (positive correction) only corrects non-zero values. The second method (threshold adaptation) identifies a threshold for which the proportion of zero values in the data to be corrected matches the proportion of zero values in the reference data. The third method (direct approach) directly applies CDFt to all values, including zeros. The final method ("Singularity Stochastic Removal") replaces values below the observed reference data threshold with small randomly-generated values, corrects all values using CDFt, then resets values below the threshold to zero. In addition, the methods were combined with a moving window as suggested in Famien et al. (2018). The data for all stations/grid points within an event were mixed for the analysis.

Based on the above initial bias correction methods exploration, the threshold adaptation method with a rolling window over positive values provided the best results. We therefore propose a two-step bias correction process. First, a threshold is found so that the percentage of values below this threshold for the entire CP4 simulation is equal to the percentage of zero values in AMMA-CATCH data. All values below the threshold are set to zero. Second, CDFt is applied in a moving window of 20 days over the season in order to correct the magnitude of values. After CDFt is applied within each overlapping window, bias-corrected values are averaged at each data point to obtain the final values.

The effectiveness of the two-step bias correction method will be evaluated in several ways: first, graphically and numerically via the Stochastorm parameters calibrated on CP4, bias-corrected CP4, and AMMA-CATCH; and second, via the outputs of the hydrological model from the biased and unbiased data sets. The modified seasonal CDF-t method will be evaluated both for its capacity to correct the absolute distribution of values and its ability to correct seasonal characteristics.

The bias correction function applied to correct the 1997-2006 CP4 simulations will be transferred to CP4 future simulations. First, a threshold below which all values are set to zero will be identified for the future simulations so that the ratio between the proportion of zero values in the future versus the present remains the same in the original data set and the bias-corrected data set:

$$\frac{Prop0_{CP4present}}{Prop0_{CP4future}} = \frac{Prop0_{CP4present,bias-corrected}}{Prop0_{CP4future,bias-corrected}} \quad (4.1)$$

where $Prop0$ is the proportion of zero values in each corresponding data set. The correction is applied to the pooled data points of each data set. It is possible for the zero-value threshold used for CP4 1997-2006 to be different from the zero-value threshold for future CP4 projections.

Then, the CDFt function calculated between CP4 present and AMMA-CATCH for each moving window will be applied to the same moving window for future projections.

4.6.2 Stochastic precipitation model

Although CP4 provides many advantages, due to large computational demands, only 10 years of simulations for the present and 10 for a projected future period exist at this time. It is useful to have a larger amount of scenarios for use in hydrological modeling in order to explore the impact of the stochastic variability within the physical and deterministic CP4 simulations.

In order to generate additional scenarios, CP4 is used to calibrate the stochastic precipitation model Stochastorm (Wilcox et al., in preparation). Stochastorm was designed specifically for modeling precipitation events that retain the spatiotemporal properties of convective storms in the tropics. Stochastorm first simulates storm occurrence from poisson like process based on the exponential distribution of the time between two events. For each simulated event, a rain field of the cumulative event precipitation values for the

storm system is generated (kilometric resolution) using a meta- Gaussian function whose marginal distribution combines a set of zero values which represents the spatial intermittency of the field, then for positive values a mixture of a Gamma distribution plus a GPD distribution for the greatest values (above a given threshold). Finally, temporal disaggregation is performed on the cumulative rain fields to transform the values into sub-event intensities (typically five minutes). The transformation takes into account a storm propagation model and the disaggregation via a synthetic hyetogram.

The ability of Stochastorm to replicate the original data characteristics has already been validated using AMMA-CATCH data (1990-2017). The same methodology proposed for the application in Wilcox et al. (in preparation) is used, notably the classification of events as large or small and having separate parameter sets associated with each category. Large events are defined as having 30% or more of stations/grid points with more than 0.12mm of registered precipitation during an event (0.12mm being the minimum detected amount for the AMMA-CATCH rain gauges).

Stochastorm is calibrated using each of the following data/simulations:

- AMMA-CATCH 1997-2006 (control)
- CP4, 1997-2006
- Bias-corrected CP4 1997-2006 (according to Section 4.6.1)
- CP4, future horizon (2090-2100)
- Bias-corrected CP4 future

The parameters of Stochastorm (marginal distributions, spatial structure, etc.) are used as an analytical tool to provide a comparison of the properties of the precipitation sources.

Ten simulated scenarios of ten years from Stochastorm calibrated on each of the five precipitation sources are produced.

4.6.3 Hydrological model description: Phorm

Each of the ten Stochastorm-generated scenarios of ten years, plus the original CP4 simulations, are then used as inputs to a hydrological model.

The process-oriented rainfall-runoff model Phorm (Purely Hortonian Runoff Model) developed specifically for the semi-arid West African Sahel

(Quantin et al., 2017) was used to test the sensitivity of hydrological response to changes in precipitation. The model is implemented on the Dargol River basin (7600 km²), one of the right-bank Sahelian tributaries of the Niger River located near to the AMMA-CATCH Niger rain gauges. Its size is compatible with that of Stochastorm outputs.

Phorm represents the dominant processes responsible for flood generation in the Sahel. Runoff in the Sahel is primarily generated by Hortonian processes (Peugeot et al., 1997), where runoff is generated once the infiltration capacity of the soil is reached. Subsurface flow plays a negligible role and is ignored in the model (Peugeot et al., 2003). As antecedent soil moisture conditions are of negligible influence on runoff production in the area (Malam Abdou, 2014), the model simply represents the infiltration capacity by a constant infiltration rate equal to the hydraulic conductivity (Ks). A hydraulic conductivity value is associated with each subbasin and determines the volume of precipitated water that arrives to the river channel after a precipitation event. Once in the channel, model dynamics are governed by river geometry parameters (channel and floodplain), the roughness coefficient (Manning coefficient), and riverbed infiltration loss. Previous tests have already shown that Phorm produces realistic outlet discharge values when using AMMA-CATCH rainfall records as inputs (Quantin et al., 2017).

4.7 Results and discussion

4.7.1 Bias correction results

Bias-corrected CP4: present

Although the original unbiased CP4 simulations had an excess of (mostly small) events (Figure 4.5a), it underestimated the average annual cumulative rainfall (Figure 4.5b). Bias correction methods increased the annual cumulative rainfall. Cumulative rainfall is now overestimated, but less severely than the previous underestimation.

Of note is the correction in the seasonal signal of storm extent (proportion of zero values) and cumulative event rainfall (Figure 4.6). The correction method for the proportion of zero values within a rainfield brought values much closer to those of AMMA-CATCH (Figure 4.6a). Although seasonality was not explicitly included in the bias-correction method, the corrected

dataset has an improved seasonal signal, more comparable to that of AMMA-CATCH.

The underestimation of average event rainfall was also mostly corrected (Figure 4.6b), especially during the middle of the rainy season. There is still a small underestimation, but this may be in part due to the lack of seasonal correction of the proportion of zero values. As the combination of timing, extent, and magnitude may have an important impact on local hydrology, the correction in the seasonal signal and storm extent may compensate for some inaccuracy in cumulative annual rainfall values.

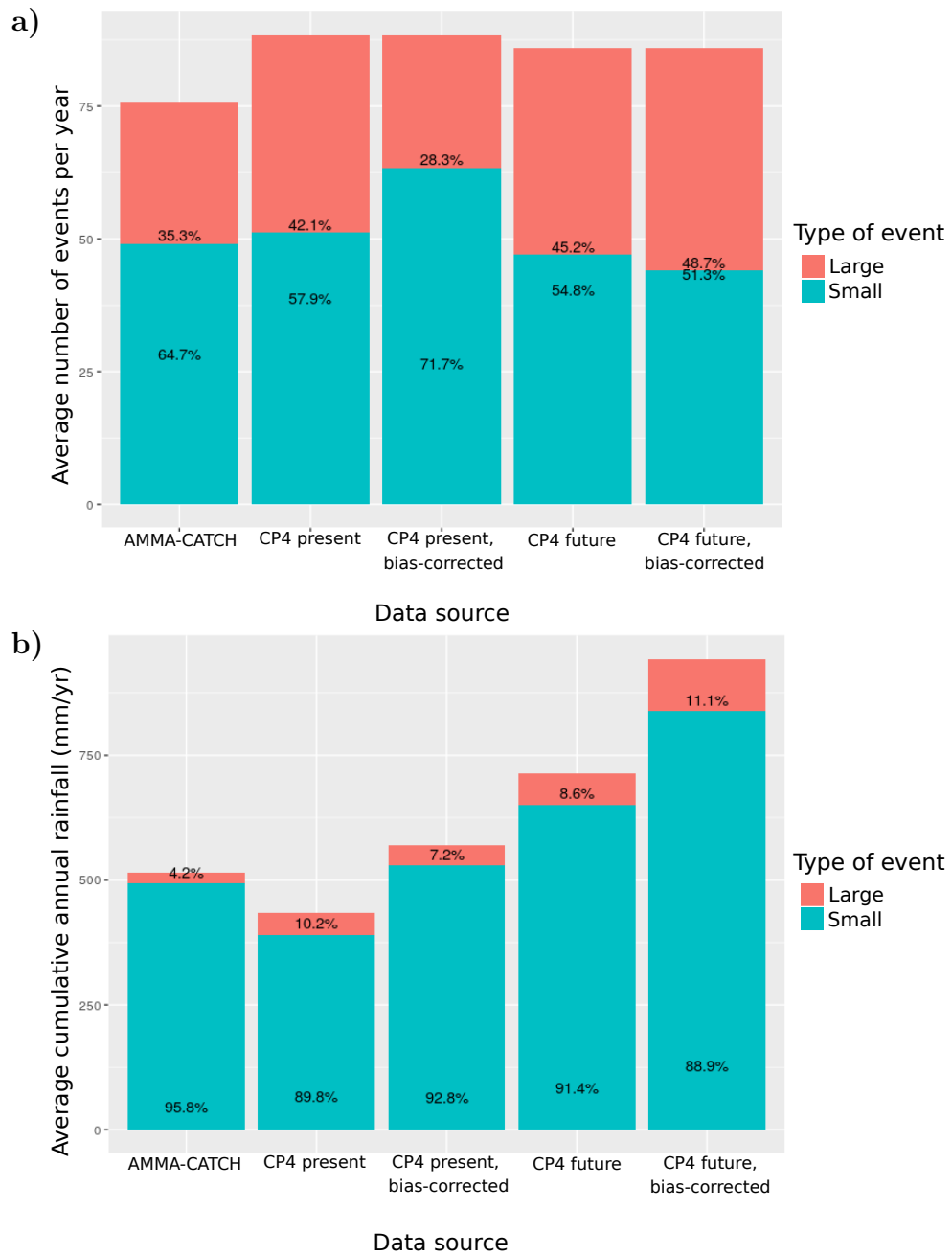
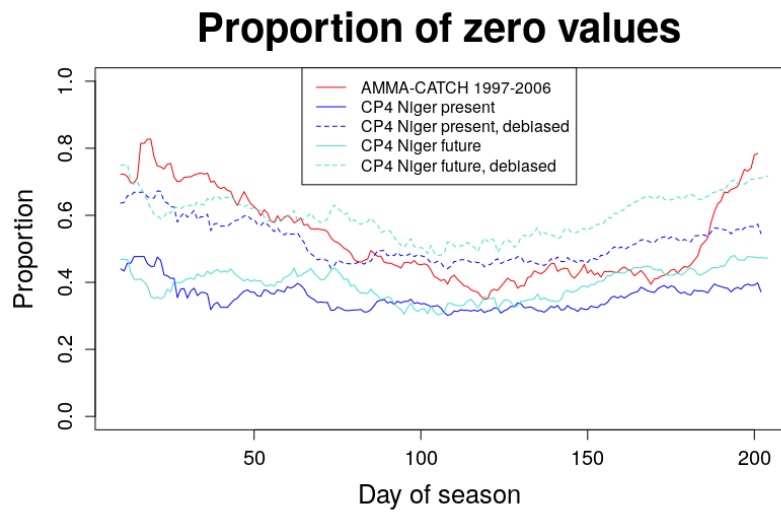


Figure 4.5: The relative contributions of large and small events to a) total events per year and b) total cumulative annual rainfall. CP4 projects that annual rainfall will increase in the future in the study region.

a)



b)

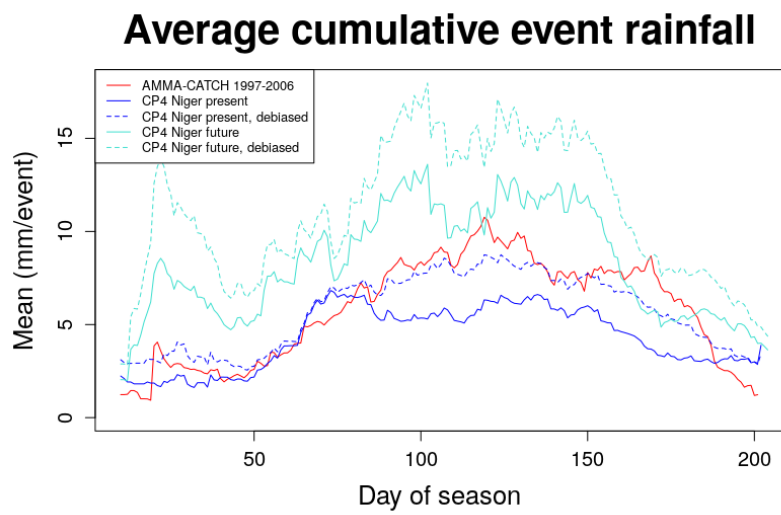


Figure 4.6: Results after applying bias correction methods. a) The proportion of zero values in CP4 before and after correction, compared to AMMA-CATCH data. b) The average cumulative event rainfall before and after correction.

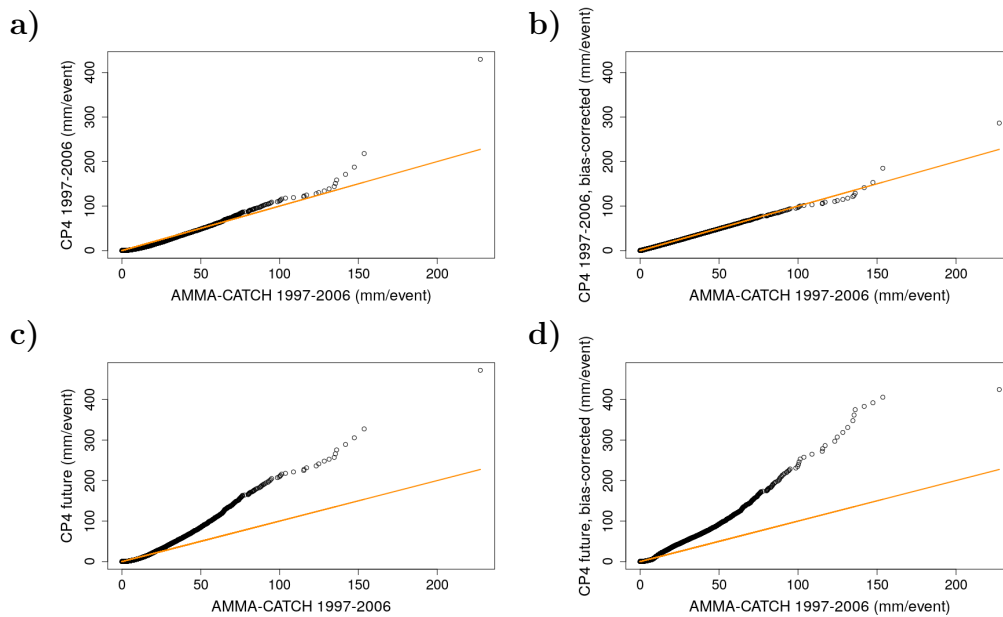


Figure 4.7: Results of bias correction on quantiles. Moderate values are corrected for CP4 1997-2006, and extreme values are overall reduced (a,b). For future projections, the increase in mid-range values becomes more pronounced while only the most extreme are reduced (c,d).

Bias-corrected CP4: future

CP4 projected that precipitation would increase in the future. The number of events would stay approximately the same (even decrease slightly - see Figure 4.5a), but the average precipitation per event would increase significantly (Figure 4.6b), leading to an increase in the annual cumulative rainfall (Figure 4.5b). After bias correction, the annual projected cumulative rainfall increased greatly.

4.7.2 Hydrological modeling results

CP4 present: before and after bias correction

Figure 4.8 shows the average hydrological regime of the Dargol over ten years (observed or simulated). The confidence intervals were established from the 10 stochastic scenarios of 10 years for each case tested.

When used as inputs to the hydrological model, Stochastorm scenarios calibrated on AMMA-CATCH data produce comparable results to the observations (Figure 4.8). This indicates the ability of Stochastorm to capture the main storm features that drive hydrological processes in the region, as demonstrated in Chapter 3

Using CP4 directly as inputs, however, produced significantly underestimated flow results (Figure 4.8a). Both annual flow volumes and peak annual discharge were approximately half of observed values. The timing of the seasonal signal remained well-represented, aside from the underestimation.

Precipitation scenarios from Stochastorm calibrated on CP4 improved results over the basic CP4 precipitation simulations (Figure 4.8b). Using CP4-based Stochastorm scenarios improves flow volumes, but underestimates peak season values and overestimates the variability.

The improvements when using Stochastorm outputs may be due to the fact that CP4 simulations have a 15-minute time step and Stochastorm outputs based on CP4 have a 5-minute time step. The higher-resolution intensities would be less smoothed and have a higher impact on Hortonian runoff generation. Since the temporal disaggregation method in Stochastorm is empirically based on observed AMMA-CATCH intensities, sub-event intensities of CP4-based Stochastorm scenarios may be more realistic than the original CP4 run. Using CP4-based Stochastorm scenarios instead of directly using the CP4 simulations may also have corrected intensities at the event scale (CP4 tends to produce events that are longer in time than those measured by the AMMA-CATCH rain gauges).

Figure 4.8c shows hydrological model outputs from CP4-based precipitation scenarios after bias correction. The bias-corrected scenarios generate hydrological model outputs that correct the underestimation and match more closely to those of AMMA-CATCH.

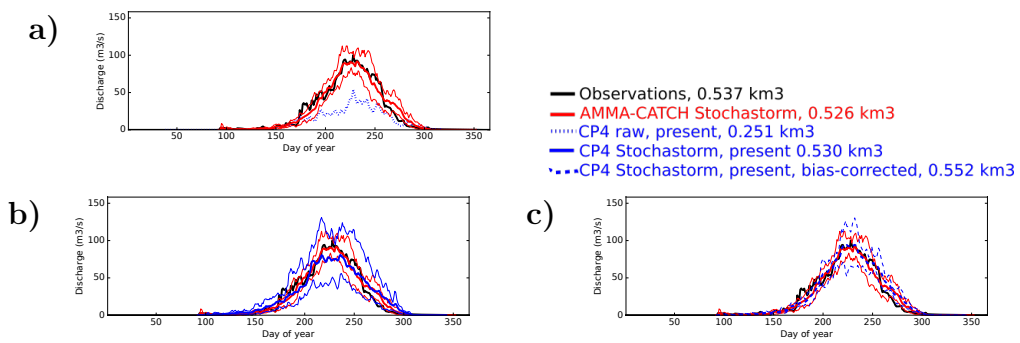


Figure 4.8: Hydrological modeling results (discharge at outlet), with 10% and 90% quantiles for results based on Stochastorm scenarios. Comparisons between observations (black), hydrological model outputs using AMMA-CATCH stochastorm scenarios as inputs, and: outputs driven by CP4 in its original form (a); outputs driven by Stochastorm outputs calibrated by CP4 (b); and Stochastorm outputs calibrated by bias-corrected CP4 (c). Average annual volumes are shown in the legend.

CP4 future

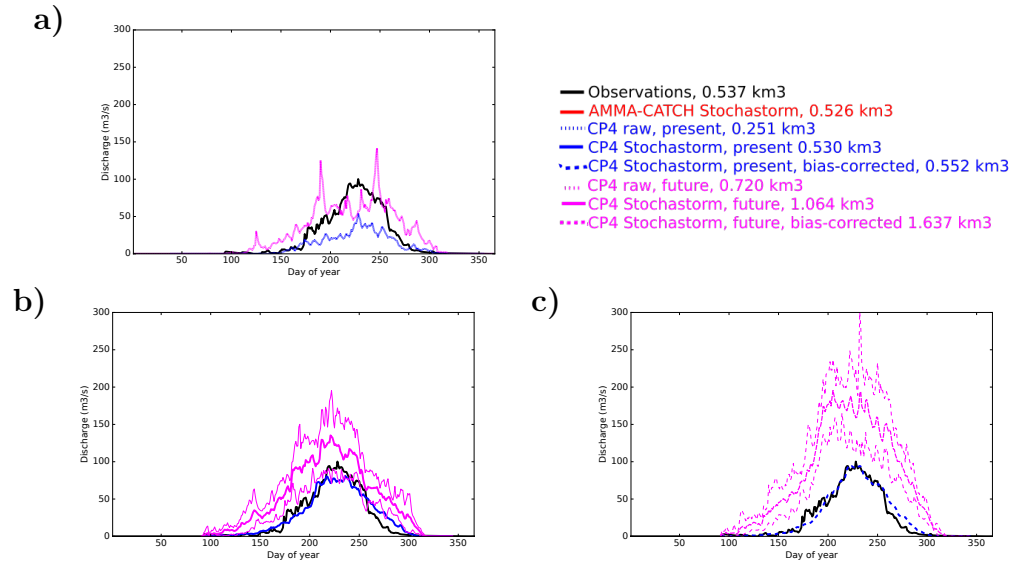


Figure 4.9: Hydrological modeling results (discharge at outlet) for future projections, with 10% and 90% quantiles for results based on Stochastorm scenarios. Results using the original CP4 simulations (a), CP4-based Stochastorm scenarios (b), and bias-corrected CP4-based Stochastorm scenarios (c) are shown. Average annual volumes are shown in the legend.

Figure 4.9 shows the results for using future CP4 and CP4+Stochastorm scenarios to drive the hydrological model. Even before bias correction, annual volumes and peak flow values are projected to be greater than the values in the observed record (Figure 4.9a). Future CP4-based Stochastorm scenarios generated streamflow values that were approximately 1.5 times more than the present for peak streamflow and nearly twice as much for annual volume (Figure 4.9b). After bias correction of the precipitation inputs, average peak discharge is projected to be approximately double and average annual flow volumes approximately triple currently observed values.

4.8 Conclusions and perspectives

4.8.1 Methodological advances

In this study, a modeling chain for future hydrological projections was developed and presented. The first high-resolution convection-permitting RCM for Africa, CP4, was evaluated for its promising ability to replicate precipitation in the region. A stochastic precipitation simulator was calibrated using CP4 and used to generate multiple CP4-like precipitation schemes. CP4 plus the rainfall scenarios were used as inputs in a hydrological model that replicates processes in the Sahelian study region. Finally, outputs of the hydrological model were evaluated. Results showed that streamflow will potentially double over the next century in the Sahelian Niger River basin.

The study demonstrates that convection-permitting RCMs provide promising information for impact studies. Stochastic precipitation generators and bias correction methods can link RCMs to hydrological models for producing additional realistic scenarios and exploring variability.

4.8.2 Limitations and future work

CP4 has many strong points in its ability to correctly replicate Sahelian precipitation. However, it also presents certain limitations. Only a limited number of years of simulations are currently available. It is also biased, as shown; while we were able to eliminate much of the bias thanks to AMMA-CATCH control data, that is not the case for all of Africa. We can use the transfer function for the AMMA-CATCH Niger study area to apply the same bias correction approach to CP4 in a different part of Africa, but this uses the assumption that the bias is consistent throughout CP4. One could perhaps make the assumption that the bias is consistent within regions having relatively homogenous climate features - such as within the Sahel - but the assumption becomes less valid in other regions. The tools and methods should be verified in other regions by using for instance the other AMMA-CATCH sites in Sudanian climate (Benin) and possibly satellite remote sensing rainfall products (even if their skills are still limited over the region and their scale are coarser than the expected kilometric resolutions).

Future projections from CP4 are based only on one GCM initialization with one RCP scenario. Other GCMs under different hypotheses could potentially lead to vastly different conclusions about how the climate will change

in the future, as the conditions of the initializing GCM have a significant impact on RCM's accuracy (Jenkins et al., 2002). There is currently a joint project between the IGE, CEH, Met office, and University of Reading to investigate the impacts of GCM initialization choices on CP4 projections.

One limitation of the study is that the only factor considered for future hydrological projections was changes in precipitation. Land use changes, already shown to have significant impacts in the Sahel historically, were not taken into account. As the population in West Africa is undergoing rapid growth and demographic change which is projected to continue, anthropic changes are potentially an important factor in changing land surface and as a result changing infiltration capacity and runoff. Changes in land surface from climate changes itself are also probable.

These questions lead towards the question of attribution: Which factor has a more significant impact for future changes in hydrology, precipitation/climate changes or land surface changes? Additional methodology is required in order to evaluate the relative impacts in a robust manner. The capacity for non-stationary land surface properties is already implemented in hydrological model.

Despite the aforementioned limitations, our results suggest concerning projections that would bring societal implications. If peak streamflow may double and annual discharge volumes triple, what are the impacts on local populations? What adaptations measures are required for flood protection given the potential increase in flow? On the other hand, how might the increase in flow benefit local populations due to the increased available water resources, especially if structures for irrigation are put in place? More evaluation is necessary in order to understand the potential implications of hydrological change (Blöschl and Montanari, 2010). However, these questions highlight the importance of pursuing the development of hydrological projections in order to provide sound and relevant indicators for decision makers in charge of water resources and hydrological risk management in the region.

Chapter 5

Conclusions and future research directions

5.1 Summary and implications of thesis work

This thesis focuses on detecting changes in extreme hydrological events and modeling the systems that produce those events. It adopts an original approach based on taking into account the most important processes in the genesis of hydrological extremes within a continuum from the past to the future, from global climate to river discharge.

The thesis work is conducted in West Africa with a particular focus on the Sahel, the semi-arid band crossing the region from east to west between latitudes 12°N and 18°N.

In the intertropical zone, West Africa is recognized as one of the most critical regions with regard to the global changes underway. The livelihood of local populations is essentially based on rainfed agriculture which is highly dependent on the limited available water resources. The marked seasonality of rainfall tied to the West African monsoon that produces it is thus an intrinsic factor of vulnerability. The variability is also strong at the decennial scale, as illustrated during the last century by the abrupt transition between two periods: relatively wet in the 1950s and 1960s followed nearly 30 years of drought whose intensity and scale remain unmatched in the modern world.

There is great variability of precipitation at the inter-annual scale, particularly in recent years where dry and wet years can be mixed together in a seemingly haphazard way. The last three decades, although on average

slightly wetter than during the great drought period, have continued to be subject to dry sequences with detrimental impacts on crops. At the same time they have witnessed an increasing number of severe floods that caused widespread fatalities and damages.

The magnitude of the flood risk problem in West Africa has led the scientific community to look into the possible mechanisms behind the apparent increase in risk. The main hypotheses for the increase in risk were mainly based on the undeniable increase in population "exposure" to floods, particularly because of the high population growth in this region of the world in cities prone to expansion of habitants in floodplains.

The "hazard" component of flood risk was less documented. A few previous studies discussed the potential causes of floods, mentioning two multiplicative effects related to (i) soil degradation resulting from the combined impact of agricultural intensification and the great drought, and (ii) intensification of rainfall which has proven to be a major marker of climate change over the last three decades in the Sahel with a tripling of the frequency of extreme monsoon storms.

On the other hand, there was very little information on how these two factors actually affect the magnitude of the floods, or how their future development might continue to influence flooding in the coming decades.

This led to several lines of research that guided my thesis work. The first concerned the quantification of the flood trend, an evaluation that is central to understanding the past trajectory of flood risk and attributing the causes. The second concerned the possibility of analyzing the impact of rain in the genesis of floods. The focus was on the characteristics of monsoon storms, as they are at the interface between changes in the properties of the atmosphere and hydrological impacts.

I therefore conducted my work on both flood trend detection problems (Chapter 2) and stochastic modeling of monsoon storm systems (Chapter 3) with the aim of contributing to set up a chain of model from climate to hydrology to project the impact of future precipitation changes on floods in the Sahel (Chapter 4). In the first part of this chapter, I summarize below the approach adopted and the main results obtained for each major question posed by the thesis.

In the second part of the chapter, the next steps identified for the continuation of research given the current limitations are presented. The third part focuses on perspectives for creating a robust attribution framework for trends in hydrological extremes.

Q1: Is there a significant trend in extreme streamflow in West Africa, or are the documented flooding events isolated incidences

Methodological advances: The study on trends in extremes in West Africa provided non-stationary GEV distributions for hydrological annual maxima with flexible representations of non-stationarity. The use of an underlying non-stationary distribution allows for estimation of uncertainty, calculation of return levels, and confidence intervals on both parameter values and return levels, all of which were conducted in the study. An estimation of the magnitude of the trend was also provided. The trend detection methodology was specifically designed for extreme values, unlike other statistical tests which assume the data is normally distributed. A robust model selection procedure was applied. Two regions with distinct hydrological characteristics were compared in the study: the Sahelian area of the Niger River basin and the Sudano-Guinean area of the Senegal River basin. The methods were implemented using R software which is freely available.

Findings: For all data series studied, the non-stationary GEV was significantly more representative of the data than the stationary GEV. The study confirmed significant trends in extreme streamflow in West Africa with greater than 99% confidence.

Trends in the Sudano-Guinean region of the Senegal River are in contrast with trends in the Sahelian Niger River. All trends are positive for the modern period, but started increasing in the 1980s in the Senegal River basin, whereas the increase started earlier (1970s) and at a greater rate in the Sahel.

For the right-bank tributaries of the Niger river, return levels have greatly increased. The 2-year return levels have more than doubled since the end of the 1960s and the 10-year return levels are currently over 1.5 times higher than they were before. Shorter-period return levels (2- and 5-year) estimated with a non-stationary GEV are 95% certain to be above return levels estimated with a stationary distribution. Uncertainty increases with longer return periods.

Implications: The results have direct impacts for the design of hydraulic structures and for river basin management. Hydraulic structures are commonly designed according to the magnitude of a given return level. The use

of a stationary distribution to calculate return levels in the right bank of the Niger River and for a few stations in the Senegal River basin would underestimate return level values. If the structure was designed for flood protection, this would lead to populations and infrastructure being at greater risk of flood damage. The increasing trends in extreme values indicate an increase in frequency of events of greater magnitudes.

For the Senegal River basin in particular, accurate estimation of return levels is essential for management of existing dams and construction of additional planned hydroelectric structures.

Limitations : The study made use of a limited selection of parametric models in the range of model choices for representing temporal evolution of GEV parameters, although a few additional parametric functions were evaluated during sensitivity testing. Only breakpoints that were a switch between two linear increasing or decreasing trends were considered, rather than other types of regime changes (e.g. abrupt shifts).

Uncertainty is high for all return levels other than for very short return periods (2-year, 5-year). Given the length of the data sets of about 60 years, naturally the 100-year return level would be accompanied by high uncertainty. Uncertainty would decrease with additional data and suitable model choice.

The uncertainties do not incorporate rating curve uncertainty, as this is challenging to estimate without additional measurements. Rating curve error could have a particularly significant impact on extreme event documentation.

Although an increase in precipitation intensity during the last two decades seems to be one of the main drivers of hydrological changes at present, it was not the case in the past (Sahelian Paradox during the 1970s-1980s drought) and it may not be the case in the future.

Q2: How can one model mesoscale convective systems in order to explore the properties of precipitation that drive streamflow?

Methodological advances: This study presented the stochastic rainfall simulator Stochastorm that provides an accurate statistical representation of mesoscale convective systems (MCSs) in the intertropical zone. It is capable of replicating the spatial covariance structure, spatial intermittency, and

magnitudes of precipitation within a storm event. It features a model for the occurrence of events throughout the season, defined season start and end points, and parameter seasonality. Extreme precipitation values were explicitly modeled via a peak-over-threshold (POT) distribution in the marginal distribution for values above a given threshold. It realistically represents the marginal distribution of cumulative event precipitation, as well as sub-event intensities.

The application to the test region in the Sahelian zone of West Africa added the feature of having different model parameters for small and large events.

A notable improvement was the use of a four-parameter Beta distribution to better model the sub-event variability of precipitation intensities. The four-parameter Beta distribution allows for the definition of upper and lower bounds and thus allows simulations to be more coherent with the physics of precipitation generation.

Findings: Precipitation scenarios produced by the simulator have the same main statistical properties as the input data used to calibrate the simulator. The advancements proposed in this thesis improve the representation of MCSs in the Sahel.

Implications: Stochastorm can generate long series of precipitation data for use in sensitivity testing and for application in areas where no measurements exist. The fact that Stochastorm realistically represents key characteristics of MCSs in the Sahel at an appropriately high resolution means it can be used to drive impact models, e.g. for hydrological and agricultural studies.

Limitations One of the major limitations of Stochastorm in the context of climate change is its lack of ability to directly incorporate nonstationary interannual trends in simulations. It can model interannual non-stationarity if the user directly changes parameters after simulating one year at a time (or by simulating two different time periods as done in Chapter 4), but this must be done "by hand" year by year. It has also only been calibrated and applied on one specific study zone in one specific climate region. Adapting it for different tropical climate regions may not be straightforward.

Q3: Based on potential precipitation changes, what trends might we see in streamflow in the future?

Methodological advances: The main methodological contribution of this study was the production of a modeling chain for hydrological projections. The RCM CP4-Africa, one of the first convection-permitting RCMs available in the region at scales that can be used for impact studies, was shown to reproduce several key characteristics of precipitation in the Sahel. CP4 was corrected for bias according to the limitations identified in the original CP4 simulations after comparison with high-resolution in-situ AMMA-CATCH data. The bias-corrected CP4 was then used to calibrate the stochastic precipitation simulator Stochastorm and produce CP4-like precipitation scenarios. Finally, scenarios for the present and for future projections were used as inputs to a hydrological model implemented in the Sahel region of the Niger River. The modeling chain is one of the few (if not the only one) that can show the hydrological impact of future evolution of convective rainfall in West Africa due to climate change.

Findings: Although the number of precipitation events was not projected to increase (number of events approximately stable), the average magnitude of each event is. The projected increase generates larger annual precipitation volumes and greater average cumulative event rainfall. Hydrological modeling results for the model implemented for the Dargol River showed that the increase in precipitation led to streamflow volumes that were three times larger on average in the future than in the present. Discharge for simulations driven by the the bias-corrected CP4 scenarios was on average nearly twice as large in the future than for the present.

Implications: The increase in river discharge calls for adaptation measures in order to reduce flood risk. At the same time, the increased precipitation and river volumes might be promising for agricultural purposes, notably irrigation (provided that suitable hydraulic structures are available to capture surface water for this purpose). More studies are needed to investigate these points as the increase in intensity and stable number of events may have varying effects. It also encourages more hydrological projections to be made so that actions and policy initiatives can be identified that are appropriate for the expected changes over specific timelines in the future. Adaptation

strategies are especially important given the projected demographic growth and change in the region.

Limitations: At the time of the research conducted for this thesis, CP4 simulations were available for ten years from 1997-2006 and ten years during a period 100 years in the future. In addition, CP4 was initialized only on one GCM with one RCP scenario. Although CP4 gives insight into potential future changes, it does not indicate what may happen in 2050, for example, nor what would happen under different future emissions scenarios and under the forcing of a different GCM. The internal model variability may also have had an impact on projection results (Hawkins and Sutton, 2011; Monerie et al., 2017), although internal variability is most able to impact climate signal projection on a short-term horizon (10-30 years) and not on the longer horizon seen in the present study.

CP4 also has some limitations regarding its coupling (or lack thereof) with various components of the global environmental system. CP4 is forced unidirectionally by the global climate model, without bilateral interactions. It is not coupled with surface processes, including vegetation which may provide feedbacks that influence regional climate. In spite of these limitations, CP4 is still the most advanced RCM available for the region at the present time.

CP4 had some remaining biases after correction with AMMA-CATCH data. It is unknown whether the bias in CP4 is constant spatially, i.e., it is unknown whether the transform applied over the AMMA-CATCH site is applicable elsewhere in Africa. This limits the ability to apply the bias correction methods to other regions of CP4 data with confidence in the results.

Arguably the major limitation of the modeling chain is that the only factor considered to impact future hydrological projections was changes in precipitation. Certainly other causal factors are possible. Land surface properties already has been shown to have an important role in runoff generation in the Sahel. The population in the region is projected to grow rapidly, which may lead to changes in land use patterns and practices in the future due to demographic pressure. In addition, the drainage basins would naturally evolve according to future changes in precipitation. In the present thesis the parameters of the hydrological model were considered stationary.

5.2 Future research directions

5.2.1 NSGEV models for trends in hydrological extremes

Updating and extending NSGEV models

Ongoing next steps in the continuation of Wilcox et al 2018 (Chapter 2) include updating NSGEV models for AMAX time series. The additional information could be in the form of longer time series as new data becomes available. It can be also in the form of updated rating curves. Rating curves play a large role in the accuracy of flow measurements. The right bank of the Niger River in the Sahel features high rates of sediment transport, meaning that rating curves might quickly become inaccurate and need to be updated more frequently (as opposed to rivers flowing on bedrock, which stays relatively stable).

One project (ANADIA project led by the Polytechnic and the University of Turin, Italy) was already completed to update rating curves for the Sirba River. I had the opportunity to update the NSGEV for the Garbe Kourou station based on the updated data set, and to collaborate to the writing of a paper recently accepted for publication in the journal *Water* (Massazza et al., 2019). Results showed that the trend in AMAX in the updated series was much greater than that previously found. 2-, 5-, and 10-year return levels estimated with the updated series were approximately double those estimated with the original series. The increase was greater for longer return levels, however uncertainty was also high. Performing the same update to other rivers as more accurate rating curves become available would improve the representation of extremes.

The same NSGEV analysis can also be extended to other stations in the region in order to further evaluate the regional contrasts or consistencies in flood changes over the last century. This would allow more insight into how return levels vary temporally and spatially if a non-stationary model is used.

Identifying other spatiotemporal factors that influence NSGEVs

One idea is to see if there is a spatial pattern in the trends of extreme values. Panthou et al 2013 already determined that there is a latitudinal gradient in extreme precipitation. The same analysis could be performed

with streamflow using spatial covariates such as latitude, longitude, elevation, etc.

Another idea is to directly use covariates that change over time to perform attribution and explain drivers of extreme hydrological values. Consider for instance the subject of whether precipitation changes or land surface changes better explained changes in extreme streamflow. This is similar to the analysis done in Risser and Wehner (2017), which attributed Hurricane Harvey to human influences using proxies for human and climate factors as covariates. In the case of extreme streamflow in the Sahel, proxies for climate could be a precipitation index: annual rainfall, average event intensity, number of events per year, etc. It could also be a factor such as potential evaporation. Potential land cover covariates could be hydraulic conductivity values (Ks), percent cover of a certain land cover/vegetation type, etc. The analysis of land cover, however, would require additional data about land surface properties, or interpolating in time between available data sets and making assumptions about the evolution.

5.2.2 Stochastic precipitation generator

Model improvements and feature additions

Immediate next steps for the stochastic precipitation simulator Stochastorm (Chapter 3) focus on using the simulator in a wider variety of contexts. A top priority would be adding the improvements developed during this thesis to an R package for Stochastorm that would facilitate additional work.

Another priority continuing to improve and validate the temporal disaggregation methods. The relationship between the maximum intensity and the cumulative event precipitation can be improved, especially for representing the most extreme intensities. Only one standard hyetograph was used, limiting the diversity of storm types and the flexibility of the storm duration associated with a given max intensity. One can imagine having multi-peak storms and relaxing the links between maximum storm intensity and other characteristics of the hyetograph.

One can envision making the season definition and seasonality parameters of Stochastorm more flexible, and their selection more automated. The end goal would be to make Stochastorm implementable in regions that do not have the stark wet season/dry season contrast that the Sahel has, and that have other forms of seasonal signal (although several covariate types are

already available in Stochastorm).

At the present moment, Stochastorm is assumed to be accurate over the entire data period. Although initial tests did not find a great difference in model parameters between the 1990s and 2000s, the model parameters may not be applicable during other time periods where the precipitation characteristics varied more drastically. In order to have continuity in the model over time, one important advancement for Stochastorm would be to implement non-stationarity into the model.

The issue of non-stationarity has particular methodological significance when considering non-stationarity in extreme values for the continued investigation of the flooding issue. If the underlying distribution of extreme values changes, how would small and mid-range values change? How to realistically represent the observed non-stationarity in precipitation characteristics in the format of stochastic model parameters?

Using Stochastorm in other regions

A major endeavor for Stochastorm would be to validate the model in other areas. One could start within the Sahel to verify the hypothesis that Stochastorm is applicable to other areas within this relatively homogenous climate zone. Then, one could test Stochastorm in other areas of West Africa where precipitation properties start to differ. The other AMMA-CATCH sites in Benin and Mali/Senegal could be useful in achieving this first goal as they provide sub-daily rainfall data suitable for documenting rainfall variability at the meso-scale (Vischel et al., 2011). This is an important step before applying Stochastorm in areas where no data is available. Eventually, one can envision validating the model for studies in regions with more greatly differing climate.

Another prerequisite for applying Stochastorm elsewhere would be to add numerical evaluation criteria that would both validate the accuracy of the model and more easily allow for comparison with other models. For example, the jackknife method could be applied to first verify model sensitivity, and the total rainfall over the modeled area could be utilized as a means of comparison with other models.

In particular, there is a need to verify that the relationship between the maximum subevent intensity and cumulative event rainfall is applicable in other areas. Many regions of the world (especially in the tropics) do not have in-situ precipitation measurements at five minutes, and the empirical

relationship between intensities and event rainfall developed using AMMA-CATCH Niger data is unlikely to be universally applicable.

5.2.3 Limits of applicability of bias-corrected CP4

Similar to the need to validate Stochastorm in other regions, validating that the bias correction method applied in Chapter 4 is applicable to all (or a given area) of CP4 in West Africa (or even Africa) is an essential next step. If the transform used to correct CP4 at the AMMA-CATCH Niger site is found to be valid over a given region, it can be used to correct biases in CP4 for areas that do not have in-situ measurements. This would be advantageous as CP4 could provide realistic precipitation simulations for regions where data is lacking.

The validation of the bias correction transform can be achieved by comparing the CDFts developed for correcting the bias of CP4 at two sites that each have in-situ data. Once again, the AMMA-CATCH data sets in other parts of West Africa can prove to be useful. Alternatively, when no sub-daily data are available, daily data from national weather services can also be of much value to assess CP4 and the related bias correction method performances.

Another important step is to evaluate the stationarity of the calibrated bias-correction transform over time. The present thesis assumed that the bias correction used for CP4 in the present period was also valid for future projections. This is a significant assumption. One way to validate it would be to confirm, once additional CP4 simulations are available for different years, that the difference between the transform function in one subperiod does not significantly differ from the transform function in another subperiod.

5.3 Attribution of trends in hydrological extremes

The modeling chain presented in Chapter 4 features qualities that advance the current research on localized hydrological projections. It uses an RCM that resolves convection, quality in-situ data to correct biases in the RCM, and a hydrological model that represents processes in the study area according to decades of previous research. The above qualities give legitimacy to the hydrological projections produced by the modeling chain.

However, in spite of the advances, it has limitations which raise numerous additional questions. One of the major limitations of the study in Chapter 4 is that it treated precipitation as the only driver of future changes in local hydrology in West Africa. Although climate is a driving factor in hydrological processes, it is not the only one. It has already been shown that land surface changes have a significant impact on runoff in the Sahel, notably the soil crusting that occurred during the drought in the 1970s and 1980s and produced the Sahelian Paradox effect of more runoff in spite of reduced precipitation (Albergel, 1987; Descroix et al., 2009; Aich et al., 2015; Cassé et al., 2016; Gal et al., 2017; Boulain et al., 2009).

The main research direction envisioned is to better identify and understand the causes of changes of extreme streamflow in West Africa. Simply considering driving factors as explanatory covariates in a non-stationary distribution as described in Section 5.2.1 can be done as a first step. However, to more fully evaluate the relative contributions of different causal factors, it is recommended to adopt the attribution framework proposed in climate change studies.

5.3.1 Background for attribution in climatology

The main next objective identified for after this thesis is to take detection and attribution (henceforth D&A) methods and apply them to the problem of flooding in the Sahel region. The goal is to develop robust methods for attributing changes in flood magnitude to either climate changes or land use changes.

The task of attribution requires several preliminary steps. First, a statistically significant trend or change in the variable of choice must be identified, one that was not caused by internal variability at a certain level of confidence. Second, the system under study must be evaluated. The given drivers (here climate and hydrological/land surface characteristics) must be well-understood, especially as an accurate representation of the internal system variability is essential for D&A methods. Next, the system must be modeled in a way that allows the user to change parameters related to hypothesized causes. Simulations are run with the model using parameters/scenarios that reflect the attribution hypotheses. Finally, model outputs are used to conduct the attribution analysis. Note that these steps are rarely followed in the studies claiming hydrological attribution (Merz et al., 2012), and even less so in West Africa.

In the field of climatology, methodologies have been developed for addressing the issue of global climate change, in particular global temperature change. In order to attribute temperature change to a particular cause, two global climate models (GCMs) simulations are compared: 1) A GCM simulations that includes only natural influences on the atmospheric greenhouse gas and energy balance, such as volcanoes and fluctuations in solar irradiance, and 2) a GCM that includes both natural and anthropogenic greenhouse gas influences. The models are run over the observation period. Multiple scenarios are produced for each model in order to have an estimate of internal variability. Then, observations are regressed against the GCM outputs typically using a form of Generalized Least Squares (GLS) regression (often called “fingerprinting” in climate change literature).

The Intergovernmental Panel on Climate Change has provided specific definitions for what is meant by both “detection” and “attribution.” Detection is the process of proving, within a certain level of confidence, that a given trend could not have been produced by “internal” (unforced) variability alone. It does not assign a cause to the change (Hegerl et al., 2010). The detection step was already completed for the case of non-stationarity of extreme hydrological events in West Africa in Chapter 2.

Attribution goes a step further by assessing if the trend is associated with one or more external drivers on the system, and not with other, physically plausible causes (bin, 2013)).

5.3.2 Methods for attribution

Researchers in the domain of climate studies have developed robust methods for detection and attribution over past decades, including the well-known attribution of increased surface temperatures to anthropogenic greenhouse gas emissions. The methods provide ways to both arrive at a given conclusion and quantify the certainty of the attribution. Although well-developed in climatology, these methods have not often been applied to hydrological issues.

Within this framework there are two main approaches to attribution: trend attribution and event attribution.

Trend attribution

Trend D&A seeks to evaluate long-term evolutions in a variable under study. Early D&A studies in climate sciences focused on this approach (see Hassel-

mann, 1993; Hegerl et al., 1997; Hasselmann, 1997 and Allen and Tett, 1999 for examples and methodology). The goal was typically to attribute a trend in a climate variable, such as mean surface temperatures, to a given cause, commonly anthropogenic greenhouse gas emissions.

Termed “optimal fingerprinting” in the climate change D&A literature, the primary method for attribution method is in essence a form of generalized least squares regression. It follows the form:

$$Y = X\beta + \epsilon$$

where Y is the vector of n observations, X is the design matrix of k factors (signal simulations generated by the model for each of k scenarios) by n realizations, β is the vector of k parameters corresponding to the magnitude of influence of each simulation x , and ϵ is the error term (estimated from model control runs). If the fingerprints in β are found to be non-zero, it is concluded that a trend is detected. The attribution stage tests the hypothesis that the β values associated with a given cause are equal to unity.

Improvements to the basic optimal fingerprinting approach have been proposed, including the application of total least squares presented in Allen and Stott (2003). Regularized optimal fingerprinting was developed by Ribes et al. (2013).

In the context of extremes, optimal fingerprinting can be used to evaluate changes in the underlying distribution of extreme values over time. Min et al. (2011) used a probability based index of extremes together with optimal fingerprinting regression methods to evaluate the human contribution to the increase in extreme precipitation.

Event attribution

Event attribution aims to determine if an event was influenced by change in a given forcing. The fraction of attributable risk (FAR) measure, common in the fields of epidemiology and environmental law has emerged as a popular method of event attribution. Simulations are conducted for the unforced scenario, or “the world that might have been,” and the scenario with the forcings under question, or “the world that was.” In the case of climate change, for example, the unforced scenario removes the effects of anthropogenic greenhouse gases.

FAR is calculated by the following equation:

$$FAR = 1 - \frac{P_{unforced}}{P_{forced}}$$

$P_{unforced}$ is the probability of a given event in the simulations without the specific forcing(s) in question, and P_{forced} is the probability of the event with those forcings.

Thermodynamic methods

Trenberth et al. (2015) argues that one should rather consider the climate system's thermodynamic state when attributing extreme weather events to either natural or anthropogenic causes, then determine if that thermodynamic state was influenced by anthropogenic climate change. The reasoning behind the thermodynamic methods could be applied by studying specific flooding events in the record and identifying associated causal factors. However, the FAR method is preferred for future studies of event attribution as it provides the advantage of quantifying the level of attribution.

5.3.3 Attribution of changes in hydrological extremes

Whereas climate change attribution focuses primarily on changes in mean values, such as mean sea surface temperature, flood attribution is concerned with changes in extremes. Heavier than usual floods are, by definition, rare, which raises additional theoretical and practical challenges. Attribution extremes is additional challenge because one can not simply perform a regression on the peak streamflow values themselves, as that would neglect the specific characteristics of extreme values. Extreme value theory (EVT) provides a framework for treating the theoretical challenges of analyzing extreme values. The aim of future work would be to couple EVT methods with attribution methodology in order to evaluate the recent hydrological changes in the Sahel region. For the case of hydrology, optimal fingerprinting (least-squares regression) can be used to attribute changes in parameters of the underlying GEV distribution of annual streamflow maxima.

As extremes are of significant concern given the recent flooding events in West Africa, future research endeavors would focus on the attribution of extreme events. However, one could imagine attributing other hydrological changes, such as annual streamflow volumes.

Most studies in the domain of hydrology that allegedly treat the attribution problem in fact only perform the detection part of the analysis. They

frequently show the correlations between the explanatory and response variables under study, but lack a sound methodology for testing the certainty of their conclusions. According to Merz et al, 2012, attribution methods must have three elements: Evidence of consistency (i.e. the produced trend is consistent with the expected impacts of the driver under question), evidence of inconsistency (the trend is not consistent with the effects produced by other, physically plausible explanations), and a provision of confidence statement Merz et al. (2012). A review of attribution research in hydrology found that most studies of flood attribution only contained the first element. Studies which contained all three criteria, in particular a statement of confidence about the results, were rare if not nonexistent. Most papers simply pointed to other studies as support for their conclusions, albeit the other studies' relevance was often questionable.

5.3.4 Precipitation or land cover? Natural or human-induced?

The following sections detail the proposed research approach in the context of attributing the recent cases of extreme flooding in the Sahel region, notably the right bank of the Niger River near Niamey, Niger.

Although other causal factors exist, it is assumed based on previous research findings that climate (precipitation) and land surface properties are two factors that may have the biggest influence on Hortonian runoff in the Sahel. Modeling and attribution efforts will therefore first concentrate on identifying the relative contribution of precipitation and human-driven land surface changes, separating out the precipitation-driven contribution to land surface changes.

Figure 5.1 shows a proposed modeling framework for attribution of hydrological extremes in its simplest form. Historical changes in precipitation are identified in AMMA-CATCH data and implemented into the rainfall simulator Stochastorm. Scenarios are generated from Stochastorm. In parallel, land cover changes are evaluated using land surface maps. In one scenario, the trends in land cover changes are implemented into hydrological model parameters, but precipitation is maintained stationary (1980s values). In another scenario, the non-stationary precipitation scenarios are used as inputs to drive the model but land surface properties stay stationary (1980s values). Another scenario could be created where both observed changes are

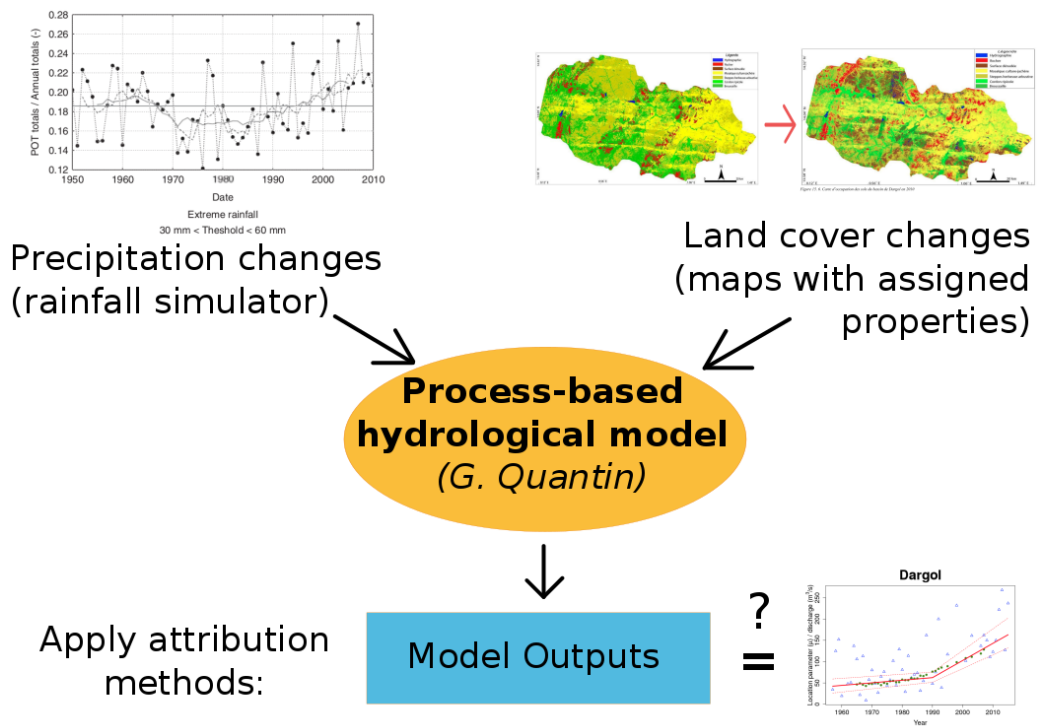


Figure 5.1: Proposed framework for attribution of hydrological extremes

implemented in the model. The methods described in Section 5.3.2 are used to attribute the observed changes in the GEV distribution of hydrological extremes shown in Chapter 2 to a given scenario.

With climate change analysis, the causal factors are relatively independent. Natural causes of atmospheric composition changes such as volcanic eruptions and solar irradiance fluctuations are arguably quite independent from human-produced greenhouse gas emissions. This is not the case when determining whether the cause of changes in hydrological extremes is precipitation or land surface properties. Precipitation has a direct impact on vegetation, which has a direct impact on surface runoff. An increase (decrease) in precipitation could lead to an increase (decrease) in vegetation. Land surface changes can likewise impact local convection and, as a result, local convective rainfall. The interactions are complex, intertwined, and often challenging to study due to lack of data and difficulty of relevant data

collection.

Determining whether changes in extreme streamflow are due to precipitation or land use changes is scientifically interesting. However, it bypasses the original question asked in climate sciences of whether changes are due to natural or anthropogenic factors. Land cover changes can be due to both natural and human causes. Human impacts include agricultural practices, grazing patterns, and urbanization. Separating out the relative contributions of natural processes and human impact from land surface changes would be another required step in the attribution process.

If one zooms out enough, precipitation changes (notably intensification) can also potentially be due to anthropogenic climate change and global warming, although that would need to be verified for the specific study region. Many climate variables are known to undergo long-term oscillations, which necessitates separating such trends from those caused by other forcings. In addition, interactions between precipitation at a specified location and larger-scale climate systems are complex, with a high degree of variability. Although global and regional climate models can be useful, it is more difficult to use them to attribute changes at a small spatial scales.

To go a step further, humans themselves respond to changes in the natural environment. Human impact on local land surfaces can in part a response to climate change. Herders in the Sahel changed the area and extent over which they let their animals graze as a response to drought conditions. This had a direct impact on local vegetation cover. Farmers change their agricultural practices in response to precipitation increases or decreases, which in turn changes the properties of the soil. Thousands of people migrate due to drought. One could attribute these “anthropic” changes to climate changes.

We see here that there are multiple potential issues to be resolved. Before proposing a modeling framework, it is important to clearly identify what the core research question is to be answered, and why. One must also determine the “box” around the hydrological system that determines at which scale the changes are attributed and which factors are considered external forcings or internal system variability.

A proposition is to focus on identifying the impacts of local anthropogenic influence on hydrological processes (for now, disregarding whether the human changes were originally due to climate). The impact of human societies on the local environment is a pertinent issue because it has relevance to how human behavior can influence floods. It can guide whether local populations and governments should change adaptation measures and how, based on which

human activities have impact on flooding.

In climate attribution studies, feedback between variables is integrated into the modeling system. For example, the atmospheric temperature response to changes in albedo from ice melting is modeled. For the hydrological attribution setup, one could envision modeling vegetation response to precipitation, local precipitation response to land surface properties, etc. Modeling feedback effects requires extensive interdisciplinary knowledge of how processes impact each other. Future research efforts would involve collecting existing knowledge about factors that affect the hydroclimatic system in West Africa, filling gaps in the understanding of the interactions between processes, representing the interactions mathematically, and incorporating the processes into an increasingly complex modeling system. Some studies have already been conducted to determine the impact one variable has on another, for example Bégué et al. (2011)'s analysis on vegetation responses to precipitation and land use changes in the Sahelian and Sudanian regions.

One could also explore theoretical methods for multiple linear regression that take into account non-independence between explanatory variables.

5.3.5 Land use scenarios

Going beyond attributing the causes of documented floods that have already occurred, one can envision making land use projections to complement the precipitation projections provided by RCMs. Making land use projection scenarios would require extended knowledge of how humans may impact their natural environment.

To better understand the human component of land surface changes, one could start by examining how people currently modify soils. There are projects underway for creating half-moons and banquettes that alter local runoff. Agricultural practices change in response to demographic pressure, changes in cultural practices, and to sudden events. There are also greening efforts underway, and regional soil rehabilitation projects. What influence do these activities have on hydrological processes? The development of land use scenarios would require interdisciplinary research on what changes in human behavior produce what changes in land surface properties.

As changes in societies are even more challenging to predict than changes in local precipitation, one could develop multiple land use/land surface scenarios based on population and demographic projections and test them in combination with precipitation projections. The factors can then be inte-

grated into the hydrological modeling system to determine impacts. Attribution methods can be applied on future projections. Appropriate adaptation measures could then be identified based on results.

5.3.6 Flood risk and societal dynamics

Besides attributing changes in floods, another research direction would consider the impact of hydrological changes and the dynamics of human populations on flood risk. Many go back to living in flood plains after a disaster. A strong population increase may also increase exposure to dangerous floods, especially in urban areas where the population increase is amplified by urban migration. One could more closely examine the factors that influence flood risk of populations. Then, one could explore future flood risk based on the hydrological projections developed. These research initiatives would provide information that could inform policy and adaptation strategies related to flood risk.

5.3.7 Practical next steps for attribution framework

Non-stationarity testing for Stochastorm

An immediate next step for developing a robust attribution framework for extremes in hydrology would be evaluating the sensitivity of the existing rainfall-runoff modeling system to trend implementation. First, the capacity for interannual trends would be implemented into Stochastorm. Then, the impact of trend parametrization must be evaluated in the output simulations of Stochastorm. If a trend is modeled in the simulator, do we see the same trend in the outputs? Or is it hidden within the variability of the simulated precipitation?

More specifically, at what signal intensity can we detect a trend in extreme precipitation values?

The suggested methodology would use a simulation period of 1980-2015. 1980 corresponds to the beginning of the linear increase in precipitation extremes in the Sahel.

Initially, only an increasing trend in Stochastorm parameters governing extremes will be tested; the other parameters (gamma distribution for non-extreme precipitation events, event frequency, time disaggregation) are kept the same. This experiment is useful for testing the sensitivity of the modeling

system. However, it raises theoretical concerns, as a change in extreme values may also indicate a change in the rest of the distribution. Future research would need to address how to realistically implement a trend in extreme precipitation in a valid statistical framework.

The proposed plan consists of testing a range of precipitation trends in Stochastorm parameters: 0%, 1%, 2%, 3% (the observed trend in extremes), 4% and 5%. The simulation outputs can then be analyzed using POT distributions with time covariates to determine the presence of trends and associated magnitudes. The output trends (if detected at a given level of significance) can then be compared with the trend implemented in Stochastorm parameters.

Another idea is to evaluate the amount of stations necessary to include in the evaluation for extracting the trend from simulation outputs.

Non-stationarity testing for Phorm (hydrological model)

Once the ability of Stochastorm to model precipitation trends is validated, a similar procedure can be repeated with the hydrological model Phorm. The goal would be to determine at what magnitude of trend would a trend in hydrological model outputs be significantly detectable within model variability.

Likewise, a range of trends over time can be implemented in land surface changes to determine the sensitivity of the model (and in particular of extreme events output by the model) to changes in land surface parameters.

Appendices

Appendix A

Supplementary information for article 1

A.1 Available data

Most of the hydrological data used in this thesis were provided by the Niger Basin Authority (in French, Autorité du Bassin de Niger - ABN) that coordinates the collective management of the Niger River and its tributaries between member countries. For the Niger River stations, all of the catchment areas were located in the Sahelian region in between the outlet of the inner delta of the Niger River and Niamey, Niger (Figure A.1).

Two additional data sets were examined within the Sahelian Niger River, for stations located in the upper reaches of the major Sahelian right-bank subbasin(s). These were of interest due to their relatively small catchment areas compared to other stations, which would potentially allow for the evaluation of the impact of catchment size on results.

The Senegal River basin is managed by the Senegal River Basin Development Authority (in French, Organisation pour la mise en valeur du fleuve Sénégal - OMVS), a transboundary organization similar to the ABN. Seven data series for the Senegal River were provided by the OMVS.

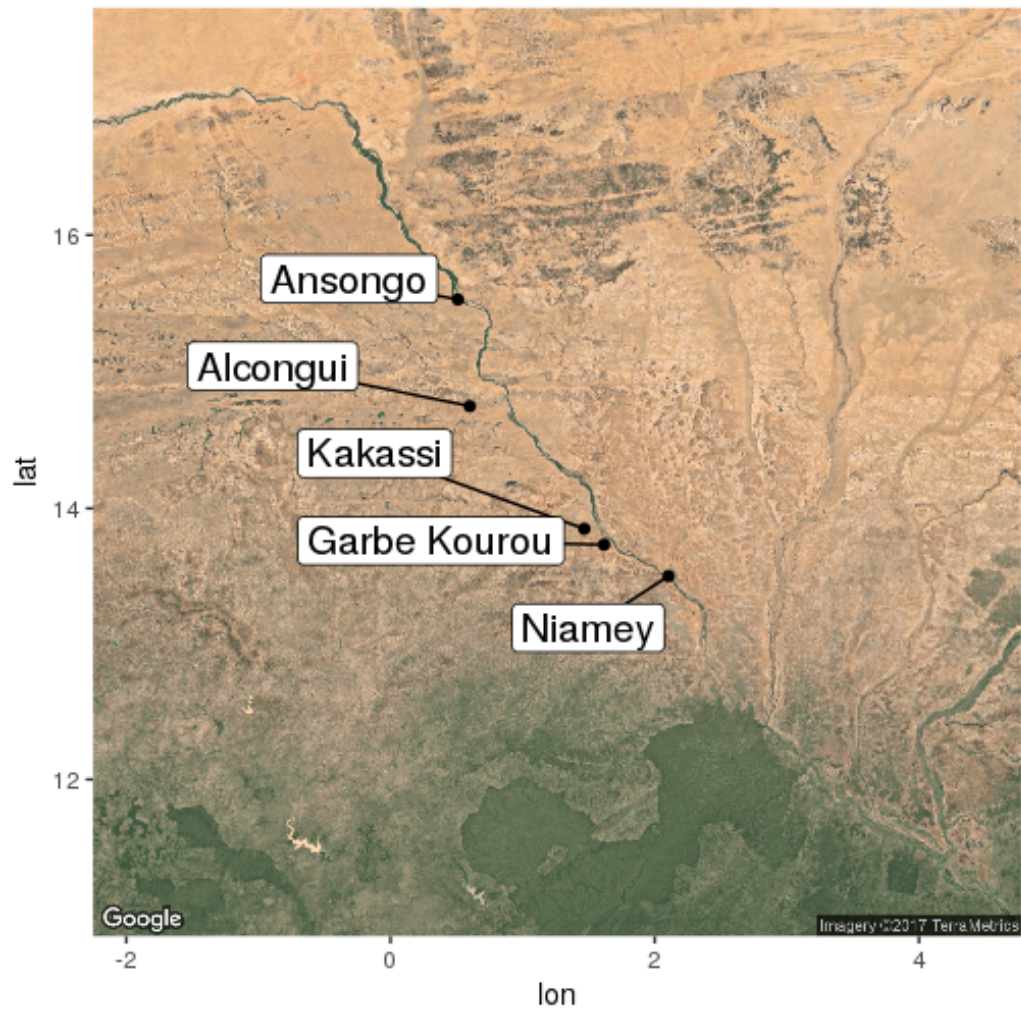


Figure A.1: map of stations on the right bank of the Niger River.

A.2 Hydrological data evaluation, selection and cleaning

Gaps and errors/inconsistencies were identified in the Niger River data. Some of the gaps were due to missing data in the original ABN time series. Three versions of the supposedly equivalent data sets were compared: two documents obtained at different times, plus the graphical interface of the ABN's NigerHycos database online. Figures A.2, A.3, and A.4 show the results of data preprocessing. Differing colors indicate a disagreement between the two documents.

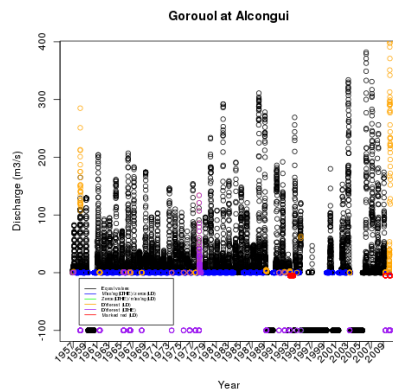


Figure A.2: Data preprocessing results for the Gorouol basin.

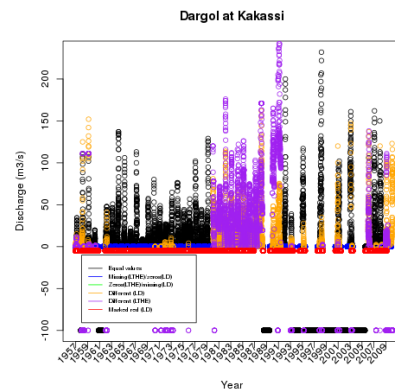


Figure A.3: Data preprocessing results for the Dargol basin.

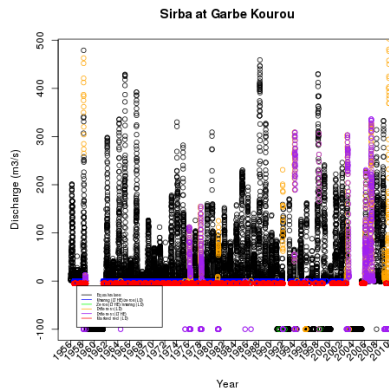


Figure A.4: Data preprocessing results for the Sirba basin.

Whereas most differing values were simply assumed zero in one data set during the dry season but marked missing in the other, a number of non-zero values were also conflicting. Figures A.5, A.6, and A.7 show only these differing nonzero values. The differing values for the Gorouol and Sirba basins appear to be mainly displaced by a short period of time, which would not affect annual maxima. However, the Dargol data sets show greater divergence. All differing data points were compared with the charts found on the ABN's website. Based on this, it was decided whether to retain the annual maximum for that year, remove it, or (if unclear) remove it only during sensitivity analysis.

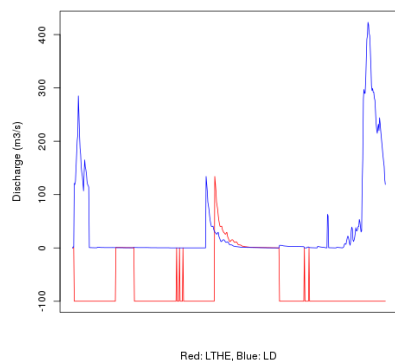


Figure A.5: Differing values between two equivalent data sets for the Gorouol basin.

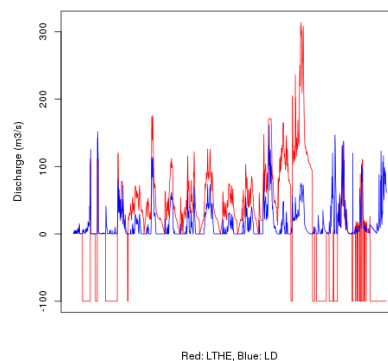


Figure A.6: Differing values between two equivalent data sets for the Dargol basin.

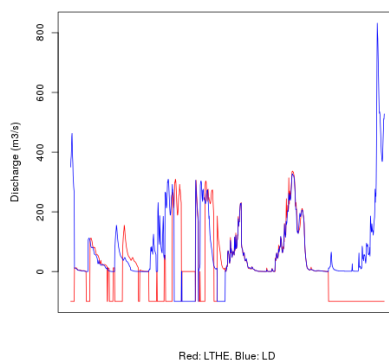


Figure A.7: Differing values between two equivalent data sets for the Sirba basin

A.3 Hydroclimatological data sensitivity testing

The article in Chapter 2 presented the most significant trend detection results for streamflow maxima in West Africa. The following sections present additional results from sensitivity testing. Data points identified to be of

questionable quality or outliers were removed to see their impact on the NS-GEV model parameters (Figures A.8-A.10). Additional data series were considered tested that were too short to be included in the primary study, but are still of interest due to their relatively small discharge area compared to the other catchments. We also further compare change points detected in the study and in the literature.

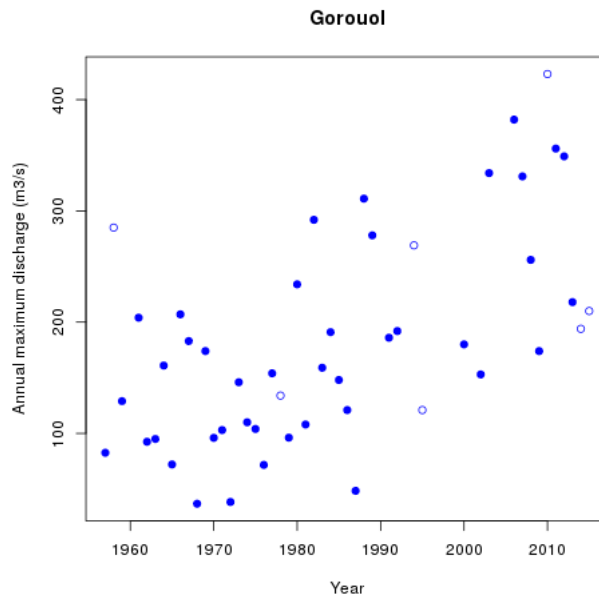


Figure A.8: Evolution of annual maxima for the Gorouol basin. The unfilled circles represent the data points which were removed for sensitivity analysis.

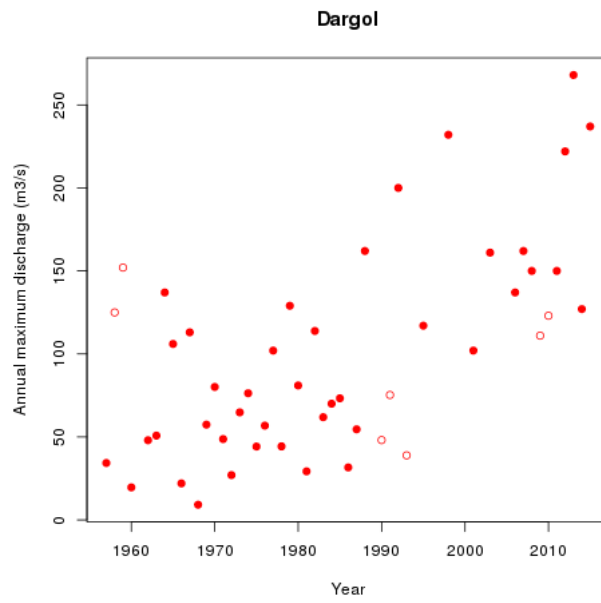


Figure A.9: Evolution of annual maxima for the Dargol basin. The unfilled circles represent the data points which were removed for sensitivity analysis.

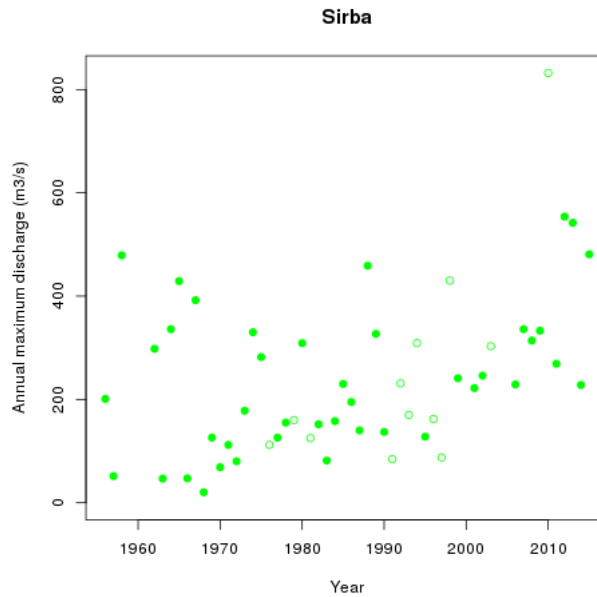


Figure A.10: Evolution of annual maxima for the Sirba basin. The unfilled circles represent the data points which were removed for sensitivity analysis.

A.3.1 Testing GEV parameters

Stress-testing of non-stationary GEV results consisted of three main trials:

- Removal of data deemed "questionable" during data preprocessing. This includes some large and rare annual maxima such as that of 2010. The removal of this data point could have a significant impact on model calibration.
- Increasing the moving average window size to 21 (a decrease was not tested as not all data sets could reach convergence with less than 15 data points).
- Adjusting the shape parameter in order to determine the sensitivity of the analysis to potential errors in shape estimation. The limits of the 95% confidence intervals of the calibrated shape parameter (ξ) were evaluated. The special case of the Gumbel distribution where $\xi=0$ was also tested.

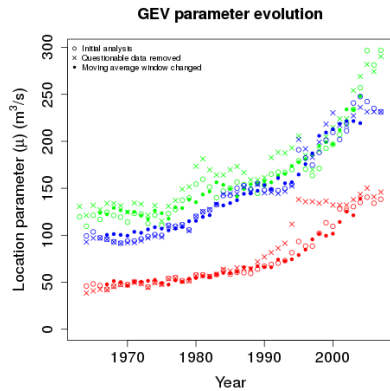


Figure A.11: Sensitivity analysis for the location parameter: testing window size and data removal.

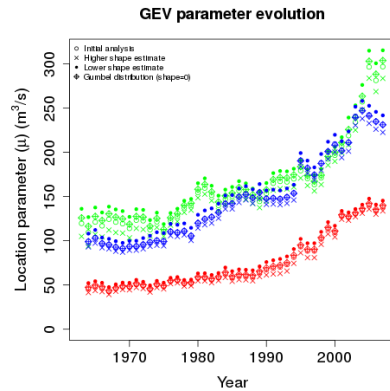


Figure A.12: Sensitivity analysis for the location parameter: testing initial shape parameter estimations.

Figures A.11 and A.12 show the results of these tests for the location parameter. Figures A.13 and A.14 likewise show the results for the scale parameter. Although the scale parameter was more sensitive to changes in data, methodology, and parameter initialization, none of the tests revealed evidence for refuting the conclusion of non-stationarity for both parameters.

A.3.2 The case of the Koriziena station

When applying the methods detailed in Chapter 2, the Koriziena station featured a linearly increasing trend for μ and no trend for σ . It did not have a break point, possibly due to the relatively short length of the time series; the data started only during the 1970s, the same time period when other Niger station models also started increasing. Model calibration would not have identified a significant break in the series.

Figure A.15 shows the effect of data quality on the Koriziena station. Models with linear non-stationary μ and stationary σ (the final model selected for this station) are tested with varying missing data criteria. Data points were kept if the series had within a given limit of missing data for the months of July, August, and September. If all AMAX values are kept without concern for missing data points within the peak wet season, the slope appears as in the first graph. If only the years with less than half of the

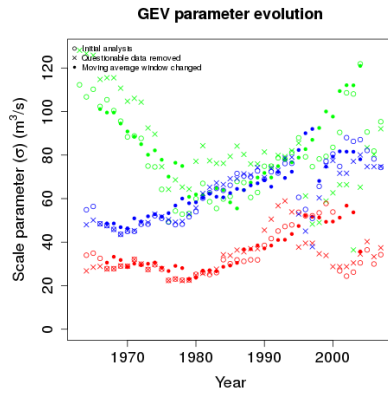


Figure A.13: Sensitivity analysis for the scale parameter: testing the window size and data removal.

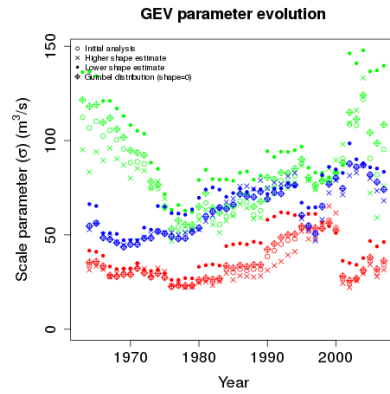


Figure A.14: Sensitivity analysis for the scale parameter: testing initial shape parameter estimations.

days missing a measurement are retained, the slope greatly decreases (second graph). If the only years used are the ones missing less than 10 percent of days, the magnitude of the estimated trend further decreases. Although in all cases the nonstationary model was significantly better than the stationary model according to the LRT, the missing data points (and consequently the size of the final data sample) had an impact on the magnitude of the model parameters. For the Koriziena station, the stationary and nonstationary components of μ and the σ parameter decreased with the reduced data sample, whereas the xi parameter strongly increased.

A.4 Specific discharge evolution

Figure A.16 shows the evolution of AMAX values when considering specific discharge.

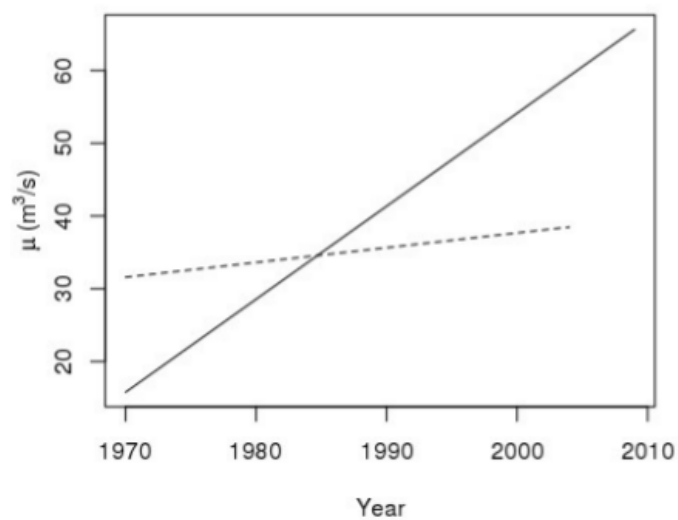


Figure A.15: NS-GEV model for the μ parameter for the Koriziena station with all data used regardless of quality (solid line) compared with the NS-GEV μ parameter if only years with less than 10% of data missing during the peak season is used (dashed line).

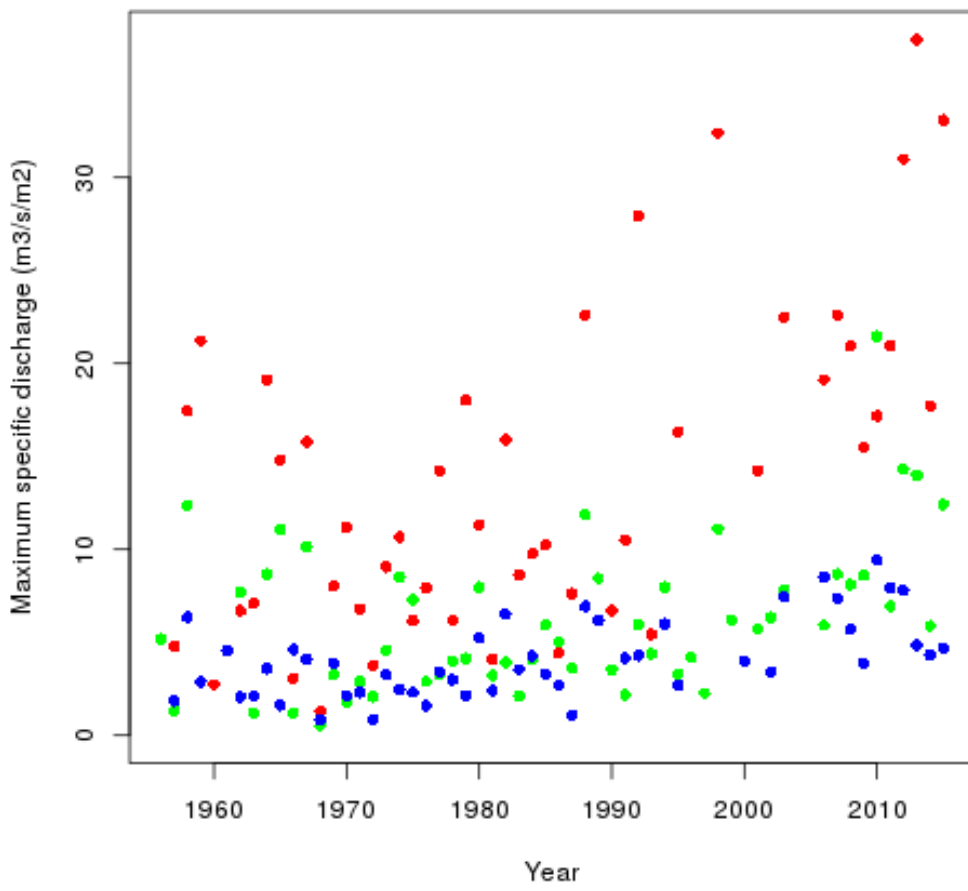


Figure A.16: Evolution of specific discharge AMAX values.

Appendix B

Supplementary information for article 2

B.1 Exploratory precipitation analysis

Several drivers could have provoked this change in the statistical characteristics of extreme streamflow. One potential key driver of hydrological extremes is an increase in precipitation, especially in the Sahel region where hydrological processes are dominated by Hortonian overland flow. If precipitation increases in intensity, the soil will more quickly exceed its infiltration capacity, which results in additional runoff. A change in precipitation could thus explain a change in streamflow.

A preliminary analysis of rainfall in the region was conducted in order to evaluate if precipitation near the study site has also changed over time. First, AMMA-CATCH data at the event scale was evaluated to determine rainfall characteristics. An exploratory analysis was conducted for the seasonal and daily cycles of rainfall near to the study site. The end goal of this variability analysis is to implement findings into the rainfield simulator developed in Vischel et al. (2009). The simulated rainfall will then be used as input into the hydrological model detailed in the perspectives chapter.

Data was used from the Niamey mesoscale site of the AMMA-CATCH data collection network, which features precipitation measurements at 30 stations. The data spans from 1990 to 2014 and has a temporal resolution of five minutes. The data was evaluated in two forms: in its original five-minute resolution, and at the event resolution. An event is defined as having touched

at least 30% of the stations. 1mm of rainfall or more must also be recorded for at least one station. A minimum of a half hour with no rainfall on any station is the criteria for distinguishing two consecutive events.

A preliminary analysis of rainfall in the region was conducted in order to evaluate if precipitation near the study site has also changed over time. Although the AMMA-CATCH data set provides rainfall data at a high temporal and spatial resolution, the time series do not extend to an early enough data for comparing any detected trends in their non-stationary GEV parameters to those of the right bank tributaries (see Chapter 2). As such, daily precipitation values for stations in and near to the hydrological study area were evaluated, as they cover a comparable range of years.

B.2 Seasonal cycle

The following parameters of interest were selected for evaluation of their seasonal and daily cyclical characteristics:

- Day of event occurrence
- Inter-event time (IET), in days
- Non-zero event rainfall
- Event duration (from the first time step registering precipitation to the last one over the entire 30 rain gage network)
- Event duration (longest at any one station during the event)
- Proportion of stations registering the event (a proxy for storm size)

The averages of each value by day for the entire time period were calculated. Figure B.1 shows the comparative evolution of these variables throughout the rainy season, each divided by their maximum to scale the values. Events become more frequent starting in late June/early July, experience another jump in frequency around late July, reach their peak around the beginning of August, then sharply decline at the end of August. Cumulative event rainfall also rises steadily and reaches its peak in early August, with a less sharp decline at the end of the season. The IET sharply decreases until

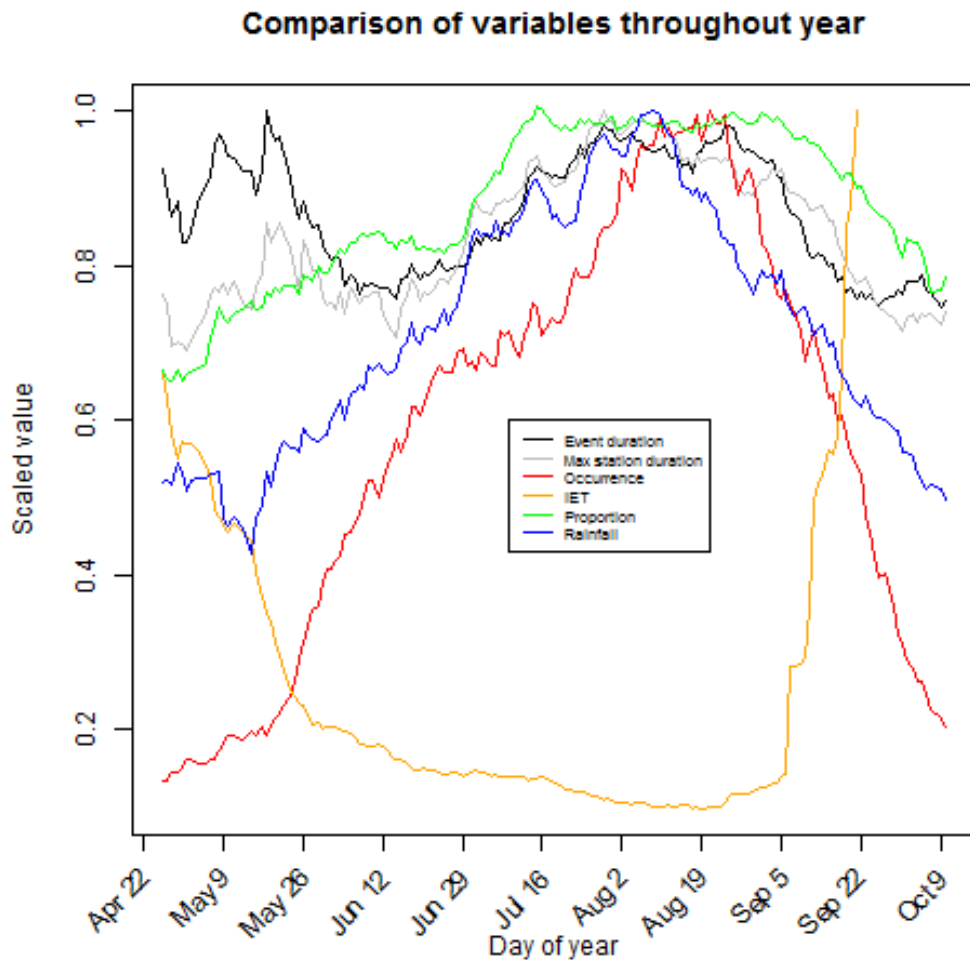


Figure B.1: Seasonal evolution of precipitation characteristics for the AMMA-CATCH data site.

the end of May, then decreases steadily but moderately until early December when it rises sharply.

The proportion of stations touched reaches its maximum earlier, in mid-June, then plateaus until the end of the season in September. This could be due to the limitations in window size; the 30 stations may not be able to capture the full size of the storm. Finally, storm duration is somewhat higher in the pre-season (although this could be due to the relatively few number of events and thus greater influence of outliers), then peaks in August along with most of the other variables. This confirms what has been observed for rainfall in the Sahel: a more variable pre-season in May and June, followed by a strong signal once the monsoon is fully underway in July and August, and a steep dropoff once the monsoon finishes around September .

Although there are clear seasonal patterns in the average values, variance around these values is also high. Figures B.2 and B.3 show the spread of values for the inter-event time (IET) (middle of season) and average event rainfall (all of the season) respectively.

B.2.1 Fitting a distribution to IET

An analysis was conducted to determine if the IET could be fitted to a given model. Figure B.4 shows the overall distribution of IET values.

Figures B.5, B.6, and B.7 show the relation between IET and cumulative event rainfall, event duration, and proportion of stations affected. IET does not appear to be correlated with any of these variables. It can be concluded that IET is independent of storm size and magnitude.

The Kolmogorov-Smirnov (KS) test was used to determine the distribution of best fit for the IET. The exponential distribution was of particular interest as a hypothesis due to only having one parameter and the possibility of then using the poisson distribution to model the occurrence rate. KS test results for both the entire season and date segments of ten days each showed that the distribution of the IETs was not exponential. However, the gamma distribution was found to be a good fit if ten-day periods were considered. Figures B.8 and B.9 show the change in calibrated gamma parameters throughout the season. Additional testing is needed to evaluate if it is possible to use the gamma distribution to accurately model the seasonality of IET in the rain field simulator.

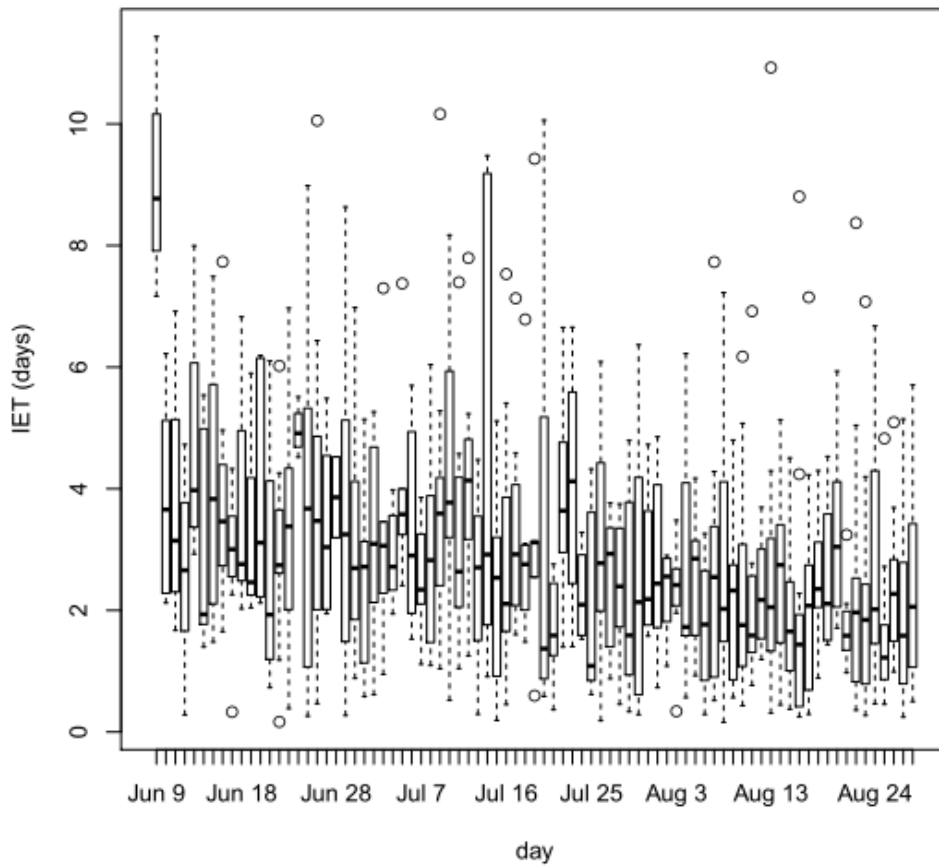


Figure B.2: Inter-event time (IET) values and their variability in the middle of the season. Values decrease steadily (i.e. more frequent storms) during the peak rainy season.

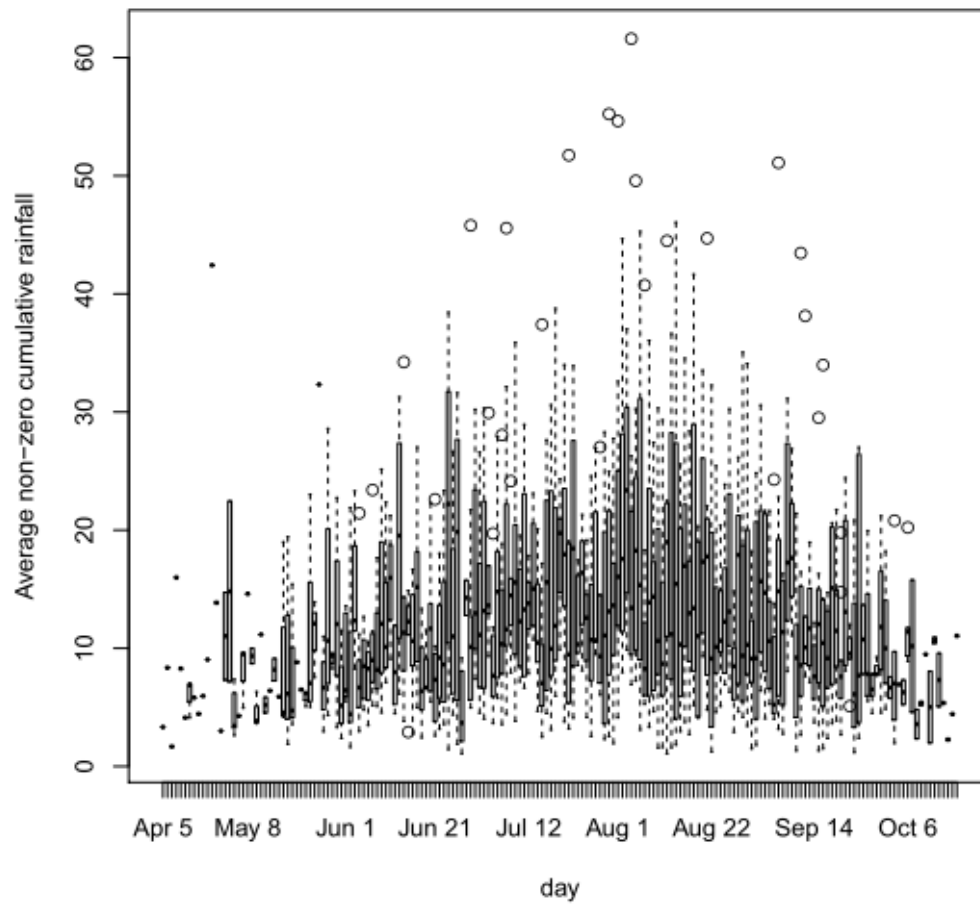


Figure B.3: Average non-zero cumulative event rainfall values and their variability throughout the rainy season.

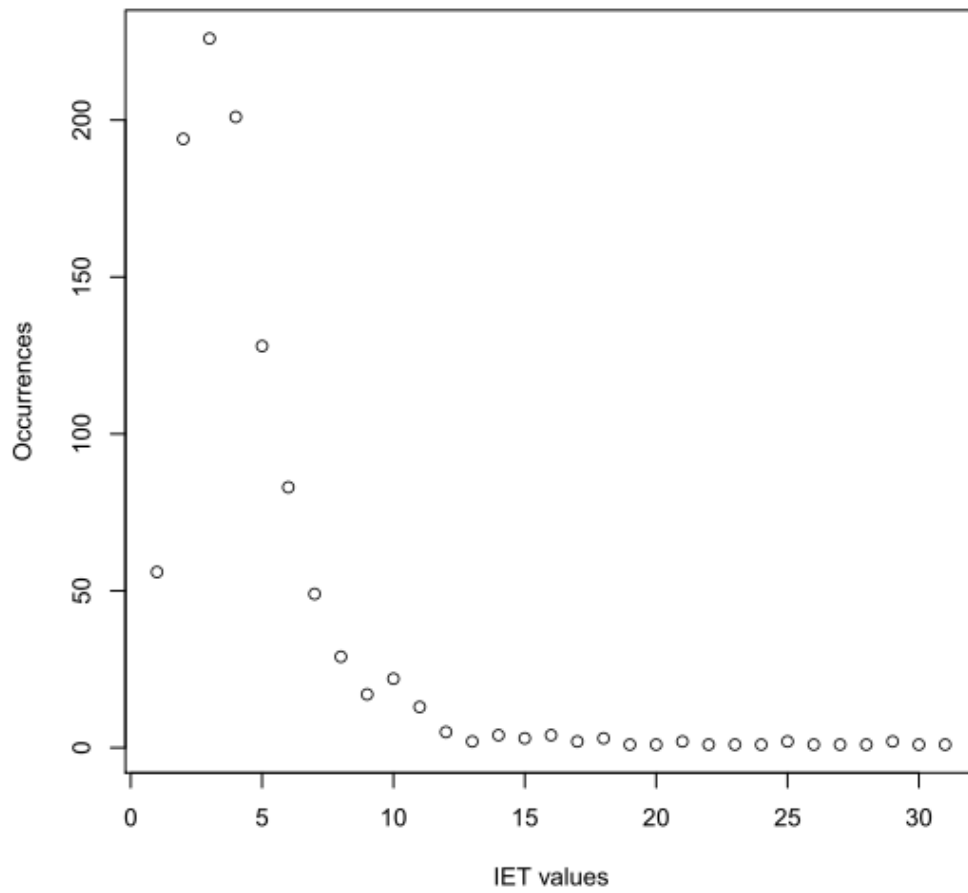


Figure B.4: Frequency of IET values by class.

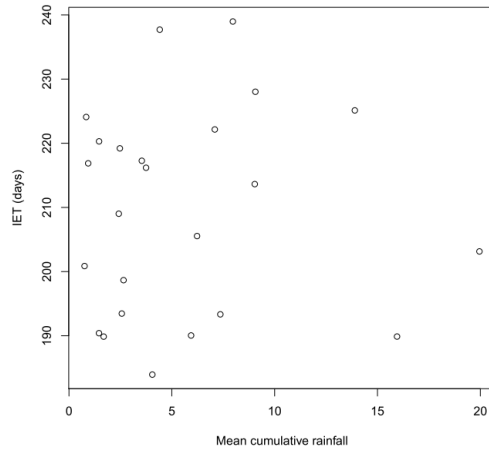


Figure B.5: Correlation between IET and cumulative event rainfall.

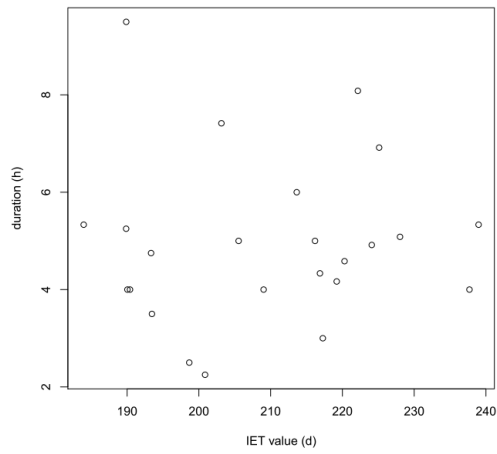


Figure B.6: Correlation between IET and event duration.

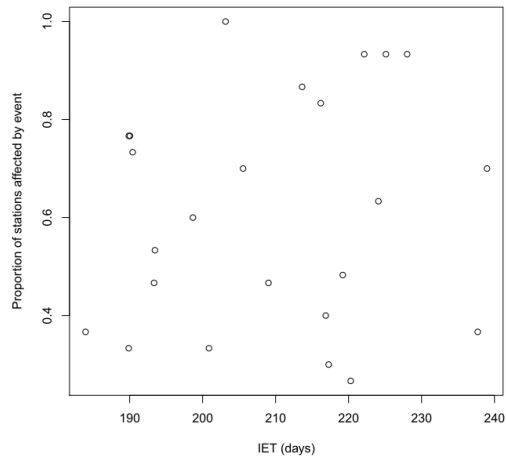


Figure B.7: Correlation between IET and proportion of stations registering precipitation.

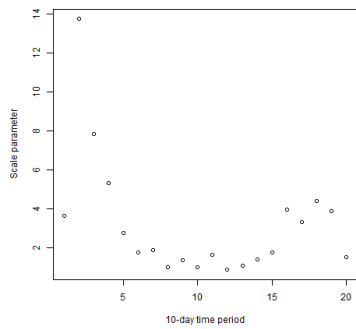


Figure B.8: Evolution of the scale parameter of the gamma distribution for IET throughout the season.

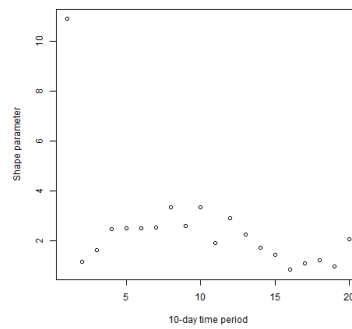


Figure B.9: Evolution of the shape parameter of the gamma distribution for IET throughout the season.

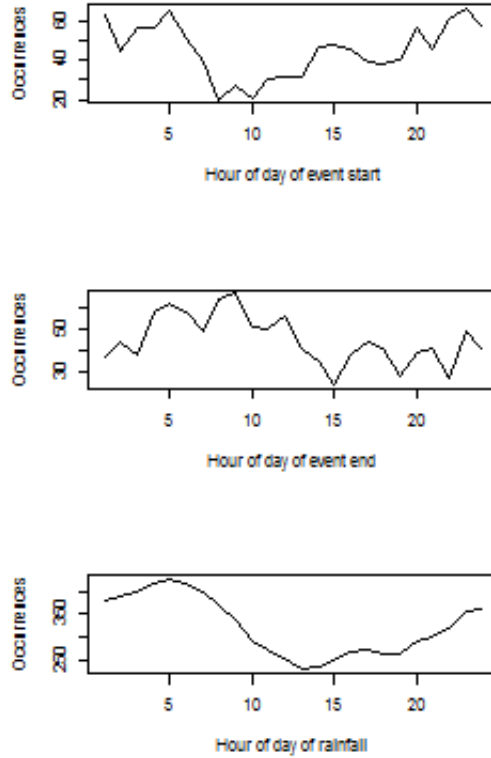


Figure B.10: Start, end, and overall times of rainfall events.

Daily cycle

Variability in the daily rainfall cycle was also examined. Figure B.10 shows the distribution throughout the day of event start times, end times, and any hour where precipitation occurs. Events have a tendency to reach the station window in the late afternoon or at night. The largest events also reflect this pattern, as seen in figure B.11; storms with the most rainfall arrive during the evening and night.

Figures B.12-B.14 display the seasonal cycle cumulative event precipitation, occurrence, and IET by hour of day of event onset. The storms forming in the morning tend to be the smallest in magnitude and least frequent, whereas those starting in the evening and night are the biggest and most frequent. There seem to be more events starting in the evening near the

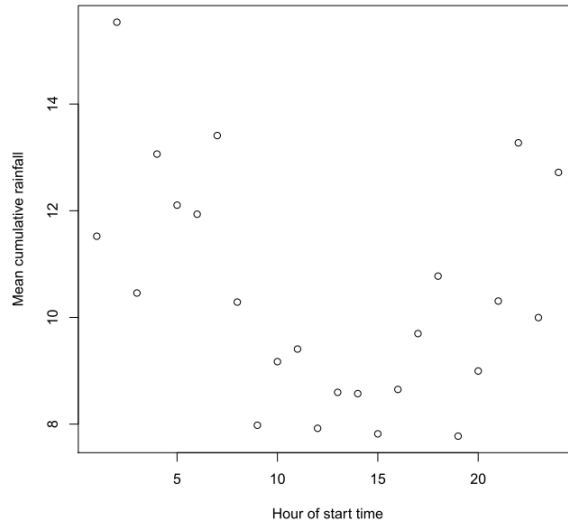


Figure B.11: Relationship between hour of precipitation event onset and cumulative rainfall amount.

beginning of the rainy season, but more events starting at night during the peak of the season. IET, however, does not show any clear distinction by hour of day.

B.3 Interannual non-stationarity

The data was divided into two segments (1990-2001 and 2002-2014) in order to check for indications of change. The occurrence, cumulative event rainfall, and event duration all showed an increase in the magnitude of the peak at the height of the season (figures B.15-B.17). However, the proportion of stations touched by a storm seemed to have decreased (figure B.18). The IET did not change significantly (figure B.19).

Sensitivity analysis must be conducted to determine if these changes are due to an overall trend, or due to a few years of particularly intense rainfall. If non-stationarity is indeed found, it could be an important factor to simulate in the rain field model.

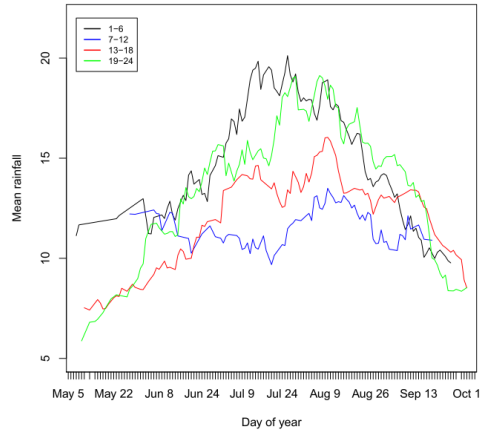


Figure B.12: Seasonal cycle of cumulative rainfall per event by time of day.

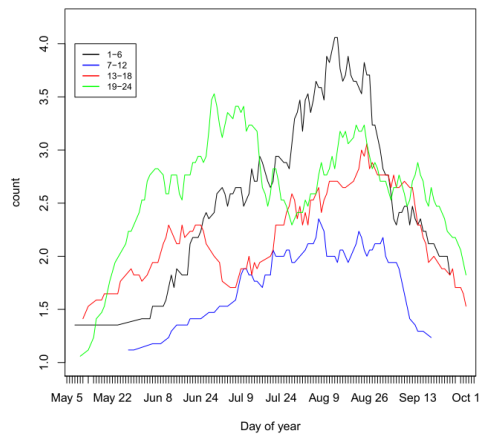


Figure B.13: Seasonal cycle of occurrence by time of day.

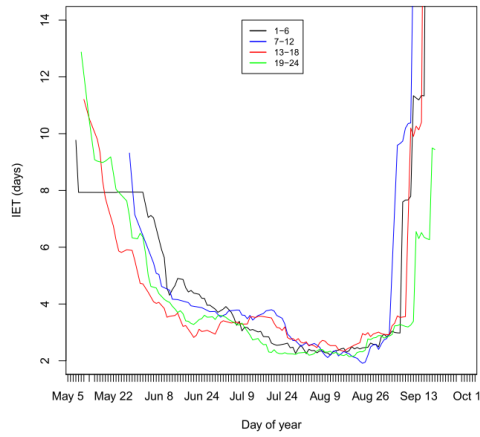


Figure B.14: Seasonal cycle of IET by time of day.

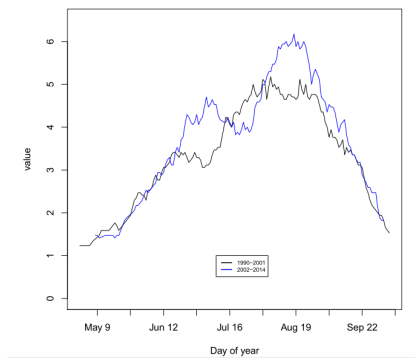


Figure B.15: Change in event frequency between 1990-2001 and 2002-2014.

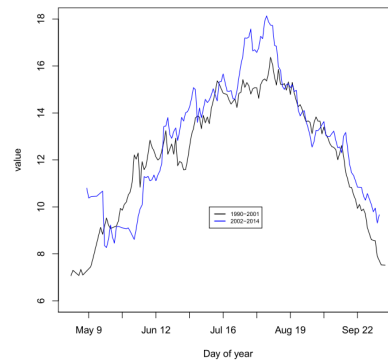


Figure B.16: Change in cumulative event rainfall between 1990-2001 and 2002-2014.

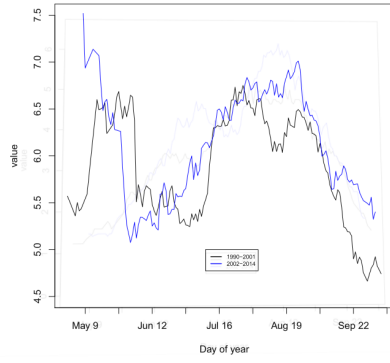


Figure B.17: Change in event duration between 1990-2001 and 2002-2014.

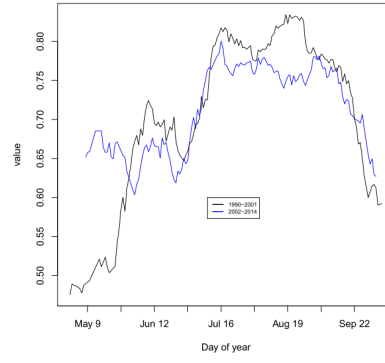


Figure B.18: Change in proportion of stations touched between 1990-2001 and 2002-2014.

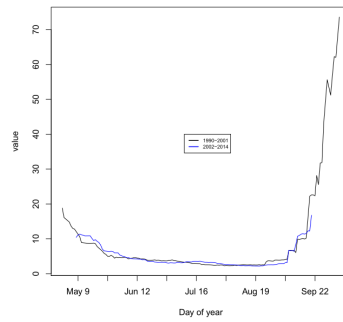


Figure B.19: Change in IET between 1990-2001 and 2002-2014.

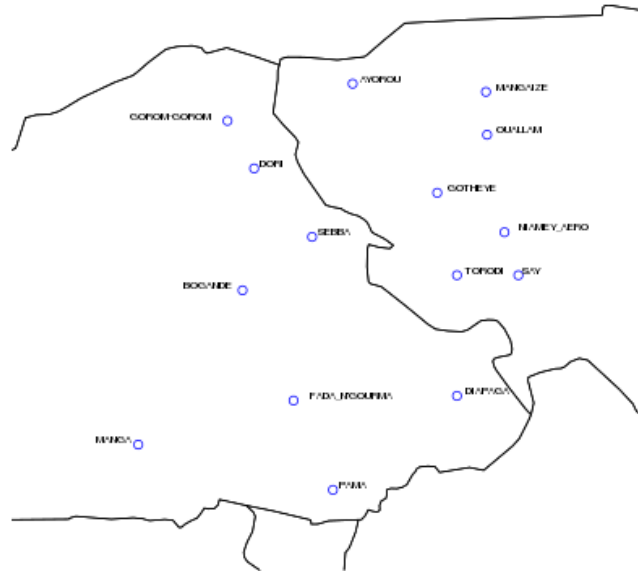


Figure B.20: Daily precipitation stations used for regional analysis. The four stations furthest to the south were not considered, as they were identified as having a different temporal evolution when compared to the other stations.

Regional rainfall non-stationary extreme value analysis

The following section applies and expands the methods used for the evaluation of temporal evolution of streamflow maxima to regional rainfall. The initial data set consisted of a sample of 15 stations that were nearest to the basins under study, extended over the same time period as the basins (1957-2015), and not missing significant portions of data. A map of these stations is shown in figure B.20. However, during the analysis it became evident that the four stations furthest to the south had a temporal evolution that differed from the other eleven stations (figure B.21). This is consistent with previous observations that rainfall characteristics in the Sahel follow a north-south gradient (Nicholson (2013a)). The final analysis kept only the eleven stations further to the north.

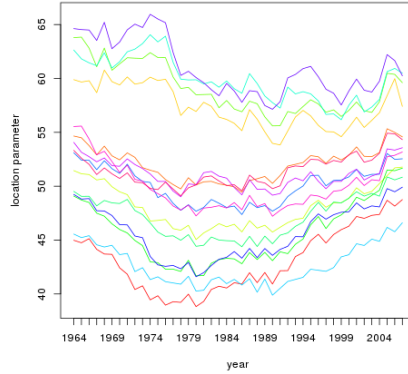


Figure B.21: Original analysis with 15 stations. The upper four lines are distinct from the other eleven. They correspond to the four stations furthest to the south.

As with the GEV analysis of streamflow, annual maxima were extracted by station. No clear spatial organization was observed in the temporal evolution of annual maxima. Instead, spatial covariates were used in order to calibrate one regional GEV to test for non-stationarity.

The analysis followed the methodology elaborated in Panthou et al. (2013). Average cumulative rainfall was used as the spatial covariate for each station. Time was then evaluated as a covariate to check for a trend.

Moving average analysis was repeated for regional precipitation, holding the shape parameter constant as done with streamflow. This method gives an indication of what type of trend might be present in the data. Figures B.22 and B.23 show these results. Of note also is the decrease in spatial dependency over time, as shown in B.24. The intercept component μ_0 of the model increases over time while the spatial dependence component μ_1 decreases. This could indicate a change in the spatial organization of extreme values.

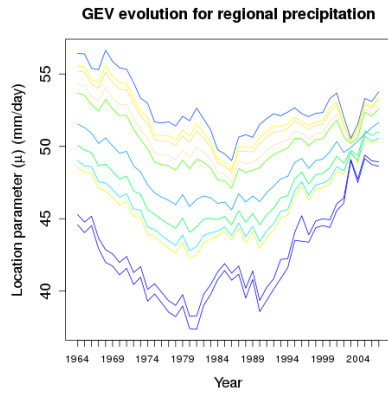


Figure B.22: Moving-average evolution of the location parameter for a regional GEV model of precipitation.

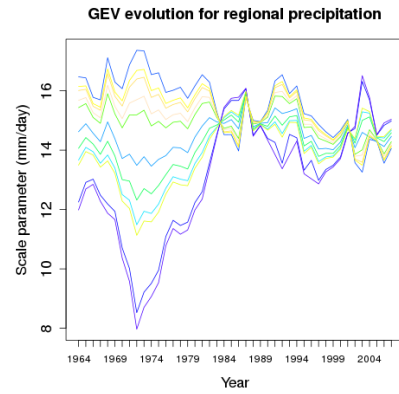


Figure B.23: Moving-average evolution of the scale parameter for a regional GEV model of precipitation.

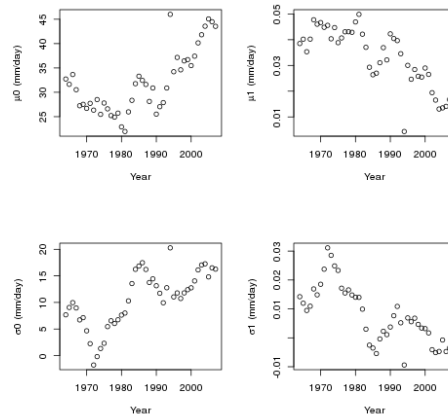


Figure B.24: Moving averages for the intercept and spatial dependency components of the regional rainfall GEV.

Maximum likelihood estimation was carried out to determine the line of best fit with various combinations of temporal and spatial covariates. Table B.1 shows the results of this analysis. Amongst the trials were the regional GEV (RGEV) and non-stationary regional GEV (NSRGEV) models tested in Panthou et al. (2013).

Using the likelihood ratio test outlined in section 2.2, the location parameter was found to have a parabolic temporal evolution of the form $\mu = \mu_0 + \mu_1(\text{spatialcovariate}) + \mu_2(t - d)^2$. Figure B.25 shows the results for maximum likelihood estimation over a range of values of d . It was determined that a displacement of 30 years provided the best fit. This indicates that the location parameter experienced a change in trend direction around the year 1984.

Adding temporal non-stationarity to the scale parameter was not shown to improve the model. Modeling the scale parameter using spatial covariates improved the model fit, but it was rejected at the 5% significance level for a likelihood ratio test comparing it to using only a non-stationary, spatialized location parameter. However, it would be accepted at a 6% significance level. A spatial model of better fit might make adding the spatial scale covariate a more significant improvement. Although regional modeling of the scale parameter may improve results, it does not seem to have the same impact as modeling the location parameter with covariates.

Another result of note was that for certain trial models, fixing the shape value at that of the model of best fit greatly improved the results. For the RGEV model, for example, fixing the shape value increased the log likelihood to that of NSRGEV, which added a temporal component and is considered a significantly improved model over the RGEV according to the likelihood ratio test. This was not the case for all trials, but it provides a clear example of the impact that a poor estimation of the shape parameter may have on final conclusions.

B.4 Conclusions

Given that rainfall maxima showed a positive trend in the evolution of their underlying distribution, and rainfall is a common driver of hydrological extremes, precipitation remains one of the principle drivers under investigation. The trend must be implemented in a representative way in the rain field simulator. Results of seasonal rainfall variability should also be incorporated in future models, particularly if suspected to have an impact on hydrological processes.

Table B.1: Maximum likelihood estimation of model of best fit for regional rainfall.

Model trial	Covariate, μ			Covariate, σ			nllh
	spatial	t	t^2	spatial	t	t^2	
Base							2764.13
1	x						2748.97
2				x			2768.39
RGEV	x			x			2761.18
3		x					2764.03
4					x		2764.12
5		x			x		2764.01
6			x				2753.94
7						x	2762.85
8			x			x	2753.94
9	x	x					2748.96
10	x		x				2738.56
11		x	x				2753.84
12	x	x	x				2738.76
13	x		x	x			2736.74
14	x		x		x		2738.48
15	x		x			x	2738.57
16	x				x		2748.88
17	x					x	2756.06
NSRGEV	x	x		x			2747.61
RGEV (shape adjusted)	x			x			2747.62

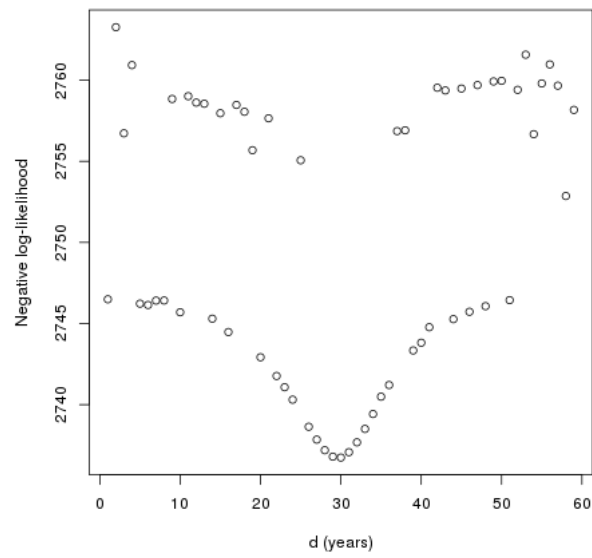


Figure B.25: Maximum likelihood estimation of the value d in the model $\mu = \mu_0 + \mu_1(\text{spatialcovariate}) + \mu_2(t - d)^2$ for regional rainfall.

Bibliography

- (2013). *Climate Change 2013: The Physical Science Basis. Contribution of Working Group I to the Fifth Assessment Report of the Intergovernmental Panel on Climate Change*, chapter Detection and Attribution of Climate Change: from Global to Regional. Cambridge University Press, Cambridge, United Kingdom and New York, NY, USA.
- Aich, V., Koné, B., Hattermann, F. F., and Paton, E. N. (2016a). Time series analysis of floods across the Niger River basin. *Water*, 8(4):165.
- Aich, V., Liersch, S., Vetter, T., Andersson, J., Müller, E. N., and Hattermann, F. F. (2015). Climate or land use? Attribution of changes in river flooding in the Sahel zone. *Water*, 7(6):2796–2820.
- Aich, V., Liersch, S., Vetter, T., Fournet, S., Andersson, J. C., Calmanti, S., van Weert, F. H., Hattermann, F. F., and Paton, E. N. (2016b). Flood projections within the niger river basin under future land use and climate change. *Science of the Total Environment*, 562:666–677.
- Aich, V., Liersch, S., Vetter, T., Huang, S., Tecklenburg, J., Hoffmann, P., Koch, H., Fournet, S., Krysanova, V., Müller, E., et al. (2014). Comparing impacts of climate change on streamflow in four large african river basins. *Hydrology and Earth System Sciences*, 18(4):1305–1321.
- Ailliot, P., Allard, D., Monbet, V., and Naveau, P. (2015). Stochastic weather generators: an overview of weather type models. *Journal de la Société Française de Statistique*, 156(1):101–113.
- Akaike, H. (1974). A new look at the statistical model identification. *IEEE transactions on automatic control*, 19(6):716–723.

- Albergel, J. (1987). Sécheresse, désertification et ressources en eau de surface: application aux petits bassins du Burkina Faso. *The influence of climate change and climatic variability on the hydrologic regime and water resources*, 168:355–365.
- Ali, A. and Lebel, T. (2009). The Sahelian standardized rainfall index revisited. *International Journal of Climatology*, 29(12):1705–1714.
- Ali, A., Lebel, T., and Amani, A. (2003). Invariance in the Spatial Structure of Sahelian Rain Fields at Climatological Scales. *Journal of Hydrometeorology*, 4(6):996–1011.
- Allan, R. P., Soden, B. J., John, V. O., Ingram, W., and Good, P. (2010). Current changes in tropical precipitation. *Environmental Research Letters*, 5(2):025205.
- Allen, M. and Stott, P. (2003). Estimating signal amplitudes in optimal fingerprinting, part i: Theory. *Climate Dynamics*, 21(5-6):477–491.
- Allen, M. R. and Tett, S. F. (1999). Checking for model consistency in optimal fingerprinting. *Climate Dynamics*, 15(6):419–434.
- Amani, A. and Paturel, J.-E. (2017). Le projet de révision des normes hydrologiques en Afrique de l’Ouest et Afrique Centrale. *La Météorologie*, (96):6–7. <http://hdl.handle.net/2042/61964> — DOI : 10.4267/2042/61964.
- Andersen, I. and Golitzen, K. G. (2005). *The Niger River basin: A vision for sustainable management*. World Bank Publications.
- Anyamba, A. and Tucker, C. J. (2005). Analysis of Sahelian vegetation dynamics using NOAA-AVHRR NDVI data from 1981–2003. *Journal of Arid Environments*, 63(3):596–614.
- Arnaud, P., Cantet, P., and Aubert, Y. (2016). Relevance of an at-site flood frequency analysis method for extreme events based on stochastic simulation of hourly rainfall. *Hydrological Sciences Journal*, 61(1):36–49.
- Arnell, N. W. and Gosling, S. N. (2016). The impacts of climate change on river flood risk at the global scale. *Climatic Change*, 134(3):387–401.

- Asadieh, B. and Krakauer, N. (2015). Global trends in extreme precipitation: climate models versus observations. *Hydrology and Earth System Sciences*, 19(2):877–891.
- Balme, M., Vischel, T., Lebel, T., Peugeot, C., and Galle, S. (2006). Assessing the water balance in the Sahel: Impact of small scale rainfall variability on runoff: Part 1: Rainfall variability analysis. *Journal of Hydrology*, 331(1–2):336–348.
- Bárdossy, A. and Pegram, G. G. (2016). Space-time conditional disaggregation of precipitation at high resolution via simulation. *Water Resources Research*, 52(2):920–937.
- Barrios, S., Bertinelli, L., and Strobl, E. (2006). Climatic change and rural–urban migration: The case of sub-saharan africa. *Journal of Urban Economics*, 60(3):357–371.
- Bathiany, S., Dakos, V., Scheffer, M., and Lenton, T. M. (2018). Climate models predict increasing temperature variability in poor countries. *Science advances*, 4(5):eaar5809.
- Baxevani, A. and Lennartsson, J. (2015). A spatiotemporal precipitation generator based on a censored latent gaussian field. *Water Resources Research*, 51(6):4338–4358.
- Bégué, A., Vintrou, E., Ruelland, D., Claden, M., and Dessay, N. (2011). Can a 25-year trend in soudano-sahelian vegetation dynamics be interpreted in terms of land use change? a remote sensing approach. *Global Environmental Change*, 21(2):413–420.
- Beguiría, S., Angulo-Martínez, M., Vicente-Serrano, S. M., López-Moreno, J. I., and El-Kenawy, A. (2011). Assessing trends in extreme precipitation events intensity and magnitude using non-stationary peaks-over-threshold analysis: a case study in northeast Spain from 1930 to 2006. *International Journal of Climatology*, 31(14):2102–2114.
- Bélisle, C. J. (1992). Convergence theorems for a class of simulated annealing algorithms on \mathbb{R}^d . *Journal of Applied Probability*, 29(4):885–895.

- Bell, T. L. (1987). A space-time stochastic model of rainfall for satellite remote-sensing studies. *Journal of Geophysical Research: Atmospheres*, 92(D8):9631–9643.
- Benoit, L. and Mariethoz, G. (2017). Generating synthetic rainfall with geostatistical simulations. *Wiley Interdisciplinary Reviews: Water*, 4(2):e1199.
- Berthou, S., Rowell, D. P., Kendon, E. J., Roberts, M. J., Stratton, R. A., Crook, J. A., and Wilcox, C. (2019). Improved climatological precipitation characteristics over west africa at convection-permitting scales. *Climate Dynamics*, pages 1–21.
- Biasutti, M. (2013). Forced sahel rainfall trends in the cmip5 archive. *Journal of Geophysical Research: Atmospheres*, 118(4):1613–1623.
- Blanchet, J., Aly, C., Vischel, T., Panthou, G., Sané, Y., and Kane, M. D. (2018). Trend in the co-occurrence of extreme daily rainfall in West Africa since 1950. *Journal of Geophysical Research: Atmospheres*.
- Blanchet, J., Molinié, G., and Touati, J. (2016). Spatial analysis of trend in extreme daily rainfall in southern France. *Climate Dynamics*, pages 1–14.
- Blöschl, G., Ardoin-Bardin, S., Bonell, M., Dorninger, M., Goodrich, D., Gutknecht, D., Matamoros, D., Merz, B., Shand, P., and Szolgay, J. (2007). At what scales do climate variability and land cover change impact on flooding and low flows? *Hydrological Processes*, 21(9):1241–1247.
- Blöschl, G. and Montanari, A. (2010). Climate change impacts—throwing the dice? *Hydrological Processes: An International Journal*, 24(3):374–381.
- Bodian, A., Dacosta, H., and Dezetter, A. (2011). Caractérisation spatio-temporelle du régime pluviométrique du haut bassin du fleuve Sénégal dans un contexte de variabilité climatique. *Physio-Géo. Géographie physique et environnement*, (Volume 5):107–124.
- Bodian, A., Dacosta, H., and Dezetter, A. (2013). Analyse des débits de crues et d'étiages dans le bassin versant du fleuve Sénégal en amont du barrage de Manantali. *Revue du LACEEDE. Climat et développement*, 15:46–56.

- Bodian, A., Dezetter, A., Deme, A., and Diop, L. (2016a). Hydrological evaluation of TRMM rainfall over the upper Senegal River basin. *Hydrology*, 3(2):15.
- Bodian, A., Ndiaye, O., and Dacosta, H. (2016b). Evolution des caractéristiques des pluies journalières dans le bassin versant du fleuve Sénégal: Avant et après rupture. *Hydrological Sciences Journal*, 61(5):905–913.
- Bonneau, M. (2001). Programme d’optimisation de la gestion des réservoirs. *Besoins en eau de l’agriculture irriguée et de l’agriculture de décrue dans la vallée du fleuve Sénégal*. IRD, OMVS, Dakar, Sénégal.
- Borgomeo, E., Hall, J. W., Fung, F., Watts, G., Colquhoun, K., and Lambert, C. (2014). Risk-based water resources planning: Incorporating probabilistic nonstationary climate uncertainties. *Water Resources Research*, 50(8):6850–6873.
- Boulain, N., Cappelaere, B., Séguis, L., Favreau, G., and Gignoux, J. (2009). Water balance and vegetation change in the Sahel: A case study at the watershed scale with an eco-hydrological model. *Journal of Arid Environments*, 73(12):1125–1135.
- Bouvier, C., Cisneros, L., Dominguez, R., Laborde, J.-P., and Lebel, T. (2003). Generating rainfall fields using principal components (pc) decomposition of the covariance matrix: a case study in mexico city. *Journal of Hydrology*, 278(1-4):107–120.
- Bower, S. S. (2010). Natural and unnatural complexities: flood control along Manitoba’s Assiniboine River. *Journal of Historical Geography*, 36(1):57–67.
- Boyer, J.-F., Dieulin, C., Rouche, N., Cres, A., Servat, E., Paturel, J.-E., and Mahe, G. (2006). SIEREM: an environmental information system for water resources. *IAHS publication*, 308:19.
- Brath, A., Montanari, A., and Moretti, G. (2006). Assessing the effect on flood frequency of land use change via hydrological simulation (with uncertainty). *Journal of Hydrology*, 324(1-4):141–153.

- Burt, C. C. (2007). *Extreme weather: a guide & record book*. WW Norton & Company.
- Butt, T. A., McCarl, B. A., Angerer, J., Dyke, P. T., and Stuth, J. W. (2005). The economic and food security implications of climate change in mali. *Climatic change*, 68(3):355–378.
- Byrd, R. H., Lu, P., Nocedal, J., and Zhu, C. (1995). A limited memory algorithm for bound constrained optimization. *SIAM Journal on Scientific Computing*, 16(5):1190–1208.
- Camberlin, P., Beltrando, G., Fontaine, B., and Richard, Y. (2002). Pluviométrie et crises climatiques en Afrique tropicale: changements durables ou fluctuations interannuelles? *Historiens et Géographes*, (379):263–273.
- Camberlin, P., Janicot, S., and Pocard, I. (2001). Seasonality and atmospheric dynamics of the teleconnection between african rainfall and tropical sea-surface temperature: Atlantic vs. enso. *International Journal of Climatology: A Journal of the Royal Meteorological Society*, 21(8):973–1005.
- Cameron, D., Beven, K., and Naden, P. (2000). Flood frequency estimation by continuous simulation under climate change (with uncertainty). *Hydrology and Earth System Sciences Discussions*, 4(3):393–405.
- Cappelaere, B., Descroix, L., Lebel, T., Boulain, N., Ramier, D., Laurent, J.-P., Favreau, G., Boubkraoui, S., Boucher, M., Moussa, I. B., et al. (2009). The AMMA-CATCH experiment in the cultivated Sahelian area of southwest Niger—investigating water cycle response to a fluctuating climate and changing environment. *Journal of Hydrology*, 375(1-2):34–51.
- Cappus, P. (1960). Etude des lois de l’écoulement-Application au calcul et à la prévision des débits. *La houille blanche*, pages 493–520.
- Carney, M. C., Babić, M., and Mesghinna, W. (2008). On the importance of spatial correlation in stochastic precipitation used in water supply modeling. *Proc., AGU Hydrology Days, Colorado State Univ., Fort Collins, CO*.
- Cassé, C. and Gosset, M. (2015). Analysis of hydrological changes and flood increase in Niamey based on the PERSIANN-CDR satellite rainfall estimate and hydrological simulations over the 1983–2013 period. *Proceedings of the International Association of Hydrological Sciences*, 370:117–123.

- Cassé, C., Gosset, M., Vischel, T., Quantin, G., and Tanimoun, B. A. (2016). Model-based study of the role of rainfall and land use–land cover in the changes in the occurrence and intensity of Niger red floods in Niamey between 1953 and 2012. *Hydrology and Earth System Sciences*, 20(7):2841–2859.
- Chardon, J., Hingray, B., Favre, A.-C., Autin, P., Gailhard, J., Zin, I., and Obled, C. (2014). Spatial similarity and transferability of analog dates for precipitation downscaling over france. *Journal of Climate*, 27(13):5056–5074.
- Coles, S., Bawa, J., Trenner, L., and Dorazio, P. (2001). *An introduction to statistical modeling of extreme values*, volume 208. Springer.
- Coles, S. G. and Tawn, J. A. (1996). A Bayesian analysis of extreme rainfall data. *Applied statistics*, pages 463–478.
- Condon, L., Gangopadhyay, S., and Pruitt, T. (2015). Climate change and non-stationary flood risk for the upper Truckee River basin. *Hydrology and Earth System Sciences*, 19(1):159.
- Cowden, J. R., Watkins Jr, D. W., and Mihelcic, J. R. (2008). Stochastic rainfall modeling in west africa: Parsimonious approaches for domestic rainwater harvesting assessment. *Journal of Hydrology*, 361(1-2):64–77.
- Cowpertwait, P., O’Connell, P., Metcalfe, A., and Mawdsley, J. (1996). Stochastic point process modelling of rainfall. ii. regionalisation and disaggregation. *Journal of Hydrology*, 175(1-4):47–65.
- Cunderlik, J. M. and Burn, D. H. (2003). Non-stationary pooled flood frequency analysis. *Journal of Hydrology*, 276(1-4):210–223.
- Dai, A., Trenberth, K. E., and Qian, T. (2004). A global dataset of Palmer Drought Severity Index for 1870–2002: Relationship with soil moisture and effects of surface warming. *Journal of Hydrometeorology*, 5(6):1117–1130.
- Dairaku, K., Emori, S., and Nozawa, T. (2008). Impacts of global warming on hydrological cycles in the asian monsoon region. *Advances in Atmospheric Sciences*, 25(6):960–973.

- D'amato, N. and Lebel, T. (1998). On the characteristics of the rainfall events in the sahel with a view to the analysis of climatic variability. *International Journal of Climatology*, 18(9):955–974.
- Davison, A. C. and Hinkley, D. V. (1997). *Bootstrap methods and their application*, volume 1. Cambridge University Press.
- Descroix, L., Genthon, P., Amogu, O., Rajot, J.-L., Sighomnou, D., and Vauclin, M. (2012). Change in Sahelian rivers hydrograph: The case of recent red floods of the Niger River in the Niamey region. *Global and Planetary Change*, 98:18–30.
- Descroix, L., Guichard, F., Grippa, M., Lambert, L. A., Panthou, G., Mahé, G., Gal, L., Dardel, C., Quantin, G., Kergoat, L., Bouaïta, Y., Hiernaux, P., Vischel, T., Pellarin, T., Faty, B., Wilcox, C., Malam Abdou, M., Mamadou, I., Vandervaere, J.-P., Diongue-Niang, A., Ndiaye, O., Sané, Y., Dacosta, H., Gosset, M., Cassé, C., Sultan, B., Barry, A., Amogu, O., Nka Nnomo, B., Barry, A., and Paturel, J.-E. (2018). Evolution of surface hydrology in the sahelo-sudanian strip: An updated review. *Water*, 10(6).
- Descroix, L., Mahé, G., Lebel, T., Favreau, G., Galle, S., Gautier, E., Olivry, J., Albergel, J., Amogu, O., Cappelaere, B., et al. (2009). Spatio-temporal variability of hydrological regimes around the boundaries between Sahelian and Sudanian areas of West Africa: A synthesis. *Journal of Hydrology*, 375(1-2):90–102.
- Di Baldassarre, G., Montanari, A., Lins, H., Koutsoyiannis, D., Brandimarte, L., and Blöschl, G. (2010). Flood fatalities in Africa: from diagnosis to mitigation. *Geophysical Research Letters*, 37(22).
- Dibike, Y. B. and Coulibaly, P. (2005). Hydrologic impact of climate change in the saguenay watershed: comparison of downscaling methods and hydrologic models. *Journal of hydrology*, 307(1-4):145–163.
- Diop, L., Yaseen, Z. M., Bodian, A., Djaman, K., and Brown, L. (2017). Trend analysis of streamflow with different time scales: a case study of the upper Senegal River. *ISH Journal of Hydraulic Engineering*, pages 1–10.
- Doocy, S., Daniels, A., Murray, S., and Kirsch, T. D. (2013). The human impact of floods: a historical review of events 1980-2009 and systematic literature review. *PLoS currents*, 5.

- d'Orgeval, T., Polcher, J., and Rosnay, P. d. (2008). Sensitivity of the West African hydrological cycle in ORCHIDEE to infiltration processes. *Hydrology and Earth System Sciences*, 12(6):1387–1401.
- Douville, H., Chauvin, F., Planton, S., Royer, J.-F., Salas-Melia, D., and Tyteca, S. (2002). Sensitivity of the hydrological cycle to increasing amounts of greenhouse gases and aerosols. *Climate Dynamics*, 20(1):45–68.
- Druyan, L. M. (2011). Studies of 21st-century precipitation trends over west africa. *International Journal of Climatology*, 31(10):1415–1424.
- d'Orgeval, T., Polcher, J., and Li, L. (2006). Uncertainties in modelling future hydrological change over west africa. *Climate dynamics*, 26(1):93–108.
- Efron, B. (1979). Computers and the theory of statistics: thinking the unthinkable. *SIAM review*, 21(4):460–480.
- Efron, B. and Tibshirani, R. J. (1994). *An introduction to the bootstrap*. CRC press.
- Elmer, F., Hoymann, J., Düthmann, D., Vorogushyn, S., and Kreibich, H. (2012). Drivers of flood risk change in residential areas. *Natural Hazards and Earth System Sciences*, 12(5):1641–1657.
- Emery, X. (2002). Conditional simulation of nongaussian random functions. *Mathematical Geology*, 34(1):79–100.
- Erb, K.-H., Lauk, C., Kastner, T., Mayer, A., Theurl, M. C., and Haberl, H. (2016). Exploring the biophysical option space for feeding the world without deforestation. *Nature communications*, 7:11382.
- Evin, G., Favre, A.-C., and Hingray, B. (2018). Stochastic generation of multi-site daily precipitation focusing on extreme events. *Hydrology and Earth System Sciences*, 22(1):655–672.
- Famien, A. M., Janicot, S., Ochou, A. D., Vrac, M., Defrance, D., Sultan, B., and Noel, T. (2018). A bias-corrected cmip5 dataset for africa using the cdf-t method: a contribution to agricultural impact studies. *Earth System Dynamics*, 9(1):313–338.

- Favreau, G., Cappelaere, B., Massuel, S., Leblanc, M., Boucher, M., Boulain, N., and Leduc, C. (2009). Land clearing, climate variability, and water resources increase in semiarid southwest Niger: A review. *Water Resources Research*, 45(7).
- Faye, c. (2015). Impact du changement climatique et du barrage de Manantali sur la dynamique du régime hydrologique du fleuve Sénégal à Bakel (1950-2014). *BSGLg*.
- Féral, L., Sauvageot, H., Castanet, L., and Lemorton, J. (2003). Hycell—a new hybrid model of the rain horizontal distribution for propagation studies: 1. modeling of the rain cell. *Radio Science*, 38(3).
- Ferraris, L., Gabellani, S., Reborá, N., and Provenzale, A. (2003). A comparison of stochastic models for spatial rainfall downscaling. *Water Resources Research*, 39(12).
- Fiorillo, E., Crisci, A., Issa, H., Maracchi, G., Morabito, M., and Tarchiani, V. (2018). Recent changes of floods and related impacts in niger based on the anadia niger flood database. *Climate*, 6(3):59.
- Fletcher, R. and Reeves, C. M. (1964). Function minimization by conjugate gradients. *The computer journal*, 7(2):149–154.
- François, B., Schlef, K., Wi, S., and Brown, C. (2019). Design considerations for riverine floods in a changing climate—a review. *Journal of Hydrology*.
- Furrer, E. M. and Katz, R. W. (2008). Improving the simulation of extreme precipitation events by stochastic weather generators. *Water Resources Research*, 44(12).
- Gal, L., Grippa, M., Hiernaux, P., Pons, L., and Kergoat, L. (2017). The paradoxical evolution of runoff in the pastoral Sahel: analysis of the hydrological changes over the Agoufou watershed (Mali) using the KINEROS-2 model. *Hydrology and Earth System Sciences*, 21(9):4591.
- Galle, S., Grippa, M., Peugeot, C., Moussa, I. B., Cappelaere, B., Demarty, J., Mougín, E., Panthou, G., Adjomayi, P., Agbossou, E., et al. (2018). Amma-catch, a critical zone observatory in west africa monitoring a region in transition. *Vadose Zone Journal*, 17(1).

- Galle, S., Peugeot, C., Grippa, M., Chaffard, V., Afouda, S., Agbossou, E., Ago, E., Arjounin, M., Awessou, B., Boucher, M., et al. (2016). Amma-catch: un observatoire hydrologique, météorologique et écologique de long terme en afrique de l'ouest: résultats importants et données disponibles.
- Gascon, T., Vischel, T., Lebel, T., Quantin, G., Pellarin, T., Quatela, V., Leroux, D., and Galle, S. (2015). Influence of rainfall space-time variability over the Ouémé basin in Benin. *Proceedings of the International Association of Hydrological Sciences*, 368:102–107.
- Gerbaux, M., Hall, N., Dessay, N., and Zin, I. (2009). The sensitivity of sahelian runoff to climate change. *Hydrological Sciences Journal*, 54(1):5–16.
- Giannini, A., Salack, S., Lodoun, T., Ali, A., Gaye, A., and Ndiaye, O. (2013). A unifying view of climate change in the sahel linking intra-seasonal, interannual and longer time scales. *Environmental Research Letters*, 8(2):024010.
- Giorgi, F., Im, E.-S., Coppola, E., Diffenbaugh, N., Gao, X., Mariotti, L., and Shi, Y. (2011). Higher hydroclimatic intensity with global warming. *Journal of Climate*, 24(20):5309–5324.
- Guan, K., Sultan, B., Biasutti, M., Baron, C., and Lobell, D. B. (2015). What aspects of future rainfall changes matter for crop yields in west africa? *Geophysical Research Letters*, 42(19):8001–8010.
- Guha-Sapir, D., Below, R., and Hoyois, P. (2016). Em-dat: international disaster database—www. emdat. be. université catholique de louvain.
- Guillot, G. and Lebel, T. (1999a). Approximation of sahelian rainfall fields with meta-gaussian random functions. *Stochastic Environmental Research and Risk Assessment*, 13(1-2):113–130.
- Guillot, G. and Lebel, T. (1999b). Disaggregation of Sahelian mesoscale convective system rain fields: Further developments and validation. *Journal of Geophysical Research: Atmospheres*, 104(D24):31533–31551.
- Guillot, P. (1993). The arguments of the gradex method: a logical support to assess extreme floods. *IAHS PUBLICATION*, pages 287–287.

- Gumbel, E. (1957). Extreme values in technical problems. Technical report, Technical report T-7A, Department of Engineering, Columbia Univ., Press, New York, AD120920.
- Hagemann, S., Chen, C., Haerter, J. O., Heinke, J., Gerten, D., and Piani, C. (2011). Impact of a statistical bias correction on the projected hydrological changes obtained from three gcms and two hydrology models. *Journal of Hydrometeorology*, 12(4):556–578.
- Hallegatte, S., Green, C., Nicholls, R. J., and Corfee-Morlot, J. (2013). Future flood losses in major coastal cities. *Nature climate change*, 3(9):802.
- Hasselmann, K. (1993). Optimal fingerprints for the detection of time-dependent climate change. *Journal of Climate*, 6(10):1957–1971.
- Hasselmann, K. (1997). Multi-pattern fingerprint method for detection and attribution of climate change. *Climate Dynamics*, 13(9):601–611.
- Hawkins, E. and Sutton, R. (2011). The potential to narrow uncertainty in projections of regional precipitation change. *Climate Dynamics*, 37(1-2):407–418.
- Heffernan, J. E., Stephenson, A. G., and Gilleland, E. (2016). *ismev: An Introduction to Statistical Modeling of Extreme Values*. R package version 1.41.
- Hegerl, G. C., Hasselmann, K., Cubasch, U., Mitchell, J., Roeckner, E., Voss, R., and Waszkewitz, J. (1997). Multi-fingerprint detection and attribution analysis of greenhouse gas, greenhouse gas-plus-aerosol and solar forced climate change. *Climate Dynamics*, 13(9):613–634.
- Hegerl, G. C., Hoegh-Guldberg, O., Casassa, G., Hoerling, M. P., Kovats, R., Parmesan, C., Pierce, D. W., and Stott, P. A. (2010). Good practice guidance paper on detection and attribution related to anthropogenic climate change. In *Meeting Report of the Intergovernmental Panel on Climate Change Expert Meeting on Detection and Attribution of Anthropogenic Climate Change*. IPCC Working Group I Technical Support Unit, University of Bern, Bern, Switzerland.
- Held, I. M. and Soden, B. J. (2006). Robust responses of the hydrological cycle to global warming. *Journal of climate*, 19(21):5686–5699.

- Hewlett, J. D. (1961). *Soil moisture as a source of base flow from steep mountain watersheds*. US Department of Agriculture, Forest Service, Southeastern Forest Experiment Station.
- Hewlett, J. D. and Hibbert, A. R. (1967). Factors affecting the response of small watersheds to precipitation in humid areas. *Forest hydrology*, 1:275–290.
- Hirabayashi, Y., Mahendran, R., Koirala, S., Konoshima, L., Yamazaki, D., Watanabe, S., Kim, H., and Kanae, S. (2013). Global flood risk under climate change. *Nature Climate Change*, 3(9):816.
- Horton, R. E. (1933). The role of infiltration in the hydrologic cycle. *Eos, Transactions American Geophysical Union*, 14(1):446–460.
- Hosking, J. R. M. and Wallis, J. R. (1997). *Regional frequency analysis: an approach based on L-moments*. Cambridge University Press.
- Intergovernmental Panel on Climate Change (2018). *Global warming of 1.5°C*. OCLC: 1056192590.
- Jalbert, J., Mathevet, T., and Favre, A.-C. (2011). Temporal uncertainty estimation of discharges from rating curves using a variographic analysis. *Journal of Hydrology*, 397(1-2):83–92.
- Janicot, S., Trzaska, S., and Pocard, I. (2001). Summer sahel-enso teleconnection and decadal time scale sst variations. *Climate Dynamics*, 18(3-4):303–320.
- Jenkins, G. S., Adamou, G., and Fongang, S. (2002). The challenges of modeling climate variability and change in west africa. *Climatic Change*, 52(3):263–286.
- Jimoh, O. and Webster, P. (1999). Stochastic modelling of daily rainfall in nigeria: intra-annual variation of model parameters. *Journal of Hydrology*, 222(1-4):1–17.
- Judt, F. (2018). Insights into atmospheric predictability through global convection-permitting model simulations. *Journal of the Atmospheric Sciences*, 75(5):1477–1497.

- Kahle, D. and Wickham, H. (2013). ggmap: Spatial visualization with ggplot2. *The R Journal*, 5(1):144–161.
- Katz, R. W., Parlange, M. B., and Naveau, P. (2002). Statistics of extremes in hydrology. *Advances in water resources*, 25(8-12):1287–1304.
- Kim, H., Kim, S., Shin, H., and Heo, J.-H. (2017). Appropriate model selection methods for nonstationary generalized extreme value models. *Journal of Hydrology*, 547:557–574.
- Koren, V., Finnerty, B., Schaake, J., Smith, M., Seo, D.-J., and Duan, Q.-Y. (1999). Scale dependencies of hydrologic models to spatial variability of precipitation. *Journal of Hydrology*, 217(3-4):285–302.
- Koutsoyiannis, D. (2004). Statistics of extremes and estimation of extreme rainfall: II. Empirical investigation of long rainfall records/Statistiques de valeurs extrêmes et estimation de précipitations extrêmes: II. Recherche empirique sur de longues séries de précipitations. *Hydrological Sciences Journal*, 49(4).
- Koutsoyiannis, D., Efstratiadis, A., and Georgakakos, K. (2007). Uncertainty assessment of future hydroclimatic predictions: A comparison of probabilistic and scenario-based approaches. *Journal of Hydrometeorology*, 8(3):261–281.
- Krysanova, V., Vetter, T., Eisner, S., Huang, S., Pechlivanidis, I., Strauch, M., Gelfan, A., Kumar, R., Aich, V., Arheimer, B., et al. (2017). Intercomparison of regional-scale hydrological models and climate change impacts projected for 12 large river basins worldwide—a synthesis. *Environmental Research Letters*, 12(10):105002.
- Kundzewicz, Z., Graczyk, D., Maurer, T., Pińskwar, I., Radziejewski, M., Svensson, C., and Szwed, M. (2005a). Trend detection in river flow series: 1. Annual maximum flow / Détection de tendance dans des séries de débit fluvial: 1. Débit maximum annuel. *Hydrological Sciences Journal*, 50(5).
- Kundzewicz, Z. W., Ulbrich, U., Graczyk, D., Krüger, A., Leckebusch, G. C., Menzel, L., Pińskwar, I., Radziejewski, M., Szwed, M., et al. (2005b). Summer floods in central Europe—climate change track? *Natural Hazards*, 36(1-2):165–189.

- Lamb, P. J. (1983). Sub-saharan rainfall update for 1982; continued drought. *International Journal of Climatology*, 3(4):419–422.
- Lambin, E. F., Geist, H. J., and Lepers, E. (2003). Dynamics of land-use and land-cover change in tropical regions. *Annual review of environment and resources*, 28(1):205–241.
- Lambourne, J. and Stephenson, D. (1987). Model study of the effect of temporal storm distributions on peak discharges and volumes. *Hydrological sciences journal*, 32(2):215–226.
- Le Barbé, L. and Lebel, T. (1997). Rainfall climatology of the HAPEX-Sahel region during the years 1950–1990. *Journal of Hydrology*, 188:43–73.
- Le Barbé, L., Lebel, T., and Tapsoba, D. (2002). Rainfall variability in West Africa during the years 1950–90. *Journal of climate*, 15(2):187–202.
- Lebel, T. and Ali, A. (2009). Recent trends in the Central and Western Sahel rainfall regime (1990–2007). *Journal of Hydrology*, 375(1-2):52–64.
- Lebel, T., Braud, I., and Creutin, J.-D. (1998). A space-time rainfall disaggregation model adapted to sahelian mesoscale convective complexes. *Water Resources Research*, 34(7):1711–1726.
- Lebel, T., Cappelaere, B., Galle, S., Hanan, N., Kergoat, L., Levis, S., Vieux, B., Descroix, L., Gosset, M., Mougin, E., et al. (2009). Amma-catch studies in the sahelian region of west-africa: an overview. *Journal of Hydrology*, 375(1-2):3–13.
- Lebel, T., Diedhiou, A., and Laurent, H. (2003). Seasonal cycle and interannual variability of the Sahelian rainfall at hydrological scales. *Journal of Geophysical Research: Atmospheres*, 108(D8).
- Leblanc, M. J., Favreau, G., Massuel, S., Tweed, S. O., Loireau, M., and Cappelaere, B. (2008). Land clearance and hydrological change in the Sahel: Southwest Niger. *Global and Planetary Change*, 61(3-4):135–150.
- Lee, T. (2018). Multisite stochastic simulation of daily precipitation from copula modeling with a gamma marginal distribution. *Theoretical and Applied Climatology*, 132(3-4):1089–1098.

- Leong, D. N. and Donner, S. D. (2015). Climate change impacts on stream-flow availability for the athabasca oil sands. *Climatic change*, 133(4):651–663.
- L'Hote, Y., Mahé, G., Somé, B., and Triboulet, J. P. (2002). Analysis of a Sahelian annual rainfall index from 1896 to 2000; the drought continues. *Hydrological Sciences Journal*, 47(4):563–572.
- Li, K., Coe, M., Ramankutty, N., and De Jong, R. (2007). Modeling the hydrological impact of land-use change in West Africa. *Journal of Hydrology*, 337(3-4):258–268.
- Li, Z., Huang, G., Wang, X., Han, J., and Fan, Y. (2016). Impacts of future climate change on river discharge based on hydrological inference: A case study of the grand river watershed in ontario, canada. *Science of the Total Environment*, 548:198–210.
- Li, Z., Lü, Z., Li, J., and Shi, X. (2017). Links between the spatial structure of weather generator and hydrological modeling. *Theoretical and applied climatology*, 128(1-2):103–111.
- Loireau, M. (1998). *Espaces-Ressources-Usages: Spatialisation des interactions dynamiques entre les systèmes sociaux et les systèmes écologiques au Sahel nigérien*. PhD thesis, Université de Montpellier 3.
- Lombardo, F., Volpi, E., Koutsoyiannis, D., and Serinaldi, F. (2017). A theoretically consistent stochastic cascade for temporal disaggregation of intermittent rainfall. *Water Resources Research*, 53(6):4586–4605.
- Lorenz, E. N. (1963). Deterministic nonperiodic flow. *Journal of the atmospheric sciences*, 20(2):130–141.
- Loveridge, M. and Rahman, A. (2018). Monte carlo simulation for design flood estimation: a review of australian practice. *Australasian Journal of Water Resources*, 22(1):52–70.
- Ly, M., Traore, S. B., Alhassane, A., and Sarr, B. (2013). Evolution of some observed climate extremes in the West African Sahel. *Weather and climate extremes*, 1:19–25.

- Mahé, G., Olivry, J.-C., Dessouassi, R., Orange, D., Bamba, F., and Servat, E. (2000). Relations eaux de surface–eaux souterraines d’une rivière tropicale au Mali. *Comptes Rendus de l’Académie des Sciences-Series IIA-Earth and Planetary Science*, 330(10):689–692.
- Mahé, G., Olivry, J. C., and Servat, E. (2005). Sensibilité des cours d’eau ouest-africains aux changements climatiques et environnementaux: extrêmes et paradoxes. *Regional Hydrological Impacts of Climatic Change—Hydroclimatic Variability*, edited by S. Frank, T. Wagener, E. Bøgh, HV Gupta, L. Bastidas, C. Nobre and C. de Oliveira Galvão, pages 169–177.
- Mahé, G. and Paturel, J.-E. (2009). 1896–2006 Sahelian annual rainfall variability and runoff increase of Sahelian rivers. *Comptes Rendus Geoscience*, 341(7):538–546.
- Malam Abdou, M. (2014). *États de surface et fonctionnement hydrodynamique multi-échelles des bassins sahéliens; études expérimentales en zones cristalline et sédimentaire*. PhD thesis, Université Joseph Fourier.
- Mamadou, I., Gautier, E., Descroix, L., Noma, I., Moussa, I. B., Maiga, O. F., Genthon, P., Amogu, O., Abdou, M. M., and Vandervaere, J.-P. (2015). Exorheism growth as an explanation of increasing flooding in the Sahel. *Catena*, 131:130–139.
- Marty, C. and Blanchet, J. (2012). Long-term changes in annual maximum snow depth and snowfall in Switzerland based on extreme value statistics. *Climatic Change*, 111(3-4):705–721.
- Massazza, G., Tamagnone, P., Wilcox, C., Belcore, E., Pezzoli, A., Vischel, T., Panthou, G., Housseini Ibrahim, M., Tiepolo, M., Tarchiani, V., and Rosso, M. (2019). Flood Hazard Scenarios of the Sirba River (Niger): Evaluation of the Hazard Thresholds and Flooding Areas. *Water*, 11(5).
- Mathon, V., Laurent, H., and Lebel, T. (2002). Mesoscale convective system rainfall in the sahel. *Journal of applied meteorology*, 41(11):1081–1092.
- McWilliams, J. C. (2019). A perspective on the legacy of edward lorenz. *Earth and Space Science*.

- Merz, B., Vorogushyn, S., Uhlemann, S., Delgado, J., and Huntecha, Y. (2012). HESS Opinions” More efforts and scientific rigour are needed to attribute trends in flood time series”. *Hydrology and Earth System Sciences*, 16(5):1379–1387.
- Miao, Q. (2018). Are we adapting to floods? evidence from global flooding fatalities. *Risk Analysis*.
- Michelangeli, P.-A., Vrac, M., and Loukos, H. (2009). Probabilistic down-scaling approaches: Application to wind cumulative distribution functions. *Geophysical Research Letters*, 36(11).
- Millar, R. J., Fuglestedt, J. S., Friedlingstein, P., Rogelj, J., Grubb, M. J., Matthews, H. D., Skeie, R. B., Forster, P. M., Frame, D. J., and Allen, M. R. (2017). Emission budgets and pathways consistent with limiting warming to 1.5 c. *Nature Geoscience*, 10(10):741.
- Milly, P. C., Betancourt, J., Falkenmark, M., Hirsch, R. M., Kundzewicz, Z. W., Lettenmaier, D. P., and Stouffer, R. J. (2008). Stationarity is dead: Whither water management? *Science*, 319(5863):573–574.
- Min, S.-K., Zhang, X., Zwiers, F. W., and Hegerl, G. C. (2011). Human contribution to more-intense precipitation extremes. *Nature*, 470(7334):378–381.
- Monerie, P.-A., Sanchez-Gomez, E., Pohl, B., Robson, J., and Dong, B. (2017). Impact of internal variability on projections of sahel precipitation change. *Environmental Research Letters*, 12(11):114003.
- Mora, C., Spirandelli, D., Franklin, E. C., Lynham, J., Kantar, M. B., Miles, W., Smith, C. Z., Freel, K., Moy, J., Louis, L. V., et al. (2018). Broad threat to humanity from cumulative climate hazards intensified by greenhouse gas emissions. *Nature Climate Change*, page 1.
- Morlot, T., Perret, C., Favre, A.-C., and Jalbert, J. (2014). Dynamic rating curve assessment for hydrometric stations and computation of the associated uncertainties: Quality and station management indicators. *Journal of Hydrology*, 517:173–186.

- Naveau, P., Huser, R., Ribereau, P., and Hannart, A. (2016). Modeling jointly low, moderate, and heavy rainfall intensities without a threshold selection. *Water Resources Research*, 52(4):2753–2769.
- Nelder, J. A. and Mead, R. (1965). A simplex method for function minimization. *The computer journal*, 7(4):308–313.
- Nicholson, S. (2013a). The West African Sahel: A review of recent studies on the rainfall regime and its interannual variability. *ISRN Meteorology*, 2013:1–32.
- Nicholson, S. (2013b). The West African Sahel: A review of recent studies on the rainfall regime and its interannual variability. *ISRN Meteorology*, 2013:1–32.
- Nicholson, S. E. (2000). The nature of rainfall variability over Africa on time scales of decades to millenia. *Global and planetary change*, 26(1-3):137–158.
- Nka, B., Oudin, L., Karambiri, H., Paturel, J.-E., and Ribstein, P. (2015). Trends in floods in West Africa: analysis based on 11 catchments in the region. *Hydrology and Earth System Sciences*, 19(11):4707–4719.
- Nyong, A. and Niang-Diop, I. (2006). Impacts of climate change in the tropics: the african experience. *Avoiding dangerous climate change*, page 237.
- O’Gorman, P. A. (2012). Sensitivity of tropical precipitation extremes to climate change. *Nature Geoscience*, 5(10):697–700.
- Olsen, J. R., Lambert, J. H., and Haines, Y. Y. (1998). Risk of extreme events under nonstationary conditions. *Risk Analysis*, 18(4):497–510.
- Onibon, H., Lebel, T., Afouda, A., and Guillot, G. (2004). Gibbs sampling for conditional spatial disaggregation of rain fields. *Water Resources Research*, 40(8).
- Oriani, F., Ohana-Levi, N., Marra, F., Straubhaar, J., Mariethoz, G., Renard, P., Karnieli, A., and Morin, E. (2017). Simulating small-scale rainfall fields conditioned by weather state and elevation: A data-driven approach based on rainfall radar images. *Water Resources Research*, 53(10):8512–8532.

- Over, T. M. and Gupta, V. K. (1994). Statistical analysis of mesoscale rainfall: Dependence of a random cascade generator on large-scale forcing. *Journal of Applied Meteorology*, 33(12):1526–1542.
- Ozer, P., Hountondji, Y., and Laminou Manzo, O. (2009). Evolution des caractéristiques pluviométriques dans l’est du Niger de 1940 à 2007. *Geo-Eco-Trop*, 33:11–30.
- Panthou, G., Lebel, T., Vischel, T., Quantin, G., Sane, Y., Ba, A., Ndiaye, O., Diongue-Niang, A., and Diopkane, M. (2018). Rainfall intensification in tropical semi-arid regions: the sahelian case. *Environmental Research Letters*, 13(6):064013.
- Panthou, G., Vischel, T., and Lebel, T. (2014). Recent trends in the regime of extreme rainfall in the Central Sahel. *International Journal of Climatology*, 34(15):3998–4006.
- Panthou, G., Vischel, T., Lebel, T., Blanchet, J., Quantin, G., and Ali, A. (2012). Extreme rainfall in West Africa: A regional modeling. *Water Resources Research*, 48(8).
- Panthou, G., Vischel, T., Lebel, T., Quantin, G., Pugin, A.-C. F., Blanchet, J., and Ali, A. (2013). From pointwise testing to a regional vision: An integrated statistical approach to detect nonstationarity in extreme daily rainfall. application to the Sahelian region. *Journal of Geophysical Research: Atmospheres*, 118(15):8222–8237.
- Paquet, E., Garavaglia, F., Garçon, R., and Gailhard, J. (2013). The SCHADEX method: A semi-continuous rainfall–runoff simulation for extreme flood estimation. *Journal of Hydrology*, 495:23–37.
- Park, J.-S., Kang, H.-S., Lee, Y. S., and Kim, M.-K. (2011). Changes in the extreme daily rainfall in South Korea. *International Journal of Climatology*, 31(15):2290–2299.
- Pechlivanidis, I., Arheimer, B., Donnelly, C., Hundecha, Y., Huang, S., Aich, V., Samaniego, L., Eisner, S., and Shi, P. (2017). Analysis of hydrological extremes at different hydro-climatic regimes under present and future conditions. *Climatic Change*, 141(3):467–481.

- Peleg, N. and Morin, E. (2014). Stochastic convective rain-field simulation using a high-resolution synoptically conditioned weather generator (hires-wg). *Water Resources Research*, 50(3):2124–2139.
- Peres, D. and Cancelliere, A. (2018). Modeling impacts of climate change on return period of landslide triggering. *Journal of Hydrology*, 567:420–434.
- Peugeot, C., Cappelaere, B., Vieux, B. E., Séguis, L., and Maia, A. (2003). Hydrologic process simulation of a semiarid, endoreic catchment in sahelian west niger. 1. model-aided data analysis and screening. *Journal of Hydrology*, 279(1-4):224–243.
- Peugeot, C., Esteves, M., Galle, S., Rajot, J., and Vandervaere, J. (1997). Runoff generation processes: results and analysis of field data collected at the East Central Supersite of the HAPEX-Sahel experiment. *Journal of Hydrology*, 188-189:179–202.
- Population-Reference-Bureau (2016). 2016 world population data sheet with a special focus on human needs and sustainable resources.
- Quantin, G., Vischel, T., Panthou, G., Vandervaere, J.-P., Wilcox, C., Malam-Abdou, M., and Descroix, L. (2017). Un modèle hydrologique pour le Sahel et son implémentation sur le bassin du Dargol. Note Technique, Institut des Géosciences de l’Environnement.
- Raut, B. A., Seed, A. W., Reeder, M. J., and Jakob, C. (2018). A multiplicative cascade model for high-resolution space-time downscaling of rainfall. *Journal of Geophysical Research: Atmospheres*, 123(4):2050–2067.
- Re, M. and Barros, V. R. (2009). Extreme rainfalls in SE South America. *Climatic Change*, 96(1-2):119–136.
- Renard, B., Kavetski, D., Leblois, E., Thyer, M., Kuczera, G., and Franks, S. W. (2011). Toward a reliable decomposition of predictive uncertainty in hydrological modeling: Characterizing rainfall errors using conditional simulation. *Water Resources Research*, 47(11).
- Ribes, A., Planton, S., and Terray, L. (2013). Application of regularised optimal fingerprinting to attribution. part i: method, properties and idealised analysis. *Climate dynamics*, 41(11-12):2817–2836.

- Risser, M. D. and Wehner, M. F. (2017). Attributable human-induced changes in the likelihood and magnitude of the observed extreme precipitation during hurricane harvey. *Geophysical Research Letters*, 44(24):12–457.
- Robertson, A. W., Kirshner, S., and Smyth, P. (2004). Downscaling of daily rainfall occurrence over northeast brazil using a hidden markov model. *Journal of climate*, 17(22):4407–4424.
- Rochette, C. et al. (1974). *Le bassin du fleuve Senegal*. ORSTOM.
- Rogelj, J., Den Elzen, M., Höhne, N., Fransen, T., Fekete, H., Winkler, H., Schaeffer, R., Sha, F., Riahi, K., and Meinshausen, M. (2016). Paris agreement climate proposals need a boost to keep warming well below 2 c. *Nature*, 534(7609):631.
- Roudier, P., Ducharne, A., and Feyen, L. (2014). Climate change impacts on runoff in west africa: a review. *Hydrology and Earth System Sciences*, 18:2789–2801.
- Salathé Jr, E. P., Hamlet, A. F., Mass, C. F., Lee, S.-Y., Stumbaugh, M., and Steed, R. (2014). Estimates of twenty-first-century flood risk in the pacific northwest based on regional climate model simulations. *Journal of Hydrometeorology*, 15(5):1881–1899.
- Samimi, C., Fink, A., and Paeth, H. (2012). The 2007 flood in the Sahel: causes, characteristics and its presentation in the media and FEWS NET. *Natural Hazards and Earth System Sciences*, 12(2):313.
- Sanogo, S., Fink, A. H., Omotosho, J. A., Ba, A., Redl, R., and Ermert, V. (2015). Spatio-temporal characteristics of the recent rainfall recovery in West Africa. *International Journal of Climatology*, 35(15):4589–4605.
- Schumacher, R. S. and Johnson, R. H. (2005). Organization and environmental properties of extreme-rain-producing mesoscale convective systems. *Monthly weather review*, 133(4):961–976.
- Seguis, L., Cappelaere, B., Milési, G., Peugeot, C., Massuel, S., and Favreau, G. (2004). Simulated impacts of climate change and land-clearing on runoff from a small Sahelian catchment. *Hydrological Processes*, 18(17):3401–3413.

- Serinaldi, F. (2010). Multifractality, imperfect scaling and hydrological properties of rainfall time series simulated by continuous universal multifractal and discrete random cascade models. *Nonlinear Processes in Geophysics*, 17(6):697–714.
- Shanno, D. F. (1970). Conditioning of quasi-Newton methods for function minimization. *Mathematics of computation*, 24(111):647–656.
- Sheen, K., Smith, D., Dunstone, N., Eade, R., Rowell, D., and Vellinga, M. (2017). Skillful prediction of sahel summer rainfall on inter-annual and multi-year timescales. *Nature communications*, 8:14966.
- Shi, P., Yang, X., Fang, J., Xu, W., Han, G., et al. (2016). Mapping and ranking global mortality, affected population and gdp loss risks for multiple climatic hazards. *Journal of Geographical Sciences*, 26(7):878–888.
- Sighomnou, D., Descroix, L., Genthon, P., Mahé, G., Moussa, I. B., Gautier, E., Mamadou, I., Vandervaere, J.-P., Bachir, T., Coulibaly, B., et al. (2013). La crue de 2012 à Niamey: un paroxysme du paradoxe du Sahel? *Science et changements planétaires/Sécheresse*, 24(1):3–13.
- Singer, M. B. and Michaelides, K. (2017). Deciphering the expression of climate change within the lower colorado river basin by stochastic simulation of convective rainfall. *Environmental Research Letters*, 12(10):104011.
- Sørup, H. J. D., Christensen, O. B., Arnbjerg-Nielsen, K., and Mikkelsen, P. S. (2016). Downscaling future precipitation extremes to urban hydrology scales using a spatio-temporal neyman–scott weather generator. *Hydrology and Earth System Sciences*, 20(4):1387–1403.
- Steffen, W., Rockström, J., Richardson, K., Lenton, T. M., Folke, C., Liverman, D., Summerhayes, C. P., Barnosky, A. D., Cornell, S. E., Crucifix, M., et al. (2018). Trajectories of the earth system in the anthropocene. *Proceedings of the National Academy of Sciences*, 115(33):8252–8259.
- Stocker, T. F., Qin, D., Plattner, G., Tignor, M., Allen, S., Boschung, J., Nauels, A., Xia, Y., Bex, V., and Midgley, P. (2013). Climate change 2013: the physical science basis. intergovernmental panel on climate change, working group i contribution to the ipcc fifth assessment report (ar5). *New York*.

- Stratton, R. A., Senior, C. A., Vosper, S. B., Folwell, S. S., Boutle, I. A., Earnshaw, P. D., Kendon, E., Lock, A. P., Malcolm, A., Manners, J., et al. (2018). A pan-african convection-permitting regional climate simulation with the met office unified model: Cp4-africa. *Journal of Climate*, 31(9):3485–3508.
- Sun, F., Roderick, M. L., Lim, W. H., and Farquhar, G. D. (2011). Hydroclimatic projections for the murray-darling basin based on an ensemble derived from intergovernmental panel on climate change ar4 climate models. *Water Resources Research*, 47(12).
- Sun, X., Renard, B., Thyer, M., Westra, S., and Lang, M. (2015). A global analysis of the asymmetric effect of enso on extreme precipitation. *Journal of Hydrology*, 530:51–65.
- Tan, J., Jakob, C., Rossow, W. B., and Tselioudis, G. (2015). Increases in tropical rainfall driven by changes in frequency of organized deep convection. *Nature*, 519(7544):451.
- Tarhule, A. (2005). Damaging rainfall and flooding: the other Sahel hazards. *Climatic change*, 72(3):355–377.
- Tarhule, A., Zume, J. T., Grijzen, J., Talbi-Jordan, A., Guero, A., Dessouassi, R. Y., Doffou, H., Kone, S., Coulibaly, B., and Harshadeep, N. R. (2015). Exploring temporal hydroclimatic variability in the Niger Basin (1901–2006) using observed and gridded data. *International Journal of Climatology*, 35(4):520–539.
- Taylor, C. M., Belušić, D., Guichard, F., Parker, D. J., Vischel, T., Bock, O., Harris, P. P., Janicot, S., Klein, C., and Panthou, G. (2017). Frequency of extreme Sahelian storms tripled since 1982 in satellite observations. *Nature*, 544(7651):475.
- Trenberth, K. E. (1999). Conceptual framework for changes of extremes of the hydrological cycle with climate change. In *Weather and Climate Extremes*, pages 327–339. Springer.
- Trenberth, K. E. (2011). Changes in precipitation with climate change. *Climate Research*, 47(1-2):123–138.

- Trenberth, K. E., Dai, A., Rasmussen, R. M., and Parsons, D. B. (2003). The changing character of precipitation. *Bulletin of the American Meteorological Society*, 84(9):1205–1218.
- Trenberth, K. E., Fasullo, J. T., and Shepherd, T. G. (2015). Attribution of climate extreme events. *Nature Climate Change*.
- Troutman, B. M. (1983). Runoff prediction errors and bias in parameter estimation induced by spatial variability of precipitation. *Water Resources Research*, 19(3):791–810.
- Tschakert, P., Sagoe, R., Ofori-Darko, G., and Codjoe, S. N. (2010). Floods in the Sahel: an analysis of anomalies, memory, and anticipatory learning. *Climatic Change*, 103(3-4):471–502.
- UNEP (2011). Livelihood security: Climate change, migration and conflict in the sahel.
- Valdes, J., Nakamoto, S., Shen, S., and North, G. (1990). Estimation of multidimensional precipitation parameters by areal estimates of oceanic rainfall. *Journal of Geophysical Research: Atmospheres*, 95(D3):2101–2111.
- Verdin, A., Rajagopalan, B., Kleiber, W., Podestá, G., and Bert, F. (2018). A conditional stochastic weather generator for seasonal to multi-decadal simulations. *Journal of Hydrology*, 556:835–846.
- Villarini, G., Serinaldi, F., Smith, J. A., and Krajewski, W. F. (2009). On the stationarity of annual flood peaks in the continental United States during the 20th century. *Water Resources Research*, 45(8).
- Vincent, K. (2004). Creating an index of social vulnerability to climate change for africa. *Tyndall Center for Climate Change Research. Working Paper*, 56(41).
- Vischel, T. and Lebel, T. (2007). Assessing the water balance in the Sahel: Impact of small scale rainfall variability on runoff. Part 2: Idealized modeling of runoff sensitivity. *Journal of Hydrology*, 333(2-4):340–355.
- Vischel, T., Lebel, T., Massuel, S., and Cappelaere, B. (2009). Conditional simulation schemes of rain fields and their application to rainfall–runoff modeling studies in the Sahel. *Journal of Hydrology*, 375(1):273–286.

- Vischel, T., Panthou, G., Peyrillé, P., Roehrig, R., Quantin, G., Lebel, T., Wilcox, C., Beucher, F., and Budiarti, M. (2019). Precipitation extremes in the west african sahel: Recent evolution and physical mechanisms. In *Tropical Extremes*, pages 95–138. Elsevier.
- Vischel, T., Quantin, G., Lebel, T., Viarre, J., Gosset, M., Cazenave, F., and Panthou, G. (2011). Generation of high-resolution rain fields in West Africa: Evaluation of dynamic interpolation methods. *Journal of Hydrometeorology*, 12(6):1465–1482.
- Vrac, M. and Friederichs, P. (2015). Multivariate—intervariable, spatial, and temporal—bias correction. *Journal of Climate*, 28(1):218–237.
- Vrac, M., Noël, T., and Vautard, R. (2016). Bias correction of precipitation through singularity stochastic removal: Because occurrences matter. *Journal of Geophysical Research: Atmospheres*, 121(10):5237–5258.
- Vu, T. M., Mishra, A. K., Konapala, G., and Liu, D. (2018). Evaluation of multiple stochastic rainfall generators in diverse climatic regions. *Stochastic Environmental Research and Risk Assessment*, 32(5):1337–1353.
- Wang, H., Xiao, W., Wang, Y., Zhao, Y., Lu, F., Yang, M., Hou, B., and Yang, H. (2019). Assessment of the impact of climate change on hydropower potential in the nanliujiang river basin of china. *Energy*, 167:950–959.
- Wang, S. and Wang, Y. (2019). Improving probabilistic hydroclimatic projections through high-resolution convection-permitting climate modeling and markov chain monte carlo simulations. *Climate Dynamics*, pages 1–24.
- Wilcox, C., Aly, C., Vischel, T., Panthou, G., Blanchet, J., Quantin, G., and Lebel, T. (in preparation). Stochastorm: a stochastic rainfall simulator for the intertropical zone.
- Wilcox, C., Vischel, T., Panthou, G., Bodian, A., Blanchet, J., Descroix, L., Quantin, G., Cassé, C., Tanimoun, B., and Kone, S. (2018). Trends in hydrological extremes in the senegal and niger rivers. *Journal of Hydrology*, 566:531–545.
- Wilks, D. (1998). Multisite generalization of a daily stochastic precipitation generation model. *Journal of Hydrology*, 210(1-4):178–191.

- Wilks, D. S. (1999). Interannual variability and extreme-value characteristics of several stochastic daily precipitation models. *Agricultural and Forest Meteorology*, 93(3):153–169.
- Wilks, D. S. (2010). Use of stochastic weathergenerators for precipitation downscaling. *Wiley Interdisciplinary Reviews: Climate Change*, 1(6):898–907.
- Wilks, D. S. and Wilby, R. L. (1999). The weather generation game: a review of stochastic weather models. *Progress in physical geography*, 23(3):329–357.
- Wilson, C. B., Valdes, J. B., and Rodriguez-Iturbe, I. (1979). On the influence of the spatial distribution of rainfall on storm runoff. *Water Resources Research*, 15(2):321–328.
- Zhang, X., Zwiers, F. W., Hegerl, G. C., Lambert, F. H., Gillett, N. P., Solomon, S., Stott, P. A., and Nozawa, T. (2007). Detection of human influence on twentieth-century precipitation trends. *Nature*, 448(7152):461.
- Zipser, E. J., Cecil, D. J., Liu, C., Nesbitt, S. W., and Yorty, D. P. (2006). Where are the most intense thunderstorms on earth? *Bulletin of the American Meteorological Society*, 87(8):1057–1072.